Title
Investigation of the Enhancement of Drug Synergy by Co-Delivery in Targeted Liposomes

Author
Riviere, Kareen

Publication Date
2009

Peer reviewed|Thesis/dissertation

Investigation of the Enhancement of Drug Synergy by Co-Delivery in Targeted Liposomes

by

Kareen Riviere

DISSERTATION

Submitted in partial satisfaction of the requirements for the degree of

DOCTOR OF PHILOSOPHY

in

Pharmaceutical Sciences and Pharmacogenomics

ACKNOWLEDGEMENTS

Most especially, I would like to acknowledge Dr. Francis C. Szoka, Jr. for his novel ideas as well as his mentorship and guidance throughout my doctoral training.

I would like to thank the faculty members that served on my dissertation committee: Dr. Francis C. Szoka Jr., Dr. Leslie Z. Benet, and Dr. Scott Kogan as well as on my oral examination committee: Dr. Leslie Z. Benet, Dr. Scott Kogan, Dr. Deanna L. Kroetz, and Dr. Christopher Cullander.

Additionally, I would like to express my gratitude to all those who have made contributions to the research in this dissertation, including Dr. Zhaohua Huang for his guidance on the synthesis and purification of the FA-PEG2000-DSPE, FA-PEG3350-DSPE and FITC-DSPE; Caroline Larregieu and Sarah B. Shugarts for their assistance with HPLC-MS/MS analysis of the biodistribution of the liposome combination drugs; Katherine Jerger and Nichole Macaraeg for their superb technical skills that were essential for executing the animal studies; Dr. Daryl Drummond, Dr. Dmitri Karpotin, and Hermes, Inc. for the generous gift of sucrose octasulfate, Dr. Gaetano Capasso for his assistance with investigating irinotecan remote loading methods; and Dr. Dipali Ruhela for her guidance and partnership on the hyaluronan targeted liposome delivery project. I would also like to thank my laboratory mates: Dr. Douglas Watson, Dr. Grace Huynh, Dr. Joshua Park, Dr. Richard Cohen, Emily Perttu, Virginia Platt, Dr. Juliane Nguyen, Dr. Bo Chen, and Edward Dy for collegial conversations and suggestions about my research.

This work was funded by NIH Grant GM061851, the UNCF-Merck Graduate Science Research Dissertation Fellowship, and the PhRMA Foundation Pre-Doctoral Fellowship in Pharmaceutics.

Finally, I must express my profound appreciation for the love and support of my family – notably Anne-Marie Riviere, Serge F. Riviere, Regine Riviere, and Joelle Pierre; my friends – especially Tamara Edwards, Tanya Nichols, Dr. Erika Tate, and Debbie Acoba; and all of my educators throughout the years.

My dissertation is dedicated to my younger brother, Patrick, who is the source of my inspiration.

Investigation of the Enhancement of Drug Synergy by Co-Delivery in Targeted Liposomes

by Kareen Riviere

ABSTRACT

Synergistic anti-cancer drug combinations have superior tumor-killing activity, the potential to reduce drug toxicity to healthy tissues, and the ability to minimize the development of drug resistance. Since drug synergism is dependent on the ratio of the combined drugs, synergistic agents must be maintained at fixed ratios to achieve the maximum therapeutic effect *in vivo*. We hypothesize that targeted liposomes can enhance the efficacy of synergistic anti-cancer drug combinations *in vivo* by facilitating the intracellular delivery of both drugs at their synergistic ratio and dose. To test this hypothesis, select combinations of anti-cancer drugs were screened *in vitro* for synergism in KB folate receptor over-expressing cancer cells. The combination activity of drug pairs was evaluated with the median effect method. Irinotecan (IRN) and 5-fluoroorotic acid (FOA) emerged as the most synergistic pair in the screen since they exhibited synergism at a wide range of concentrations and molar ratios. Investigating my hypothesis required that I devise and validate new encapsulation techniques for liposome formulations of IRN, FOA, and the combination of IRN + FOA. Safety studies with the single agents in non-targeted liposomes (NTLs) were conducted in normal mice to identify the maximum tolerated dose. Therapeutic studies in HT29 and C26 tumor mouse models confirmed that the new NTL formulations had anti-cancer potency. We designed folate-targeted liposomes (FTLs) that target the folate receptors on KB tumor cells *in vitro* and *in vivo*

when as little as 0.03 mol% of the synthesized folate ligand was displayed on the liposome surface. Biodistribution and anti-tumor studies in the KB model with liposome encapsulated doxorubicin confirmed that FTLs deliver chemotherapeutics to the tumor and have anti-tumor activity. The anti-tumor efficacy of IRN + FOA co-delivered in the same FTLs or in a mixture of FTLs was compared to their NTL counterparts in the KB model. Liposomes significantly enhanced the *in vivo* efficacy of the synergistic combinations. However, folate-targeted liposomes with IRN + FOA did not provide a statistically significant therapeutic advantage over co-delivery of this synergistic pair in non-targeted liposomes.

TABLE OF CONTENTS

List of Tables x

List of Figures xi

List of Abbreviations xii

CHAPTER 1: Introduction

1.1 Overview 1

1.2 Synergism 1

1.2.1 What is synergy? 1

1.2.2 Methods of Determining Synergism 2

1.2.3 Synergism is Drug Ratio Dependent 6

1.3 Liposome Drug Carriers for *in vivo* Delivery of Synergistic Agents 6

1.4 Targeted Liposome Delivery of Synergistic Drugs 8

CHAPTER 2: *In Vitro* Screen for Synergistic Anticancer Agents

2.1 Abstract 12

2.2 Introduction 12

2.3 Methods 15

2.3.1 Materials 15

2.3.2 Cell Culture 15

2.3.3 Cytotoxicity Assay 16

2.3.4 Evaluating Synergy 16

2.4 Results 18

2.5 Discussion 22

CHAPTER 3: Development and Evaluation of Non-Targeted Liposomal Formulations of Irinotecan and Fluoroorotate and Their Combination

3.1 Abstract 24

3.2 Introduction 25

3.3 Methods 26

3.3.1 Materials 26

3.3.2 Cell Culture 26

3.3.3 Cytotoxicity Assay 26
3.3.4 Drug Interaction Analysis 27
3.3.5 Preparing Liposomal IRN 27
3.3.6 Preparing Liposomal FOA 28
3.3.7 Liposome Co-encapsulation of IRN and FOA 30
3.3.8 Animals 31
3.3.9 NTL-IRN Chemotherapy in HT29 Mouse Model 31
3.3.10 FOA and NTL-FOA MTD Studies in Balb/c and Balb/c nu/nu Mice 32
3.3.11 Liposomal IRN+FOA Combination Therapy in C26 Mouse Model 32
3.4 Results 33
3.4.1 Synergism of IRN+FOA 33
3.4.2 Development of NTL-IRN Formulation 34
3.4.3 Therapeutic Efficacy of NTL-IRN in HT29 Tumor Model 36
3.4.4 Formulation Development of NTL-FOA 38
3.4.5 MTD Analysis of FOA and NTL-FOA in Balb/c and Balb/c nu/nu Mice 39
3.4.6 Liposome Co-encapsulation of IRN+FOA 41
3.4.7 Anti-tumor Effect in and Survival of C26 Tumor-Bearing Mice Treated with Liposomal IRN and FOA 47
3.5 Discussion 49
CHAPTER 4: Evaluation of Folate Targeted Liposome Delivery
4.1 Abstract 54
4.2 Introduction 55
4.3 Methods 56
4.3.1 Materials 56
4.3.2 Cell Culture 56
4.3.3 Synthesis and Characterization of FA-PEG-DSPE Ligands 57
4.3.4 Synthesis of FITC-DSPE 59

4.3.5 Effect of Ligand Concentration and PEG on FTL Cell Association 60
4.3.6 Animals 62
4.3.7 Circulation Profile and Biodistrubution of FTLs in KB Tumor-bearing Mice 62
4.3.8 Antitumor Activity and Survival Studies 63
4.4 Results 64
4.4.1 Effect of Ligand Density and PEG on Folate Targeting to KB Cells in vitro 64
4.4.2 Blood Concentration Profile and Biodistribution of FTLs 66
4.4.3 Effect of FTL-Dox on Tumor Growth and Survival Rate 68
4.5 Discussion 71

CHAPTER 5: Therapeutic Activity of Folate Targeted Liposome Co-encapsulated Irinotecan and Fluoroorotic Acid in a KB (FR+) Tumor Model

5.1 Abstract 76
5.2 Introduction 77
5.3 Methods 79
5.3.1 Materials 79
5.3.2 Cell Culture 79
5.3.3 Cytotoxicity Assay 79
5.3.4 Drug Interaction Analysis 80
5.3.5 Preparing Liposomal IRN 80
5.3.6 Preparing Liposomal FOA 81
5.3.7 Liposome Co-encapsulation of IRN and FOA 82
5.3.8 Drug Release Studies 83
5.3.9 Animals 83
5.3.10 Liposomal IRN and FOA Individual and Combination Therapy 83
5.4 Results 84
5.4.1 Combination Activity of IRN and FOA in KB Cells 84
5.4.2 Encapsulation and Release Profile of IRN and FOA from Liposomes 86

5.4.3 Therapeutic Activity of Individual Liposomal Agents in the KB Tumor Model 88
5.4.4 Therapeutic Activity of Liposomal Combinations in KB Tumor-bearing Mice 91
5.5 Discussion 97
CHAPTER 6: Conclusions and Future Directions 101
REFERENCES 106
APPENDIX: Hyaluronan-Lipid Conjugates for Targeted Liposomal Delivery
A.1 Abstract 113
A.2 Introduction 113
A.3 Materials and Methods 115
A.3.1 Enzymatic Digestion of HA 115
A.3.2 Size Exclusion Chromatography 115
A.3.3 Ozonolysis/Reduction of the HA Oligomers 116
A.3.4 Synthesis of the Lipooligosaccharide 117
A.4 Results and Discussion 118
A.5 References 123

LIST OF TABLES

Table 1.1 Potential Mechanisms of Drug Interactions 2
Table 1.2 Summary of Popular Drug Interaction Models 5
Table 1.3 Summary of Anticancer Drug Combinations Delivered in Liposome Carriers 7
Table 2.1 Properties of Drugs Selected for *in vitro* Screen in KB Cells 14
Table 2.2 Summary of Primary Screen in KB Cells 18
Table 2.3 Summary of SN-38 Combination Activity in KB Cells 19
Table 2.4 Summary of Vinorelbine Combination Activity in KB Cells 19
Table 2.5 Summary of Resveratrol Combination Activity in KB Cells 20
Table 2.6 Summary of Seleno-L-Methionine Combination Activity in KB Cells 20
Table 3.1 IRN + FOA Combination Activity in C26 Cells 34
Table 3.2 Summary of Conditions and Outcome to Co-encapsulate IRN + FOA into Liposomes at 1:5 Molar Ratio 43
Table 3.3 Summary of Conditions and Outcome to Co-encapsulate IRN + FOA into Liposomes at 1:1 Molar Ratio 45
Table 3.4 Drug Content in Formulations Used in Combination Therapy Study 47
Table 4.1 Summary of Formulations Prepared for Studies 61
Table 4.2 Quantification of Antitumor and Survival Data 69
Table 4.3 Multiple Statistical Comparison of Average Tumor Size Data 70
Table 4.4 Multiple Statistical Comparison of Survival Data 71
Table 5.1 Quantification of Antitumor and Survival Data 93
Table 5.2 Multiple Statistical Comparison of Average Tumor Size Data 94
Table 5.3 Multiple Statistical Comparison of Survival Data 96
Table A.1 MALDI-TOF MS (negative mode) Results for HA oligosaccharides 120
Table A.2 MALDI-TOF MS (positive mode) Results for HA_n-DPPE conjugates 121

LIST OF FIGURES

Figure 1.1 Schematic drawing illustrating non-targeted versus targeted liposomal delivery of a synergistic drug combination encapsulated at a 1:1 ratio 9

Figure 2.1 Drugs evaluated in *in vitro* screen for synergism in KB cells 13

Figure 3.1 Schematic diagram of proposed mechanism of encapsulation of IRN in liposomes 35

Figure 3.2 Effect of NTL-IRN on tumor growth and survival rate in HT29 tumor-bearing mice 37

Figure 3.3 Effect of NTL-IRN on weight of HT29 tumor-bearing mice 38

Figure 3.4 Maximum tolerated dose study of FOA 100 mg/kg and NTL-FOA 10 mg/kg 40

Figure 3.5 Effect of new dosing schedule on FOA MTD in Balb/c mice 41

Figure 3.6 Effect of IRN drug to lipid ratio on IRN and FOA co-encapsulation at 1:5 ratio 44

Figure 3.7 Effect of IRN drug to lipid ratio on IRN and FOA co-encapsulation at 1:1 ratio 46

Figure 3.8 Schematic diagram of proposed mechanism of co-encapsulation of IRN + FOA in liposomes 46

Figure 3.9 NTL-IRN-FOA combination therapy in C26 tumor-bearing mice 48

Figure 3.10 Effect of combination therapy on weight of C26 tumor-bearing mice 49

Figure 4.1 Schematic diagram of the liposome formulations 61

Figure 4.2 Cell association of FTLs with varying FA-PEG(2000)-DSPE mole percentages with KB cells 65

Figure 4.3 Cell association of FTLs with and without mPEG2000-DSPE 66

Figure 4.4 Blood circulation profile of FTLs with varying FA-PEG-DSPE mole percentages in KB tumored Balb/c nu/nu mice 67

Figure 4.5 Biodistribution of radiolabeled FTLs and PLs in KB tumored Balb/c nu/nu mice sacrificed 48 hr after i.v. injection of 1 μmol lipid 68

LIST OF FIGURES (Continued)

Figure 4.6 Antitumor activity of PL-Dox and F_{3350}PL(0.03%)-Dox 69

Figure 4.7 Effect of PL-Dox and F_{3350}PL(0.03%)-Dox on the survival of KB tumored Balb/c nu/nu mice 71

Figure 5.1 *in vitro* combination activity of IRN and FOA at fixed dose ratios in KB cells 85

Figure 5.2 Schematic diagram of proposed mechanism of co-encapsulation of IRN + FOA in liposomes 86

Figure 5.3 IRN and FOA release profile from NTL formulations 88

Figure 5.4 Efficacy of NTL and FTL formulations of IRN or FOA alone in KB tumor-bearing mice 90

Figure 5.5 Tumor growth inhibition of NTL and FTL combination therapy in KB tumor-bearing mice 92

Figure 5.6 Effect of NTL and FTL combination therapy on survival rate in KB tumor-bearing mice 95

Figure 5.7 Effect of treatments on weight of KB tumor-bearing mice 96

Figure A.1 Disaccharide repeat unit of HA 114

Figure A.2 Size exclusion profile of HA oligomer 120

Figure A.3 ^{1}H NMR spectrum of HA_4-DPPE and HA_6-DPPE 122

LIST OF SCHEMES

Scheme 4.1 Synthesis of FA-PEG3350-DSPE 59

Scheme 4.2 Synthesis FITC-DSPE 60

Scheme A.1 Ozonolysis/reduction of HA oligomers 117

Scheme A.2 Synthesis of lipooligosaccharide 118

LIST OF ABBREVIATIONS

BTCA:	1,2,3,4-butanetetracarboxylic acid
Chol:	cholesterol
CI:	combination index
D_A:	concentration of Drug A in combination
D_B:	concentration of Drug B in combination
$(D_m)_A$:	median concentration of Drug A
$(D_m)_B$:	median concentration of Drug B
$(D_x)_A$:	concentration of Drug A alone
$(D_x)_B$:	concentration of Drug B alone
D/L:	drug to lipid ratio
Dox:	doxorubicin
DSPC:	distearoylphosphatidylcholine
DSPE:	distearoylphosphatidylethanolamine
DSPG:	distearoylphosphatidylglycol
EC50:	concentration that produces 50% of effect
EC75:	concentration that produces 75% of effect
EC90:	concentration that produces 90% of effect
em:	emission wavelength
ex:	excitation wavelength
F_{2000}L:	Folate-PEG2000 liposome
F_{2000}PL:	Folate-PEG2000 PEGylated liposome
F_{3350}L:	Folate-PEG3350 liposome
F_{3350}PL:	Folate-PEG3350 PEGylated liposome
f_a:	fraction of affected cell
f_A:	fractional response of Drug A
f_B:	fractional response of Drug B
f_{AB}:	predicted fractional response of drug combination
f_{obs}:	observed fractional response of drug combination
FA:	folic acid, folate
FACS:	fluorescence activated cell sorting
FITC:	fluorescein isothiocyanate
FOA:	fluoroorotic acid, fluoroorotate
FR:	folate receptor
FTL:	folate-targeted liposome
I:	interaction index
ILS:	increase in life span
IRN:	irinotecan
i.p.:	intraperitoneal
i.v.:	intravenous
mPEG-DSPE:	methoxy-polyethylene glycol distearoylphosphatidylethanolamine
MST:	mean survival time
MTD:	maximum tolerated dose

LIST OF ABBREVIATIONS (Continued)

MW:	molecular weight
NTL:	non-targeted liposome
PEG:	polyethylene glycol
PBS:	phosphate buffered saline
PL:	PEGylated liposome
RES:	reticuloendothelial system
SRB:	sulforhodamine B
TEA:	triethylamine
TGD:	tumor growth delay
Tris:	tris(hydroxymethyl)aminomethane

CHAPTER 1:
Introduction

1.1 Overview

My hypothesis is that targeted liposomes can enhance the efficacy of synergistic anticancer drug combinations *in vivo* by facilitating the intracellular delivery of both agents at their synergistic ratio and dose. The goal for the proposed delivery strategy is to specifically deliver a combination of drugs to tumor cells, maximize the tumor intracellular amount of the combination agents at their synergistic ratio, and thereby enhance the antitumor activity of the drug combination.

1.2 Synergism

Increasingly, therapeutics are being combined to successfully treat life-threatening diseases such as cancer. The underlying principle is that multiple drugs can act against multiple targets to more effectively treat a disease. In addition, drug combinations that "synergize" have the potential to reduce drug toxicity and minimize the development of drug resistance.

1.2.1 What is synergy?

Drug synergism occurs when the combined effect of two or more drugs is greater than the additive pharmacological effect of the combinations. The mechanisms of synergism for all synergistic drug combinations are not fully understood since drugs usually have more than one mode of action, and all the modes of action of a drug may not be known [1]. However, some potential mechanisms of synergy have been discussed in the literature [2-4]. These mechanisms are listed in Table 1.1.

Table 1.1 Potential Mechanisms of Drug Interactions

i.	Drug A affects how Drug B reaches target (i.e. Drug A alters transport/metabolism of Drug B)
ii.	Drug A alters activity of Drug B (i.e. Drug A alters cell cycle kinetics)
iii.	Drugs A and B bind to separate targets on same, related, or crosstalking pathways
iv.	Drug A and B bind to same target at identical or different sites
v.	Drug A and B combine to form a new drug
vi.	Drug A is a catalyst for endogenous formation of Drug B

1.2.2 Methods of Determining Synergism

In the past century, various methods for evaluating drug interactions have arisen. Included in each method is a reference model of what is considered an additive combination effect and comparisons to this model that indicate synergism or antagonism. The most popular methods cited in the literature are briefly discussed here and are summarized in Table 1.2.

The isobologram method is one of the oldest and simplest methods for analyzing drug interactions [5]. For this method, one has to construct 2D plots called isobolograms where that x-axis is the concentration of Drug A alone and the y-axis is the concentration of Drug B alone. Lines called iso-effect curves are drawn to connect the concentration of Drug A and Drug B that produce the same effect (i.e. EC_{50}). Points on the iso-effect curve are considered additive. Measured data points from the drug combinations that fall to the left of the curve are considered synergistic while points to the right are considered antagonistic. Each plot represents a certain effect level; thus, this method requires a large data set in order to analyze the interaction at multiple concentrations. Other drawbacks of this method are that the degree of synergism cannot be quantified and statistical analysis cannot be applied. The interaction index method is a mathematical version of the isobologram method [6, 7]. An interaction index (I) < 1 indicates synergism, I = 1 indicates additivity, and I > 1 indicates antagonism. Using this model, one can quantify the level of synergism and perform limited statistics.

The Bliss independence method or the fractional product method [8, 9] is also simple. In this model, the additive effect is determined by multiplying the effect of each drug alone. Synergy is indicated if the observed effect is greater than the product of the effects of the individual agents. A major limitation of this method is that it assumes a linear dose effect relationship for the drugs. Also, only limited statistical analysis can be applied.

The most sophisticated drug interaction methods utilize response surface analysis [10-12]. The data is fitted to an interactive index type equation and is usually presented in a 2D or 3D dose-effect plot. There are interaction ranges for synergism, additivity and antagonism. This method is mathematically complex and thus requires more complicated computational modeling than the other methods. Additionally, the statistics can be difficult to interpret.

The median effect method is the most widely used model for analyzing drug interactions [1, 13-17]. This method is based on the median effect equation. Dose effect data are fitted to this equation and presented in a median effect plot (a log-log plot of dose on the x-axis and effect on the y-axis). Then, parameters are determined that are used to calculate a combination index (CI). Synergism, additivity, and antagonism are defined for $CI < 1$, $CI = 1$, and $CI > 1$, respectively. The computational analysis required for this method is facilitated by the use of a commercially available and user friendly software program called CalcuSyn (BioSoft). The software package also performs statistical analysis. The median effect method is more thoroughly discussed in Chapter 2. One major limitation of this model is that the accuracy of the parameters can be affected by transforming the dose-effect data to a logarithmic scale. Although this method has its

limitations, it is a very attractive drug interaction model because of its pharmacological basis, software availability, and popularity. Therefore, this is the method that I employed for identifying synergistic anti-cancer drug combinations.

Table 1.2 Summary of Popular Drug Interaction Models

Method	Theoretical Basis	Two-Drug Interaction Equation		Simple	Statistics	Software
Isobologram	Loewe Additivity	Graphical Analysis	Synergy: *Left of line* Additivity: *On line* Antagonism: *Right of line*	Yes	No	No
Interaction Index	Loewe Additivity	$I = \frac{D_A}{(D_x)_A} + \frac{D_B}{(D_x)_B}$	Synergy: $I < 1$ Additivity: $I = 1$ Antagonism: $I > 1$	Yes	No	No
Fractional Product	Bliss Independence	$f_{AB} = f_A f_B$	Synergy : $f_{obs} > f_{AB}$ Additivity: $f_{obs} = f_{AB}$ Antagonism: $f_{obs} < f_{AB}$	Yes	No	No
Median Effect	Mass Action Law, Enzyme Kinetics, Hill	$CI = \frac{D_A}{(D_x)_A} + \frac{D_B}{(D_x)_B}$ $CI = \frac{D_A}{(D_x)_A} + \frac{D_B}{(D_x)_B} + \frac{D_A D_B}{(D_x)_A (D_x)_B}$	Synergy: $CI < 1$ Additivity: $CI = 1$ Antagonism: $CI > 1$	Yes	Yes	Yes
Response Surface	Loewe Additivity, Median Effect Method	$I = 1 - \frac{\alpha D_A D_B}{(D_m)_A^{\frac{1}{2}} (D_m)_B^{\frac{1}{2}} (D_x)_A^{\frac{1}{2}} (D_x)_B^{\frac{1}{2}}}$	Synergy : $\alpha < 0$ $(I < 1)$ Additivity: $\alpha = 0$ $(I = 1)$ Antagonism: $\alpha > 0$ $(I > 1)$	No	Yes	Yes

α: degree of synergism; $\mathbf{D_A}$, $\mathbf{D_B}$: dose of Drug A or Drug B in combination
$\mathbf{(D_x)_A}$, $\mathbf{(D_x)_B}$: dose Drug A or Drug B alone; **CI**: combination index; **I**: interaction index
$\mathbf{f_{AB}}$: predicted fractional response of combination; $\mathbf{f_{obs}}$: observed fractional response of combination

1.2.3 Synergism is Drug Ratio Dependent

The therapeutic activity of a drug combination depends on maintaining the synergistic ratio at the target site. Some ratios of drug combinations may be synergistic while other ratios may be additive or antagonistic [18]. The most convenient and cost-effective way to determine what drugs will synergize is to systematically screen different drug combinations at various ratios and concentrations in cell culture or other preclinical models [16]. In order to produce the maximum therapeutic effect, synergistic drug combinations administered *in vivo* must remain at the identified synergistic ratio observed i*n vitro*. Because drugs have diverse biochemical properties, it can be difficult to control the pharmacokinetics of two or more drugs in a manner that causes these drugs to reach target cells at the optimal ratio and concentration. Thus, a strategy is needed to successfully translate the synergistic interactions observed *in vitro* to animal models and humans.

1.3 Liposome Drug Carriers for *in vivo* Delivery of Synergistic Agents

The application of liposomes, phospholipid bilayer vesicles, as drug delivery vehicles to enhance the therapeutic activity of anti-cancer drug combinations has been under investigation by many groups. Liposome drug carriers of 50-200 nm size can entrap 10^3 – 10^5 drug molecules [19, 20], and can therefore deliver a large payload of drugs to tumor cells. Liposomes, especially those coated with polyethylene glycol (PEG), can increase the circulation time and thus the pharmacokinetic and biodistribution profile of the encapsulated drug(s) [21]. The liposome carrier shields the loaded drug(s) from sites of metabolism in the body (i.e. liver, gut, and kidney) and also early degradation. Including PEG on the liposome surface further helps to reduce liposome clearance from the circulation by reducing the binding of opsonins on the liposome surface and by

inhibiting interactions with liver and spleen macrophages as well as other tissue of the reticuloendothelial system (RES). Liposomes are able to passively accumulate the drug(s) in tumors via the enhanced permeability and retention (EPR) effect [22]. The EPR effect is a phenomenon by which nanoparticles can permeate through the discontinuous vasculature of solid tumors or inflamed tissue and remain in these areas due to the poorly developed lymphatic drainage system of the environment. This mechanism helps to dramatically increase the tumor drug levels, decrease drug concentrations at possible sites of toxicity, and thereby improve the therapeutic index of the encapsulated drug(s) [23].

Some examples of FDA approved liposomal drugs are Doxil/Caelyx (PEGylated liposomal doxorubicin), Myocet (liposomal doxorubicin), AmBisome (liposomal amphotericin B), DepoCyt (liposomal cytosine arabinoside), and DaunoXome (liposomal daunorubicin). The liposome platform has been well studied and is under continuous investigation for various types of drugs [23]. Thus, liposomes are an established drug delivery technology.

Table 1.3 Summary of Anticancer Drug Combinations Delivered in Liposome Carriers

Drug A	Drug B	Co-encapsulated	Targeted	Cancer Type	Biological System	Reference
Doxorubicin	Vincristine	No	No	Mammary carcinoma	Cell, Mouse	24
Doxorubicin	Vincristine	Yes	No	Breast cancer	Cell, Mouse	25
Doxorubicin	Verapamil	Yes	No	Prostate cancer	Cell, Rat	26
Irinotecan	Floxuridine	Yes	No	Colorectal cancer	Cell, Mouse, Human	27, 35, 37
Cytarabine	Daunorubicin	Yes	No	Leukemia	Cell, Mouse, Human	27, 31, 36
Cisplatin	Daunorubiicn	No	No	Lung cancer	Cell, Mouse	27
Topotecan	Doxorubicin	No	No	Glioblastoma multiforme	Cell, Rat	28
Irinotecan	Doxorubicin	No	No	Glioblastoma multiforme	Cell, Rat	29
Doxorubicin	Verapamil	Yes	Yes	Leukemia	Cell	30
Irinotecan	Cisplatin	Yes	No	Small cell lung cancer	Cell, Mouse	32

Over the past 15 years, several studies have reported on the liposome delivery of drug combinations for cancer therapy [24-32]. These combinations have included diverse drug such as daunorubicin, doxorubicin, cisplatin, cytarabine, floxuridine, irinotecan, topotecan, verapamil, and vincristine (Table 1.3). Mayer and coworkers have been at the

forefront of this new paradigm of enhancing combination chemotherapy by controlling drug ratios with liposome drug carriers [33, 34]. They use the median effect method to identify the synergistic ratios of their drug combinations. The animal studies conducted by this group demonstrate that liposomes are able to maintain the encapsulated drug combination at the synergistic ratio for approximately 24hr after systemic administration in mice. Furthermore, the liposome drug combinations have significantly more therapeutic activity than free drug combinations. Mayer and coworkers have even established a company based on the concept of liposome delivery of fixed ratio agents. Celator Pharmaceuticals currently has two liposome drug combination formulations in clinical development: CPX-1 (liposomal irinotecan + floxuridine 1:1) for colorectal cancer and CPX-351 (liposomal cytarabine + daunorubicin 5:1) for acute myeloid leukemia [35-37]. Therefore, liposomes are suitable drug carriers to synchronize the pharmacokinetics and biodistribution of drug combinations and to control the ratio and dose of the drugs that reach the target site. However, can combination chemotherapy be further enhanced by targeted liposome delivery of synergistic drugs?

1.4 Targeted Liposome Delivery of Synergistic Drugs

Ligand-mediated targeting of liposome therapeutics to specific antigens over-expressed or selectively expressed on tumor cells is a well studied strategy for preferentially delivering toxic drugs to tumor diseased tissue rather than normal, healthy tissue [38, 39]. Another benefit of targeting liposomal drug carriers to tumors by tumor-specific ligands is that liposomes can be internalized into the cancer cells via receptor-mediated endocytosis. As a result, a large payload of liposome drug contents can be released within tumor cells. This is in contrast to non-targeted liposomes. Once the non-

targeted liposomes reach the tumor extracellular space, the encapsulated drugs are gradually released from the liposomes and then are taken up by the tumor cells as a free drug combination via standard mechanisms of drug uptake. Because drugs can have different mechanisms of uptake (i.e. diffusion or active transport), the drugs may get taken up in the tumor cells at a ratio that is different from the desired, synergistic ratio.

Thus, I propose that receptor-targeted liposomes can further enhance the efficacy of synergistic anticancer drug combinations *in vivo* by maintaining the optimal ratio that is delivered within tumor cells (Figure 1.1).

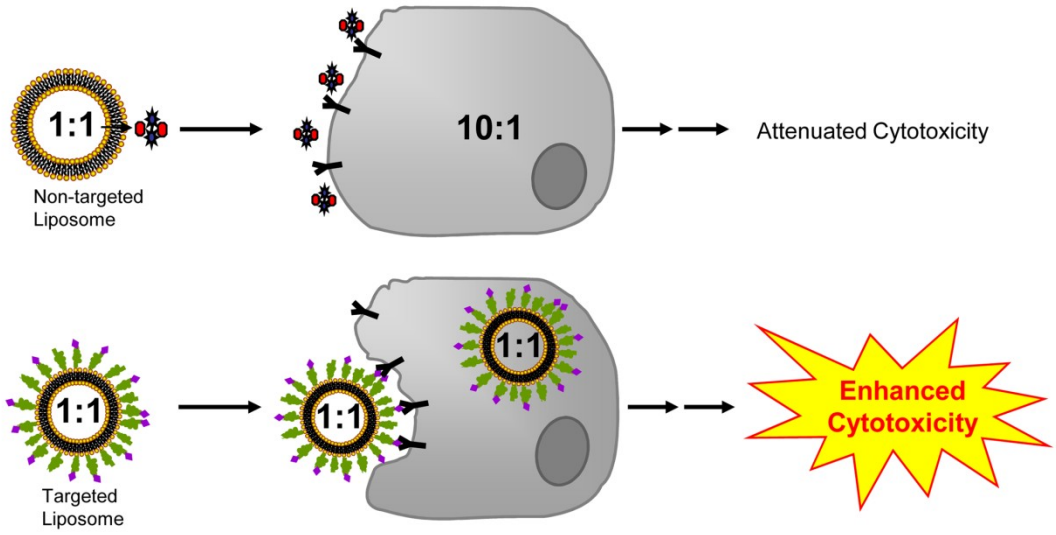

Figure 1.1 Schematic drawing illustrating non-targeted versus targeted liposomal delivery of a synergistic drug combination encapsulated at a 1:1 ratio. **Top.** Co-encapsulated drugs are released from non-targeted liposomes in the tumor interstitial fluid at their synergistic ratio (i.e. 1:1). However, the drugs enter the tumor cells at a different ratio (i.e. 10:1) due to their different mechanisms of cellular uptake. As a result of the change in drug ratio, an attenuated cytotoxic effect may be observed. **Bottom.** Targeted liposomes bind to a tumor-specific receptor and get internalized. Inside the tumor cell, the co-encapsulated drugs are released at their synergistic ratio and exert an enhanced cytotoxic effect.

Folate targeting is a well studied strategy for site-specific delivery of liposome therapeutics. Folate binds to the folate receptor (FR) with high affinity (Kd = 0.1 nM) and is internalized via receptor-mediated endocytosis [40]. FR is a 38 kDa glycosyl-phosphatidylinositol membrane anchored glycoprotein that is over-expressed on various

tumor cells types; however, it is present at low levels in most normal epithelial tissue [41]. The high folate binding affinity and tumor specificity distinguish the folate receptor as an attractive target for directed cancer therapy. Folate targeted liposomes (FTL) have successfully delivered chemotherapeutic agents as well as genes, antisense oligonucleotides, and radionuclides into FR over-expressing tumor cells [42]. Furthermore, it was reported that KB (FR+) tumor-bearing mice treated with FTL-doxorubicin had a greater reduction in tumor growth and an increase in survival compared to those that received NTL-doxorubicin or free doxorubicin [43]. Hence, folate-mediated targeting of liposomes seems an appropriate system to investigate whether the intracellular delivery of a fixed synergistic ratio of drugs will enhance the therapeutic efficacy of synergistic anti-cancer drug combinations.

In this dissertation, I conducted a series of studies to examine my hypothesis. In Chapter 2, I screened selected combinations of anti-cancer drugs in *vitro* for synergism in KB (FR+) cancer cells and evaluated the combination activity with the median effect method. Then in Chapter 3, I developed non-targeted liposomal formulations for the best synergistic combination and evaluated the therapeutic efficacy of these new formulations in normal mice as well as in tumor-bearing mouse. In Chapter 4, I evaluated folate targeted liposome delivery by characterizing the *in vitro* and *in vivo* targeting of FTLs and also the antitumor activity of FTL-doxorubicin in a KB (FR+) tumor mouse model. Finally in Chapter 5, I investigated whether folate targeting improves the therapy of the liposome co-encapsulated synergistic drug combination by performing biodistribution and antitumor studies in KB (FR+) tumor-bearing mice.

This work begins the conversation for the question “Can targeted liposome delivery of synergistic agents enhance combination chemotherapy?” and sets the stage for yet another paradigm.

CHAPTER 2:
In Vitro Screen for Synergistic Anticancer Agents

2.1 Abstract

Several two-drug combinations of the following compounds: doxorubicin, cisplatin, irinotecan, and fluoroorotic acid, vinorelbine, resveratrol, and seleno-L-methionine were screened for *in vitro* synergism. The drugs/drug combinations were chosen for their potency in cancer therapy, differing mechanisms of action, potential to be encapsulated within a liposome, and reported synergistic effect. The *in vitro* cytotoxicity of these drugs alone and in combination was evaluated in KB human nasopharyngeal cancer cells that over-express the folate receptor via the sulforhodamine B assay. To determine whether the drug combinations are synergistic, additive or antagonistic, we utilized the Median Effect Method developed by Chou and Talalay [1, 2, 17]. The results of the screen show that irinotecan + 5-fluoroorotic acid is the most synergistic combination in KB cells due to their synergism at a wide range of concentrations at particular molar ratios. In the flowing chapters, this drug combination was co-encapsulated in liposome formulations, and animal studies were conducted to validate whether the therapeutic efficacy of these liposomal drug cocktails was predicted by the *in vitro* results.

2.2 Introduction

To investigate the hypothesis that targeted liposomes can enhance the efficacy of synergistic anticancer drugs combinations, it was crucial to identify compounds that exhibited synergistic cytotoxic effects on cancer cells. We decided to screen doxorubicin [44-48], cisplatin [46-56], irinotecan [20, 44, 50, 51, 57-67], SN-38 [53, 68-71] and vinorelbine [72-77] because they are potent anticancer agents that are reported to behave

synergistically in many cancer cell lines. These drugs also possess the physicochemical properties that allow them to be stably encapsulated in liposome formulations. We also examined combinations involving fluoroorotate because it is a derivative of fluorouracil – a widely used and potent anticancer drug – that is able to be encapsulated in liposomes [50, 52, 57, 62, 72, 78-81]. In addition, combinations involving the antioxidants resveratrol [47, 82-84] and seleno-L-methionine [58-61] were investigated since they are unique compounds that are nontoxic but can enhance the cytotoxicity of other anticancer drugs. The drug candidates are shown in Figure 2.1, and their properties are summarized in Table 2.1. The published information on the synergism of these compounds was gathered in diverse cancer cell lines using various cytotoxicity assays and different mathematical models of synergism. Therefore, it was necessary to screen the candidate drug combinations in our target cancer cell line(s) with a reliable cytotoxicity assay and a widely accepted method for evaluating drug synergism.

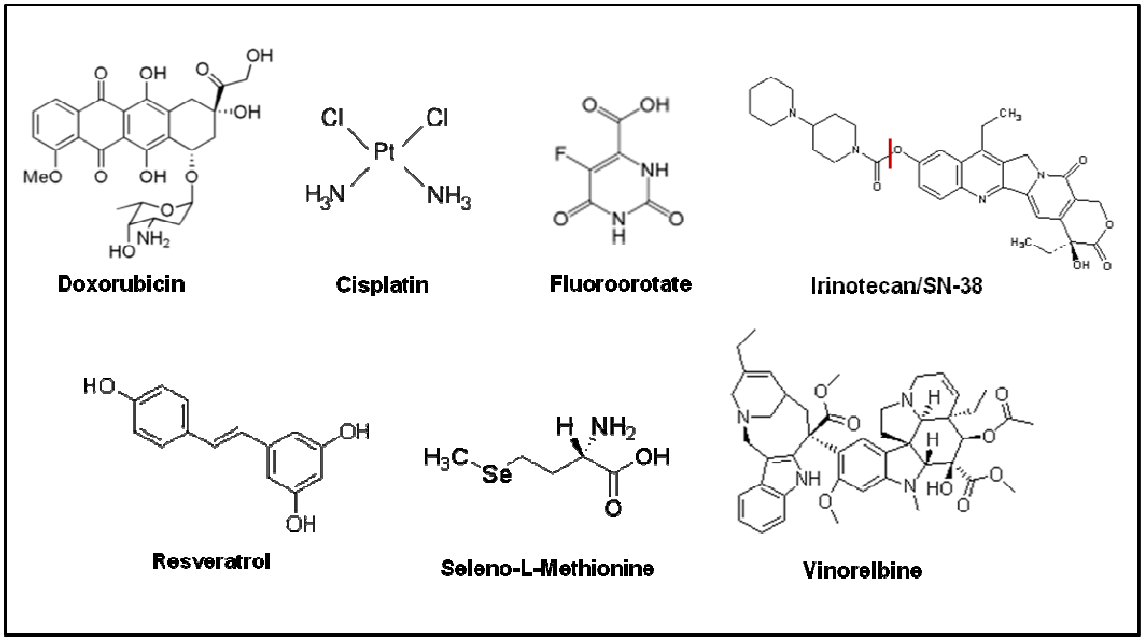

Figure 2.1 Drugs evaluated in *in vitro* screen for synergism in KB cells

Table 2.1 Properties of Drugs Selected for *in vitro* Screen in KB cells

Drug	Mechanism of Action	Synergistic Preclinical Combinations	Clinical Combinations	Cancer Types	Liposome Formulation?
Doxorubicin	topoisomerase II inhibitor	w/ cisplatin, w/ irinotecan	ABVD[1], CHOP[2], FAC[3]	breast, ovarian, lung, bladder, Hodgkin's disease, non-Hodgkin's lymphoma, sarcoma	Yes
Cisplatin	alkylating agent	w/ doxorubcin, w/ irinotecan, w/ fluoropyrimidines	w/topotecan, w/paclitaxel	testicular, ovarian, bladder, lung, esophagus, stomach	Yes
Fluoroorotate	antimetabolite; fluorouracil derivative	ND	ND	ND	Yes
Irinotecan	topoisomerase I inhibitor	w/ doxorubcin, w/ cisplatin, w/ fluoropymidines	FOLFIRI[4]	colorectal	Yes
Resveratrol	antioxidant	w/ doxorubicin, w/ cisplatin	ND	ND	Yes
Seleno-l-Methionine	antioxidant	w/ irinotecan, w/ cisplatin, w/ doxorubcin, w/ fluoropyrimidines	ND	ND	No
SN-38	topoisomerase I inhibitor; Irinotecan metabolite	w/ alkylating agent	ND	colorectal	Yes
Vinorelbine	antimototic agent	w/ cisplatin, w/ fluoropyrimidines, w/ doxorubicin	w/cisplatin	breast, non-small cell lung	Yes

[1] ABVD: adriamycin (doxorubicin) + bleomycin + vinblastine + decarbazine
[2] CHOP: cyclophosphamide + adriamycin + vincristine + prednisone
[3] FAC: 5-fluorouracil + adriamycin + cyclophosphamide
[4] FOLFIRI: 5-fluorouracil + leucovorin + irinotecan
* ND: not determined

Select drug pairs were screened for *in vitro* synergism in KB human nasopharyngeal epidermal carcinoma cells, a well studied tumor cell line that over-expresses the folate receptor and forms solid tumors in mice. Notably, we tested the synergism of the combinations due to simultaneous incubation rather than sequential addition on cells since the ultimate goal is to deliver two drugs simultaneously via liposomes. Furthermore, we tested the combinations at fixed molar ratios between 10:1 – 1:10 because we believe that stable encapsulation of two drugs can be achieved at this ratio range. The cytotoxic effects obtained with the different combinations were analyzed according to the median effect principle [15], a widely used method for evaluating drug interactions. The results of this screen are shown and discussed in this chapter.

2.3 Methods

2.3.1 Materials

Doxorubicin-HCl was purchased from LGM Pharmaceuticals (Boca Raton, FL). 5-fluoroorotic acid was purchased from Research Products International (Mt. Prospect, Illinois). Irinotecan-HCL Trihydrate and SN-38 were purchased from Ivy Fine Chemicals (Cherry Hill, NJ). Cisplatin, resveratrol, seleno-L-methionine, sulforhodamine B, and vinorelbine were purchased from Sigma-Aldrich (St. Louis, MO). KB cells were purchased from University of California, San Francisco Cell Culture Facility. Folate-free RPMI 1640 media was purchased from Invitrogen (Carlsbad, CA).

2.3.2 Cell Culture

KB cells were maintained in folate-free RPMI 1640 media supplemented with 10% fetal calf serum which provides the only source of folic acid. The cells were cultured as a monolayer in 5% CO_2 at 37 °C.

2.3.3 Cytotoxicity Assay

KB cells were seeded in 96 well plates and incubated for 24 hr at 37 °C to allow for cell attachment. Single drug or a pair of drugs in a fixed ratio (10:1, 5:1, 1:1, 1:5, and 1:10) were simultaneously added to each well at eight different doses that capture the full range of cytotoxic effects of the drug(s). The cells were continuously exposed to the drug(s) for 72 hr at 37 °C. Each concentration was tested in triplicate per plate. Cytotoxicity was evaluated using the sulforhodamine B (SRB) assay as previously described [85]. The cells were fixed with 50% trichloroacetic acid, and then stained for 30 min with 0.4% SRB in 1% acetic acid (w/v). Next, the protein bound dye was solubilized by 10 mM unbuffered Tris base, and the absorbance of each well was read at 564 nm. The effect for each dose was normalized to the untreated controls. Finally, dose-effect curves consisting of eight data points were generated for each drug alone and their combinations.

2.3.4 Evaluating Synergy

To determine whether the drug combinations are synergistic, additive or antagonistic, we utilized the median effect method developed by Chou and Talalay [1, 2, 17]. The median effect equation is derived from the law of mass action and describes the relationship between dose and effect. It is a unified theory of the Michaelis-Menten equation of enzyme kinetics, the Hill equation for higher-order ligand binding saturation, and the Scatchard equation for receptor binding [1]. The median effect equation states that the dose-effect relationship for a single drug is:

$$\frac{f_a}{f_u} = \left[\frac{D}{D_m}\right]^m, \qquad [1]$$

where D is dose, D_m is the median effect dose (i.e. EC_{50}), f_a is the fraction affected by D, f_u is the fraction unaffected by D, and m represents the shape of the dose-effect curve. For a two drug combination, the multiple drug-effect equation is:

$$\left[\frac{(f_a)_{A,B}}{(f_u)_{A,B}}\right]^{1/m} = \frac{D_A}{(D_m)_A} + \frac{D_B}{(D_m)_B} \quad , \qquad [2]$$

where D_A and D_B are the respective doses of Drug A and Drug B in the mixture, $(D_m)_A$ and $(D_m)_B$ are the respective EC_{50}s of each drug alone, $(f_a)_{A,B}$ is the fraction affected by the mixture, and $(f_u)_{A,B}$ is the fraction unaffected by the mixture. The most useful aspect of median effect method is that Eq. 2 gives rise to the combination index (CI), a term that quantitatively describes the degree of a drug interaction. The CI equation is:

$$CI_x = \frac{D_A}{(D_x)_A} + \frac{D_B}{(D_x)_B} \quad , \qquad [3]$$

where CI_x is the combination index at **x** effect (i.e. at $x = EC_{50}$ or $x = EC_{75}$), D_A and D_B are the respective doses of Drug A and Drug B in mixture that produce **x** effect, and $(D_x)_A$ and $(D_x)_B$ are the respective doses of Drug A alone and Drug B alone that produce **x** effect. Synergism is indicated for CI < 1, additivity for CI = 1, and antagonism for CI >1.

For all the drug combinations, the dose-effect data – in the form of fraction of affected (f_a) cells as a function of concentration – for Drug A alone, Drug B alone, and a fixed ratio of Drug A+B were fitted to Eq. 3 to analyze the drug interactions. CalcuSyn software (Biosoft, Ferguson, MO), a program based on the median effect principle, was used to automatically simulate the combination index at all dose levels of each drug

combination. All data were fitted to the median effect equation with a linear correlation coefficient of $r > 0.95$.

2.4 Results

The results of the *in vitro* screen for synergism in KB cells are shown in Tables 2.2-2.6. The combination index values at the EC_{50}, EC_{75}, and EC_{90} are shown for the five molar ratios of each drug pair tested. Synergistic combinations ($CI < 0.9$) are shown in green, additive combinations ($0.9 < CI < 1.1$) are shown in yellow, and antagonistic combinations ($CI > 1.1$) are shown in red.

Table 2.2 Summary of Primary Screen in KB Cells

Drug Combinations	Ratios	Combination Index		
		EC_{50}	EC_{75}	EC_{90}
Irinotecan + 5-Fluoroorotate	10:1	1.3	0.87	0.61
	5:1	1.2	0.91	0.70
	1:1	0.95	0.75	0.61
	1:5	0.85	0.77	0.76
	1:10	0.83	0.93	1.2
Irinotecan + Cisplatin	10:1	2.3	2.8	3.4
	5:1	1.5	1.6	1.7
	1:1	1.1	1.4	1.7
	1:5	1.4	1.1	0.84
	1:10	2.0	2.2	2.4
Doxorubicin + Irinotecan	10:1	2.6	2.2	2.0
	5:1	2.3	2.0	1.8
	1:1	1.3	1.3	1.4
	1:5	1.8	1.9	2.0
	1:10	2.4	2.3	2.3
Doxorubicin + Cisplatin	10:1	0.96	1.5	2.4
	5:1	1.4	1.2	1.1
	1:1	0.72	1.0	1.4
	1:5	0.88	0.78	0.70
	1:10	1.2	0.90	0.67

* Combination Index is a quantity derived from the median effect equation that describes the degree of a drug interaction. Synergism is indicated for $CI < 0.9$ **(Green)**, additivity for $0.9 < CI < 1.1$ **(Yellow)**, and antagonism for $CI > 1.1$ **(Red).**

Table 2.3 Summary of SN-38 Combination Activity in KB Cells

Drug Combinations	Ratios	Combination Index*		
		EC_{50}	EC_{75}	EC_{90}
SN-38 + Fluoroorotate	10:1	1.3	0.97	0.71
	5:1	0.36	1.1	3.2
	1:1	1.0	3.9	14.7
	1:5	1.1	0.91	0.77
	1:10	0.45	1.9	7.7
SN-38 + Cisplatin	10:1	0.53	1.8	6.2
	5:1	1.3	1.5	1.7
	1:1	1.2	1.4	1.7
	1:5	0.87	2.1	6.4
	1:10	0.48	0.87	2.3
SN-38 + Doxorubicin	10:1	2.3	3.4	5.2
	5:1	2.7	2.1	1.7
	1:1	2.6	1.5	0.96
	1:5	2.2	1.5	1.2
	1:10	1.8	1.4	1.9

Table 2.4 Summary of Vinorelbine Combination Activity in KB Cells

Drug Combinations	Ratios	Combination Index*		
		EC_{50}	EC_{75}	EC_{90}
Vinorelbine + Fluoroorotate	10:1	0.66	0.9	1.2
	5:1	0.56	0.89	1.4
	1:1	0.92	0.98	1.0
	1:5	0.70	0.92	1.2
	1:10	0.75	1.3	2.2
Vinorelbine + Doxorubicin	10:1	1.3	4.2	13
	5:1	1.2	1.2	1.2
	1:1	1.6	3.5	7.7
	1:5	1.9	3.7	7.2
	1:10	1.7	2.4	3.3
Vinorelbine + Cisplatin	10:1	0.68	0.91	1.2
	5:1	0.92	0.83	0.75
	1:1	0.93	0.76	0.63
	1:5	0.83	1.5	2.6
	1:10	1.1	1.4	2.0

* Combination Index is a quantity derived from the median effect equation that describes the degree of a drug interaction. Synergism is indicated for CI < 0.9 **(Green)**, additivity for 0.9 < CI < 1.1 **(Yellow)**, and antagonism for CI > 1.1 **(Red).**

Table 2.5 Summary of Resveratrol Combination Activity in KB Cells

Drug Combinations	Ratios	Combination Index*		
		EC_{50}	EC_{75}	EC_{90}
Doxorubicin + Resveratrol	10:1	1.1	0.93	0.75
	5:1	1.4	1.0	0.77
	1:1	1.4	1.03	0.77
	1:5	1.3	0.98	0.72
	1:10	1.4	1.1	0.86
Fluoroorotate + Resveratrol	10:1	0.89	1.5	3.3
	5:1	1.2	1.6	2.9
	1:1	1.0	1.6	3.7
	1:5	1.1	1.1	1.3
	1:10	1.0	1.0	1.1
Cisplatin + Resveratrol	10:1	0.93	1.0	1.2
	5:1	0.80	0.97	1.2
	1:1	1.1	1.1	1.2
	1:5	1.4	1.9	2.6
	1:10	1.6	2.1	2.7

Table 2.6 Summary of Seleno-L-Methionine Combination Activity in KB Cells

Drug Combinations	Ratios	Combination Index*		
		EC_{50}	EC_{75}	EC_{90}
Fluoroorotate + Seleno-l-Methionine	10:1	0.93	1.1	1.3
	5:1	0.98	1.2	1.5
	1:1	0.82	1.1	1.2
	1:5	0.62	0.76	0.98
	1:10	0.79	0.88	1.0
Doxorubicin + Seleno-l-Methionine	10:1	1.1	0.79	0.56
	5:1	1.5	1.5	1.5
	1:1	1.0	0.7	0.47
	1:5	0.95	0.95	0.94
	1:10	1.0	1.2	1.4
Irinotecan + Seleno-l-Methionine	10:1	1.0	0.93	0.84
	5:1	0.99	0.92	0.85
	1:1	0.99	0.92	0.87
	1:5	0.95	0.87	0.8
	1:10	0.74	0.94	1.2
Cisplatin + Seleno-l-Methionine	10:1	1.0	1.1	1.1
	5:1	1.3	1.3	1.2
	1:1	1.1	1.0	0.93
	1:5	1.1	1.1	0.98
	1:10	1.0	1.2	1.3

* Combination Index is a quantity derived from the median effect equation that describes the degree of a drug interaction. Synergism is indicated for CI < 0.9 **(Green)**, additivity for 0.9 < CI < 1.1 **(Yellow)**, and antagonism for CI > 1.1 **(Red).**

In the primary screen (Table 2.2), we observed drug synergy for irinotecan + fluoroorotate, irinotecan + cisplatin, and doxorubicin + cisplatin. For irinotecan + fluoroorotate, synergy occurred at 1:5 ratio at EC_{50}-EC_{90} doses, the 10:1 and 1:1 ratios at EC_{75}-EC_{90} doses, the 1:10 ratio at the EC_{50} dose, and 1:5 ratio at the EC_{90} dose. For irinotecan + cisplatin, we found that synergism occurred only at the 1:5 ratio at the EC_{90} dose. Finally, doxorubicin + cisplatin exhibited synergy at the 1:1 ratio at the EC50 dose, the 1:5 ratio at EC_{50}-EC_{90} doses, and the 1:10 ratio at the EC_{90} dose.

From the SN-38 combinations shown in Table 2.3, it was seen that SN-38 + fluoroorotate were synergistic at the 10:1 and 1:5 ratios at the EC_{90} dose, and the 5:1 and 1:10 ratios at the EC_{50} dose. Additionally, SN-38 + cisplatin were synergistic at the 1:5 ratio at the EC_{50} dose and the 1:10 ratio at EC_{75}-EC_{90} doses.

In the screen of vinorelbine combinations (Table 2.4), we observed that vinorelbine + doxorubicin were synergistic at all ratios at the EC_{50} dose only. Vinorelbine + cisplatin also displayed synergism at the 10:1 and 1:5 ratios at the EC_{50} dose, and at the 5:1 and 1:1 ratios at the EC_{75}-EC_{90} doses.

Table 2.5 demonstrates that doxorubicin + resveratrol were synergistic at all ratios at the EC_{90} doses only. However, fluoroorotate + resveratrol were only synergistic at the 5:1 ratio at the EC_{50} dose.

In the seleno-L-methionine combinations (Table 2.6), fluoroorotate + seleno-L-methionine were synergistic at the 1:1 ratio at the EC_{50} dose only, and at the 1:5 and 1:10 ratios at the EC_{50}-EC_{75} doses. Doxorubicin + seleno-L-methionine were synergistic at the 10:1 and 1:1 ratios at EC_{75}-EC_{90} doses. Finally, irinotecan + seleno-L-methionine were

synergistic at the 10:1, 5:1 and 1:1 ratios at the EC_{90} dose, as well as the 1:5 ratio at the EC_{75}-EC_{90} doses, and the 1:10 ratio at the EC_{50} dose.

The irinotecan + fluoroorotate combination was the most synergistic pair because this pair exhibited synergism at the widest range of ratios and concentrations.

2.5 Discussion

The goal of this screen was to identify compounds that exhibited synergistic cytotoxic effects on KB cancer cells. What is evident from the data is that irinotecan + fluoroorotate was the most synergistic combination because these drugs exhibited synergism at a wide range of ratios and concentrations. This result is not surprising since irinotecan + fluorouracil is clinically used to treat colorectal cancer. Thus, this is the combination that we decided to use for further studies. Interestingly, most of the combinations in this screen were more additive or antagonistic than synergistic in the KB cells. Therefore, one cannot assume that two drugs will be synergistic without testing the combination under their assay conditions (i.e. cell line, time course, cytotoxicity assay) and analyzing the data with a robust synergy model.

As can be discerned from the data, the type of drug interaction is dependent on the ratio and the concentration of the combined drugs. For example, irinotecan + fluoroorotate at the 10:1 molar ratio are antagonistic at the EC_{50} dose but are synergistic at the EC_{75} and the EC_{90} doses at this same ratio. However, this combination is synergistic at the 1:5 molar ratio at EC_{50}-EC_{90} doses. This phenomenon of ratio and dose dependent synergy was observed for every combination in our screen and has been discussed in the literature as well [33].

Since the type of interaction is dependent on the ratio and concentration of the combined drugs, we believe that it is crucial to control the ratio and dose to maximize the therapeutic effect. In the following chapters, we designed novel, non-targeted and folate targeted liposome formulations consisting of irinotecan and fluoroorotate alone or in a synergistic combination to further examine this hypothesis.

CHAPTER 3:
Development and Evaluation of Non-Targeted Liposomal Formulations of Irinotecan, Fluoroorotate, and Their Combination

3.1 Abstract

We have created a liposome formulation that co-encapsulates the synergistic drug combination, irinotecan (IRN) and fluoroorotic acid (FOA). The formulation is used to test the hypothesis that liposomes can enhance the *in vivo* anti-tumor efficacy of synergistic drug combinations. Non-targeted liposome (NTL) formulations of IRN and FOA alone and in combination were developed and evaluated in various mouse models. A variety of protocols were examined to remote load IRN into liposomes. The charged molecule 1,2,3,4-butanetetratcarboxylic acid, when encapsulated in the liposome, provided the best IRN encapsulation efficiency. To confirm that the new IRN loading procedure resulted in a formulation that was active, we treated Balb/c nu/nu mice bearing HT29 human colorectal tumors with NTL-IRN at 50 mg/kg. This dose had previously been shown to be active in a different liposome formulation. The NTL-IRN formulation had significantly more tumor growth inhibition ($p < 0.05$) and a higher survival rate than mice receiving free IRN 50 mg/kg in the HT29 model. Due to the low aqueous solubility of FOA, it was also necessary to devise an improved method to formulate NTL-FOA. Passively loading NTLs with 500 mM Li-FOA or TEA-FOA in 7 M urea provided a high concentration of FOA in liposomes. The maximum tolerated doses for FOA and NTL-FOA were established in Balb/c and Balb/c nu/nu mice. IRN and FOA have disparate physiochemical properties and have not previously been co-formulated in liposomes. We

varied the drug/lipid ratio, loading temperature and loading time to find the highest IRN + FOA co-encapsulation content. Modulating these parameters allowed for a consistent co-encapsulation of IRN + FOA at various molar ratios.

The antitumor activity of NTL-IRN, NTL-FOA, NTL-IRN-FOA at the 1:5 synergistic ratio, and the NTL-IRN + NTL-FOA mixture at the 1:5 molar ratio were examined in the C26 colorectal cancer mouse model. The most potent formulation was NTL-FOA. A single dose of the combinations exhibited a modest tumor suppressive effect. Two doses of the NTL-IRN + NTL-FOA 1:5 combination, which had the same total amount of FOA as the NTL-FOA and $1/7^{th}$ of the dose of the NTL-IRN formulation, provided a slightly lower tumor suppressive effect than NTL-FOA. Thus, liposomes prepared at a drug ratio that was synergistic in cell culture on the C26 colon carcinoma did not display synergism in the C26 tumor model. These studies point out the challenges to design synergistic treatment protocols based upon results from *in vitro* cytotoxicity studies.

3.2 Introduction

Irinotecan (IRN) and fluoropyrimidines are widely used for the treatment of colorectal cancer because of the enhanced tumor killing effect exerted by this combination. It has been shown that IRN and fluoropyrimidines can be synergistic [57, 62, 86]. Although the exact mechanism of synergism is not clearly understood, it is believed that IRN recruits cells in S phase that allows increased fluoropyrimidine incorporation into DNA and induces apoptosis [27, 57, 86]. Recently, it has been reported that the activity of IRN and fluoropyrimidines can be enhanced via liposome delivery [27, 34, 35, 37]. Therefore, we investigated the use of liposome drug delivery vehicles to

deliver IRN and fluoroorotic acid (FOA), an analog of fluorouracil that is able to be encapsulated into liposomes [79, 80, 87]. This chapter focuses on the work completed to develop effective liposomal formulations encapsulating IRN alone, FOA alone, and IRN + FOA at synergistic molar ratios in order to test to test the hypothesis that liposomes can enhance the *in vivo* efficacy of synergistic combinations.

3.3 Methods

3.3.1 Materials

5-Fluoroorotic acid (FOA) was purchased from Research Products International (Mt. Prospect, Illinois). Irinotecan-HCl Trihydrate (IRN) was purchased from Ivy Fine Chemicals (Cherry Hill, NJ). 1,2,3,4-Butanetetracarboxylic acid (BTCA), cholesterol (Chol) and sulforhodamine B (SRB) were purchased from Sigma-Aldrich (St. Louis, MO). Distearoylphosphatidylcholine (DSPC) and methoxy-polyethylene glycol (MW2000)-DSPE (mPEG2000-DSPE) were products from Genzyme (Cambridge, MA). C26 and HT29 cells were purchased from University of California, San Francisco Cell Culture Facility.

3.3.2 Cell Culture

C26 murine colorectal cancer cells were maintained in RPMI 1640 media supplemented with 10% fetal calf serum. HT29 human colorectal cancer cells were maintained in McCoy's 5A media supplemented with 10% fetal calf serum. The cells were cultured as a monolayer in 5% CO_2 at 37 °C.

3.3.3 Cytotoxicity Assay

C26 cells were seeded in 96 well plates and incubated for 24 hr at 37 °C to allow for cell attachment. IRN+FOA in a fixed ratio (10:1, 5:1, 1:1, 1:5, and 1:10) were

simultaneously added to cells at eight doses that capture the full range of cytotoxicity of the most potent drug. The cells were continuously exposed to the single drugs and pairs of drugs for 72 hr at 37 °C. Each concentration was tested in triplicate per plate. Cytotoxicity was evaluated using the sulforhodamine B assay (SRB) assay [85]. Briefly, the cells were fixed with 50% trichloroacetic acid and stained for 30 min with 0.4% SRB in 1% acetic acid (w/v). Then, the protein bound dye was solubilized with 10 mM unbuffered Tris base, and the absorbance of each well was measured at 564 nm.

3.3.4 Drug Interaction Analysis

Dose-effect curves consisting of eight data points were generated for each drug alone and in the combinations. The effect for each concentration was normalized to the untreated controls as a percent of cell survival and then converted to fraction of affected cells. CalcuSyn software (Biosoft, Ferguson, MO) was used to analyze the drug interaction between IRN and FOA. This program uses the median effect principle determine the combination index (CI) that quantitatively describes the degree of synergism or antagonism of a drug interaction [1, 15]. Synergism is indicated for $CI < 1$, additivity for $CI = 1$, and antagonism for $CI > 1$.

3.3.5 Preparing Liposomal IRN

Non-targeted liposomes (NTLs) were composed of DSPC:Chol:mPEG-DSPE at a 55:40:5 molar ratio. Lipid mixtures were dissolved in chloroform and dried into a thin film by rotary evaporation under reduced pressure then placed under high vacuum overnight. The films were subsequently hydrated with either 300 mM BTCA (adjusted to pH 5.0 with NH_4OH), 250 mM ammonium sulfate, or 650 mM phytic acid (adjusted to pH 6.0 with triethylamine) at 65 °C and vortexed to obtain a lipid concentration of 100

mM. The liposomes were then sonicated at 65 °C and extruded through 200 nm and 100 nm polycarbonate membranes (Avestin, Ottawa, CA) at 65 °C. The liposomes were exchanged into 5 mM Hepes, 5% Dextrose pH 6.5 by size exclusion chromatography using a Sephadex G25 column. IRN was loaded by incubating the drug with liposomes (0.2/1 drug to lipid molar ratio) at 65°C for 1 hr. The liposome preparation was exchanged into Hepes Buffer (5 mM Hepes, 140 mM NaCl pH 7.4) by size exclusion chromatography using a Sephadex G25 column. To measure the encapsulated IRN concentration, an aliquot of liposomes was mixed with 1% Triton X-100, heated to 100°C until the cloud point was reached, and cooled down room temperature. The encapsulated IRN concentration was determined by comparing the absorbance at 370 nm to an IRN standard curve in the appropriate buffer. The liposome diameter and particle size distribution were measured by dynamic light scattering (Malvern Instruments, Westborough, MA). The average liposome diameter was ~100 nm. For comparison, NTL-IRN was also prepared according to previously described methods [20, 88, 89].

3.3.6 Preparing Liposomal FOA

The same lipid mixture was used for FOA encapsulation and was processed as described above. The films were subsequently hydrated with 500 mM FOA in 7 M urea (adjusted to pH 7 with triethylamine or LiOH) at 65 °C and vortexed to obtain a lipid concentration of 50 mM. The multilamellar vesicles were then sonicated at 65 °C. The preparation was added to a dialysis cassette (10,000 MWCO) and dialyzed against 500 mL of 5 mM Hepes, 5% Glucose pH 7.4. For comparison, FOA was passively loaded into NTLs following the method of Heath and coworkers [80].

A previously reported method for remote loading weak acids was also investigated [90]. Non-targeted liposomes (NTLs) were composed of DSPC:DSPG:Chol at a 55:5:40 molar ratio and processed as described above. The lipid mixture was hydrated with 150 mM calcium acetate pH 7.7 or 150 mM zinc acetate pH 6.6 at 65 °C and vortexed to obtain a lipid concentration of 50 mM. Then the mixture was sonicated at 65 °C and exchanged into 10% sucrose by size exclusion chromatography using a Sephadex G25 column. FOA was incubated with liposomes (at 0.1/1 and 0.2/1 drug to lipid molar ratios) at 65 °C for 1 hr. The liposome preparation was exchanged into 10% sucrose by size exclusion chromatography using a Sephadex G25 column. In another case, the lipid mixture was hydrated with 100 mM zinc acetate pH 6 at 65 °C and vortexed to obtain a lipid concentration of 50 mM. Then the mixture was sonicated at 65 °C and exchanged into 100 mM sodium sulfate pH 6 by size exclusion chromatography using a Sephadex G25 column. FOA was incubated with liposomes (at 0.1/1, 0.2/1, 0.3/1, and 1/1 drug to lipid molar ratios) at 70°C for 15 hr. The liposome preparation was exchanged into Hepes buffer (5 mM Hepes, 140 mM NaCl pH 7.4) by size exclusion chromatography using a Sephadex G25 column.

To assay for the encapsulated FOA concentration, an aliquot of liposomes from all preparations were diluted with phosphate buffered saline (PBS; 2.16 g/L Na_2HPO_4 $7H_20$, 0.2 g/L KH_2PO_4, 0.2 g/L KCl, 8.0 g/L NaCl) and mixed with methanol:chloroform (1:1:1 v/v/v), vortexed, and centrifuged at 1,000 rpm for 10 min. Then the upper phase was mixed with 1M HCl. The encapsulated FOA concentration was determined by comparing the absorbance at 284 nm to a standard curve prepared with a solution from a

blank lipid extraction. The liposome diameter and particle size distribution were measured by dynamic light scattering. The average liposome diameter was ~120 nm.

3.3.7 Liposome Co-encapsulation of IRN and FOA

The same lipid mixture was processed into thin films as outlined above. The lipid films were subsequently hydrated with 500 mM FOA in 7 M urea (adjusted to pH 7 with triethylamine) at 65 °C and vortexed to obtain a lipid concentration of 25 mM. The resulting multilamellar vesicles were then sonicated at 65 °C. The preparations were added to a dialysis cassette (10,000 MWCO) and dialyzed against 500 ml of 5 mM Hepes, 5% glucose pH 6.5. To load IRN into the FOA containing liposomes and achieve an encapsulated IRN:FOA 1:5 molar ratio, IRN was incubated with the liposomes at drug/lipid molar ratios ranging from 0.025/1 to 0.3/1, at loading temperatures of 40, 45, 50, or 60 °C and for incubation periods of 10, 30 or 60 min. The liposome preparations were exchanged into Hepes buffer (5 mM Hepes, 140 mM NaCl pH 7.4) by size exclusion chromatography using a Sephadex G25 column. To assay the drug content of the liposomes, an aliquot was mixed with 1% Triton X-100, heated to 100°C until the cloud point was reached, and then cooled down room temperature. The encapsulated IRN concentration was determined by comparing the absorbance at 370 nm to a standard curve. A second sample was diluted with PBS and mixed with methanol:chloroform (1:1:1 v/v/v), vortexed, and centrifuged at 1000 rpm for 10 min. Then the upper phase was mixed with 1M HCl. The encapsulated FOA concentration was determined by 1) calculating the absorbance due to FOA in the co-formulation at 284 nm according to the equation $(A284)_{FOA} = (A284)_{FOA+IRN} - R(A284)_{IRN}$ where R = [IRN Dilution Factor / FOA Dilution Factor] and 2) comparing $(A284)_{FOA}$ to a standard curve. The liposome

diameter and particle size distribution were measured by dynamic light scattering. The average liposome diameter was ~120 nm.

3.3.8 Animals

Eight to ten week old athymic nu/nu mice (for HT29 model), Balb/c mice (for C26 model and maximum tolerated dose studies), and Balb/c nu/nu mice (for maximum tolerated dose studies) were obtained from Simonsen Laboratories, Inc. (Gilroy, CA). Animal maintenance and experiments adhered to the NIH principles of laboratory animal care under a protocol approved by the Committee on Animal Research at the University of California, San Francisco.

3.3.9 NTL-IRN Chemotherapy in HT29 Mouse Model

HT29 human colorectal cells ($5x10^6$), suspended in 50 μL medium, were inoculated subcutaneously in the right hind flank of each athymic nu/nu mouse. On Day 8 after tumor implantation, mice were randomly distributed into treatment groups (n = 8). NTL-IRN was prepared by hydrating lipid films with 300 mM BTCA (adjusted to pH 5.0 with NH_4OH) and incubating IRN with liposomes (0.2/1 drug to lipid molar ratio) at 65°C for 1 hr as described above. Each treatment (~200 μL) was administered by tail vein injection on Days 12, 14, 19, and 21. Mouse tumor growth, weight, and overall health were monitored on alternate days. Tumor volume was determined by measuring the tumor in two dimensions with calipers and calculated using the formula: tumor volume = ½ (length x $width^2$). The percent tumor growth delay (%TGD) was calculated from the equation %TGD = (T-C)/C x 100, where T is the mean time for the tumor volume of a treatment group to reach a designated volume of 300 mm^3 and C is the mean time of the control group to reach the designated volume of 300 mm^3. Mice were

sacrificed due to tumor burden (volume ≥ 2000 mm^3) or decrease in body weight (>20% loss). Mouse survival was analyzed by using MedCalc 8.2.1.0 for Windows (MedCalc Software, Mariakerke, Belgium).

3.3.10 FOA and NTL-FOA MTD Studies in Balb/c and Balb/c nu/nu Mice

A solution of free FOA was made by dissolving the drug in 50 mM MOPS+50 mM LiCl (pH adjusted to 7.4 with LiOH). NTL-FOA was prepared by hydrating liposomes with 500 mM FOA in 7 M urea (adjusted to pH 7 with triethylamine) as described above. In the first maximum tolerated dose (MTD) study, Balb/c mice and Balb/c nu/nu (n=2 mice/group/strain) were administered a single intravenous injection of FOA 100 mg/kg or NTL-FOA 10 mg/kg on Day 0. In another arm of the study, Balb/c mice and Balb/c nu/nu (n=2 mice/group/strain) were administered FOA 100 mg/kg or NTL-FOA 10 mg/kg by intravenous injections on a q4d schedule starting on Day 0. In a second MTD study, Balb/c mice (n=2 mice/group) were administered FOA 100 mg/kg by intravenous injections on a q7d schedule starting on Day 0. Mouse weight and overall health were monitored on alternate days. If a mouse's body weight decreased by > 15% of the original weight or if a mouse looked unhealthy, treatments were stopped for the group to which the mouse belonged. Mice were sacrificed due to decrease in body weight > 20% of original weight.

3.3.11 Liposomal IRN+FOA Combination Therapy in C26 Mouse Model

C26 murine colorectal cells ($3x10^5$) suspended in 50 μL RPMI 1640 medium were inoculated subcutaneously in the right hind flank of each Balb/c mouse. On Day 8 after tumor implantation, mice were randomly distributed into treatment groups (n = 8). NTL-IRN-FOA (1:5) was prepared by hydrating liposomes with 500 mM FOA in 7 M

urea (adjusted to pH 7 with triethylamine) and incubating IRN with liposomes (0.025/1 drug to lipid molar ratio) at 50 °C for 10 min as described above. Each treatment (~200 μL) was administered by tail vein injection on Day 8 and Day 15. Mouse tumor growth, weight, and overall heath were monitored on alternate days. Tumor volume was determined by measuring the tumor in three dimensions with calipers and calculated using the formula: tumor volume = length x width x height. Mice were sacrificed due to tumor burden (volume ≥ 2000 mm^3) or decrease in body weight (> 20% loss). Mouse survival was analyzed by using MedCalc 8.2.1.0 for Windows (MedCalc Software, Mariakerke, Belgium).

3.4 Results

3.4.1 Synergism of IRN+FOA

IRN and FOA were screened for synergy in C26 murine colorectal cancer cells at 10:1, 5:1, 1:1, 1:5, and 1:10 molar ratios. Table 3.1 shows the combination index (CI) values at the EC_{50}, EC_{75}, and EC_{90} are shown for the five molar ratios tested. Synergistic combinations (CI < 0.9) are shown in green, additive combinations (0.9 < CI < 1.1) are shown in yellow, and antagonistic combinations (CI > 1.1) are shown in red. This drug combination was very synergistic at the 1:5 molar ratio and slightly synergistic at 10:1 molar ratio over a wide range of concentrations. However, IRN+FOA was mostly antagonistic at the 5:1 and 1:1 molar ratios, and additive at the 10:1 molar ratio. The results show that synergism exhibited by IRN and FOA is ratio-dependent.

Table 3.1 IRN + FOA Combination Activity in C26 Cells

Drug Combination	Ratios	Combination Index*		
		EC50	*EC75*	*EC90*
Irinotecan + Fluoroorotate	**10:1**	**1.1**	**0.99**	**0.89**
	5:1	**1.3**	**1.2**	**1.2**
	1:1	**1.3**	**1.2**	**1.1**
	1:5	**0.20**	**0.16**	**0.13**
	1:10	**0.89**	**0.88**	**0.88**

* Combination Index is a quantity derived from the median effect equation that describes the degree of a drug interaction. Synergism is indicated for CI < 0.9 **(Green)**, additivity for 0.9 < CI < 1.1 **(Yellow)**, and antagonism for CI > 1.1 **(Red).**

To maximize the therapy of this combination, the synergistic ratio must be maintained *in vivo.* We believe that delivering IRN and FOA in liposomes will enhance the efficacy of the combination by delivering the drugs at their synergistic ratios to tumor cells. Therefore, we proceeded to develop individual liposome formulations of each drug and a liposome formulation of the drugs together in order to examine this hypothesis.

3.4.2 Development of NTL-IRN Formulation

There are several published methods for formulating liposomal irinotecan by remote loading, which is a technique used to encapsulate drugs into preformed liposomes via a transmembrane ion or pH gradient [20, 88, 89]. This strategy allows high encapsulation efficiency and stable retention of drug within liposomes, both of which are essential for effective delivery and therapy [23]. We prepared NTL-IRN using these different published methods, but we were not able to achieve the reported high encapsulation efficiencies. We also tried using ammonium sulfate (250 mM) or TEA-phytic acid (650 mM) as trapping agents, but only were able to obtain encapsulation efficiencies of 55 and 45 %, respectively.

Encapsulating IRN in NTLs containing 1,2,3,4-butanetetracarboxylic acid (BTCA) resulted in greater than 90% encapsulation efficiency of IRN. Figure 3.1 depicts the proposed mechanism of IRN encapsulation with BTCA as the trapping agent. We

believe that during the remote loading process, ammonia present in the liposome aqueous compartment partitions out of the liposome interior down its concentration gradient. This causes a transmembrane pH gradient across the liposome bilayer (high [H+] in the interior, low [H+] in the exterior). IRN in the external buffer is then able to cross the liposome bilayer and become protonated. Thus, the IRN within the liposomes that is positively charged interacts with the negatively charged BTCA and forms a complex [20, 88].We decided to prepare NTL-IRN with BTCA as the trapping agent method for the rest of the study.

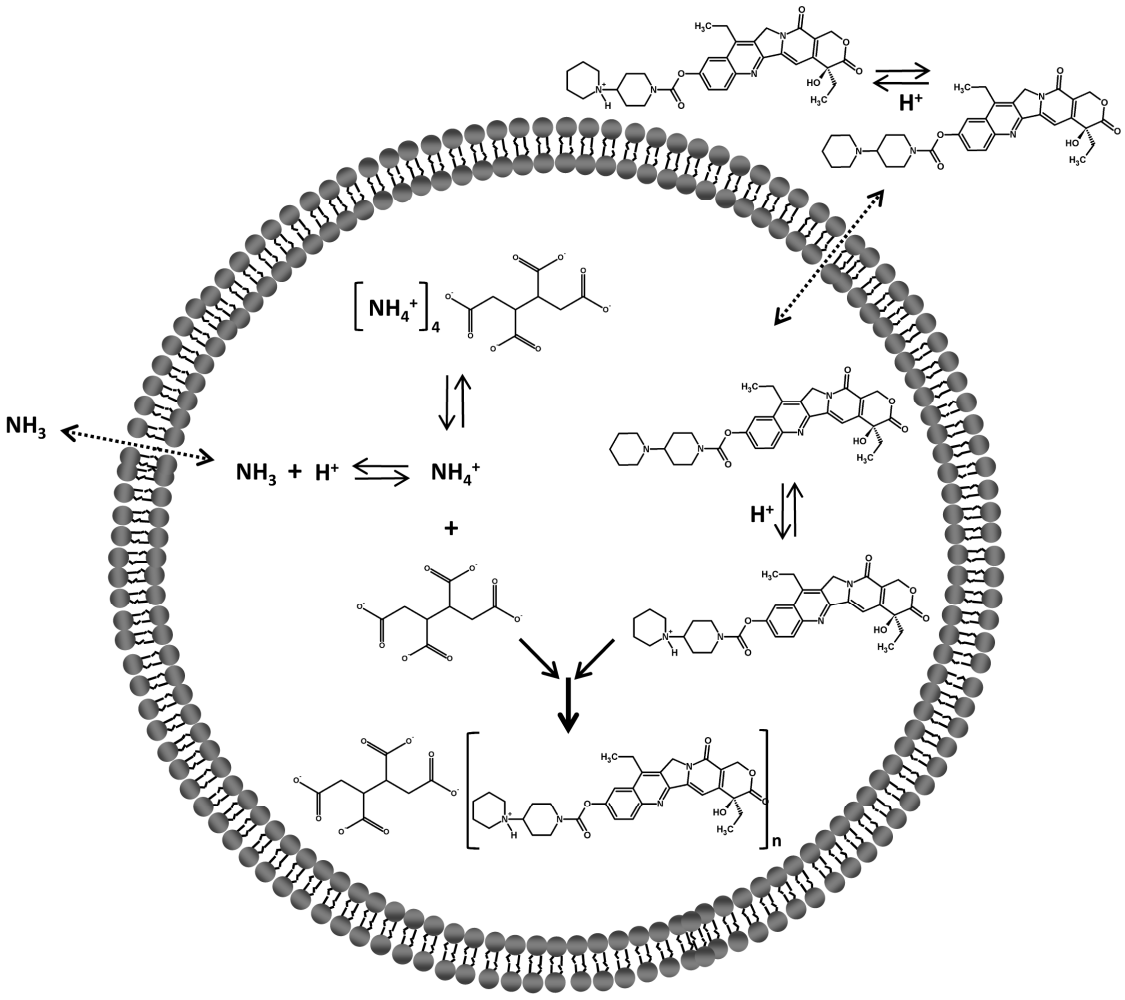

Figure 3.1 Schematic diagram of proposed mechanism of encapsulation of IRN in liposomes. BTCA is the trapping agent.

3.4.3 Therapeutic Efficacy of NTL-IRN in HT29 Tumor Model

To assess the antitumor efficacy of our NTL-IRN, we examined its antitumor activity in HT29 tumor-bearing mice. We administered free IRN and NTL-IRN at a dose of 50 mg/kg intravenously to mice twice per week for a total of four doses. This dose, which is the MTD of free IRN, and the dosing regimen have been established as safe in previous studies [20]. Figure 3.2 shows that NTL-IRN 50 mg/kg had significantly greater tumor growth inhibition than IRN 50 mg/kg ($p<0.05$). In fact, the %TGD of NTL-IRN was 114% whereas the %TGD of IRN was 36%. Also, mice treated with NTL-IRN 50 mg/kg had a slight increase in survival rate than mice treated with free IRN 50 mg/kg (% increase in life span equaling 50% and 29.3% for NTL-IRN and IRN, respectively). This NTL-IRN formulation had similar efficacy as other liposomal IRN formulations evaluated in a HT29 tumor xenograft model [20] .

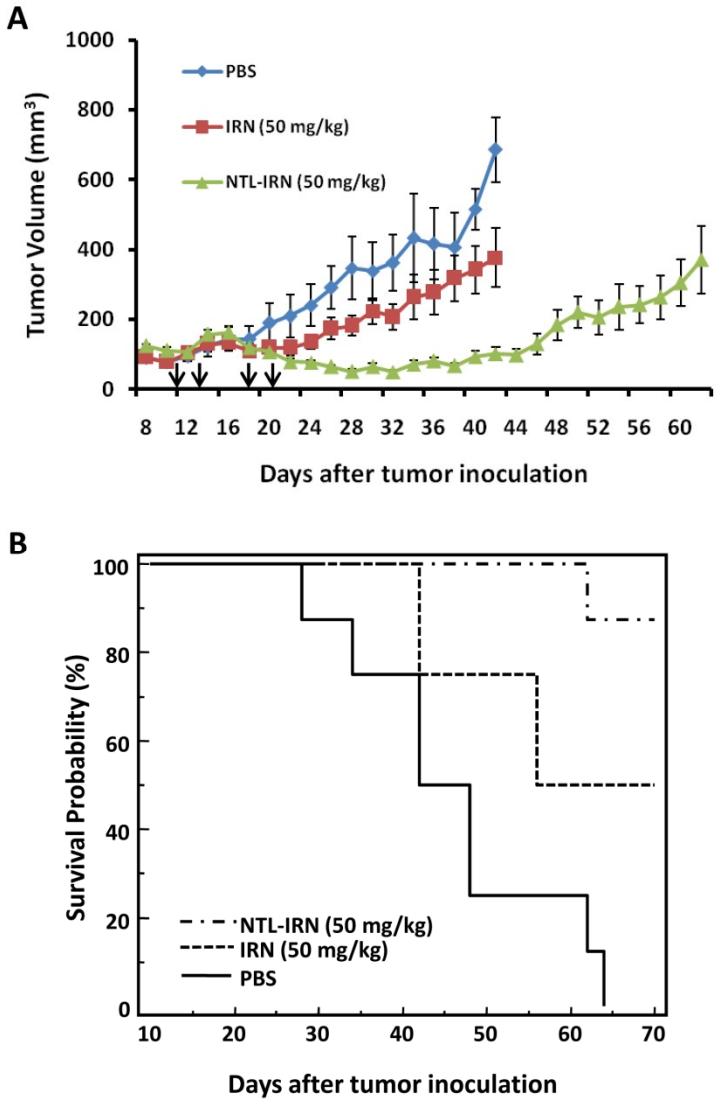

Figure 3.2 Effect of NTL-IRN on tumor growth and survival rate in HT29 tumor-bearing mice. HT29 tumored athymic nu/nu mice (n=8) were administered by i.v. injections on Days 12, 14, 19, and 21 (as indicated by arrows) with PBS, free IRN 50 mg/kg, and NTL-IRN 50 mg.kg. For NTL-IRN formulation, 9.2 µmol of lipid was injected per dose. **A**. Tumor growth inhibition. Error bars represent SEM. The NTL-IRN group had significantly smaller tumors than IRN group ($p<0.05$ Student's t-test) **B**. Survival curves.

As can be observed from Figure 3.3, NTL-IRN did not adversely affect the weight of the mice. This result indicates that at this dose there was no major acute toxicity associated with administering NTL-IRN to the mice.

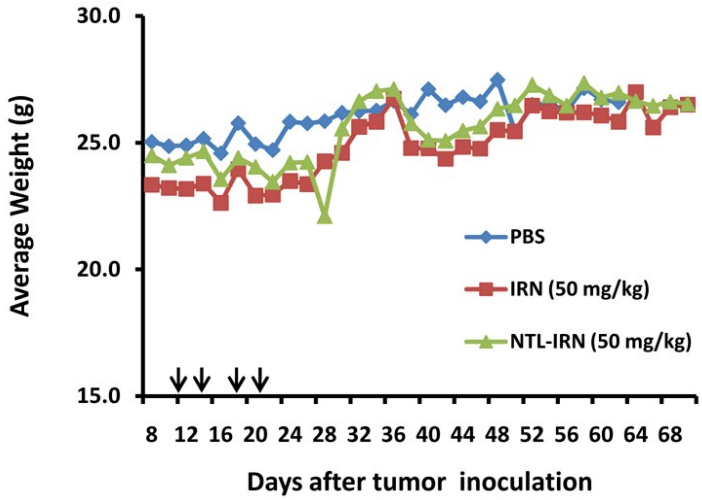

Figure 3.3 Effect of NTL-IRN on weight of HT29 tumor-bearing mice. Arrows indicate treatment days.

3.4.4 Formulation Development of NTL-FOA

FOA is a weak acid and is charged in aqueous solution; thus it is difficult to actively load into pre-formed liposomes. Therefore, we investigated passive loading methods for encapsulating FOA within liposomes. Passive loading is the process of hydrating lipids with an aqueous buffer or a drug-containing solution. Initially, we prepared NTL-FOA using an approach developed by Heath and coworkers [80]. In this method, the lipid films were hydrated with 50 mM FOA solution that resulted in the liposomes encapsulating only 1-3 mM of FOA. This concentration range is low and would require high injection volumes in order to achieve a high drug concentration that might be required for treatment since FOA is only a moderately potent anticancer drug. Therefore, our next attempts focused on ways to increase FOA concentration in liposomes. We decided to increase the solubility of FOA in order to make a more concentrated drug solution for passive loading. We selected the chaotropic agent 7M urea to dissolve FOA and adjusted the pH to 7 with either LiOH or TEA. By this tactic, we were able to obtain as high as 650 mM FOA. This permitted the preparation NTL-FOA formulations encapsulating 4-15 mM FOA by passively loading NTLs with 500 mM of

TEA-FO or Li-FOA. We also investigated remote loading using zinc acetate or calcium acetate [90]; however, we could not encapsulate FOA using these methods.

3.4.5 MTD Analysis of FOA and NTL-FOA in Balb/c and Balb/c nu/nu Mice

The toxicity of free FOA in mice as well as the activity of FOA against tumors has been previously tested [78, 91]. However, liposomal FOA has only been evaluated *in vitro* [79-81]. The toxicity of FOA and NTL-FOA was evaluated by performing MTD studies at dosing schedules similar to what is used for IRN treatment. Figure 3.4 shows the results from the first MTD study in Balb/c and Balb/c nu/nu mice. The weight of mice did not significantly decrease after one i.v. dose of FOA 100 mg/kg or NTL-FOA 10 mg/kg during the course of the study. Therefore, one i.v. dose of both formulations was well tolerated. A 2xq4d schedule of FOA 100 mg/kg was toxic in both mouse strains. In Balb/c mice, a 2xq4d schedule of NTL-FOA 10 mg/kg was toxic; however, in Balb/c nu/nu mice NTL-FOA 10 mg/kg was toxic at a 3xq4d schedule.

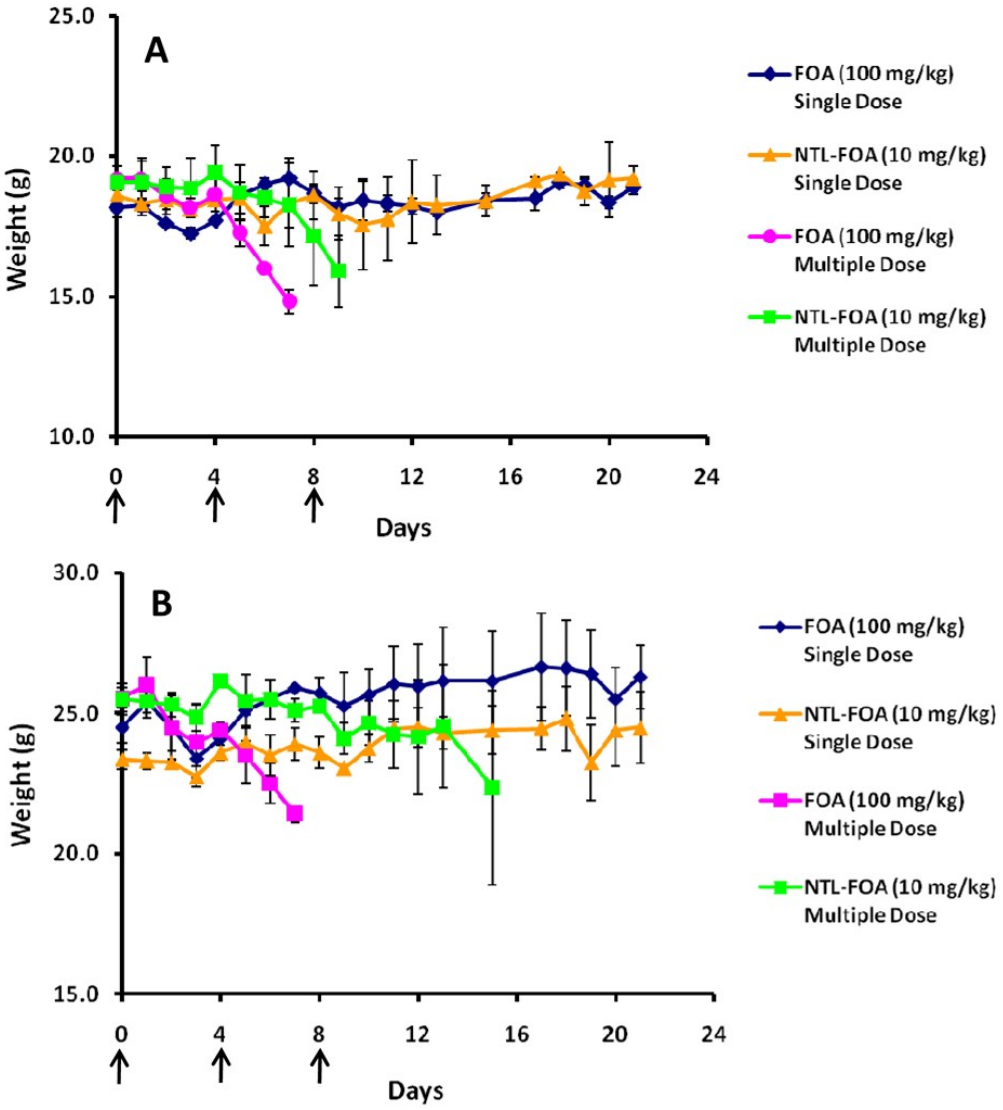

Figure 3.4 Maximum tolerated dose study of FOA 100 mg/kg and NTL-FOA 10 mg/kg. For single dose, FOA and FTL-FOA administered i.v. on Day 0. For multiple dose, FOA and NTL-FOA administered i.v. on Day 0 and four days apart (as indicated by arrows). **A**. Balb/c mice. **B**. Balb/c nu/nu mice.

In a second MTD study (Figure 3.5), FOA 100 mg/kg and NTL-FOA10 mg/kg were administered i.v. on a 3xq7d schedule starting on Day 0 to Balb/c mice. The weight of mice showed a downward trend for twenty-one days after initiating dosing but it was not a statistically significantly decrease. The weight of the animals then recovered indicating that this dose and schedule was an acceptable maximum tolerated dose.

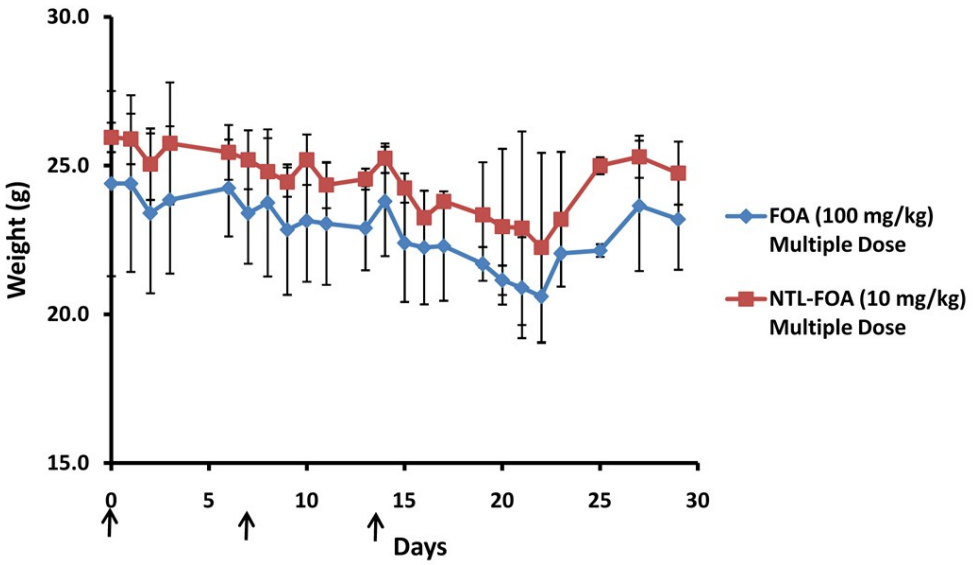

Figure 3.5 Effect of new dosing schedule on MTD in Balb/c mice. FOA 100 mg/kg and NTL-FOA 10 mg/kg administered i.v. on a 3xq7d schedule starting on Day 0.

3.4.6 Liposome Co-encapsulation of IRN+FOA

To investigate whether liposomes can maintain the synergistic ratio *in vivo*, we formulated liposomes co-encapsulating both drugs. The approach we pursued was to first passively load FOA into the liposomes and then to use the weak acid on FOA to remote load IRN. Cholesterol content, drug/lipid ratio, loading temperature, and incubation time can influence co-encapsulation of drugs into liposomes [89]. Therefore, various IRN drug/ lipid ratios, loading temperatures, and incubations times were tested in order to load IRN into the FOA encapsulated liposomes and achieve an IRN/FOA 1:5 molar ratio. The various approaches examined are listed in Table 3.2. We found that the encapsulated FOA concentration is significantly reduced during IRN remote loading. Decreasing the initial IRN drug/ lipid ratio, loading temperature, and incubation time increase the retention of FOA in the liposomes. However, increasing the initial IRN drug/lipid ratio and incubation time generally increase the encapsulated IRN concentration. Loading

temperature did not significantly affect IRN encapsulation. Thus, the protocol developed had to balance the competing tendency of the two drugs.

There is a strong correlation between the initial IRN drug/lipid ratio and 1) the final encapsulated IRN concentration, 2) the final encapsulated FOA concentration, and 3) the co-encapsulated drug ratio (Figure 3.6). We determined that an IRN/FOA 1:5 co-encapsulated molar ratio could be consistently achieved when remote loading IRN at a 0.025/1 drug/lipid ratio at 50 °C for 30 min. We also investigated how the aforementioned parameters as well as cholesterol content would affect co-encapsulation of the drugs at a 1:1 molar ratio (Table 3.3). Again, there was a strong correlation between the initial IRN drug/lipid ratio and the final co-encapsulated drug ratio (Figure 3.7). Cholesterol did not affect the amount of encapsulated IRN. Surprisingly, more FOA was retained in liposomes during remote loading when the mol% of Chol was decreased. We determined that an IRN/FOA 1:1 co-encapsulated molar ratio could be consistently achieved when remote loading IRN at a 0.1375/1 drug/lipid ratio at 50 °C for 10 min. Thus, we were able to optimize loading parameters to co-encapsulate IRN and FOA at a 1:5 or 1:1 molar ratio in the NTL formulations.

The proposed mechanism of co-encapsulation is shown in Figure 3.8. We hypothesize that during the remote loading process, triethylamine present in the liposome internal buffer partitions out of the liposome interior. This causes a transmembrane pH gradient across the liposome bilayer (high [H+] in the interior, low [H+] in the exterior). IRN in the external buffer is then able to cross the liposome bilayer and become protonated. IRN within the liposomes that is positively charged (pKa = 8.1) interacts with FOA that is negatively charged (pKa = 2.4) and probably forms a complex [92].

Table 3.2 Summary of Conditions and Outcomes of IRN+FOA Co-encapsulation into Liposomes at 1:5 Ratio

Trial	$[FOA]_o$ (mM)	IRN D/L Ratio	Load Temp (°C)	Load Time (min)	$[IRN]_f$ (mM)	$[FOA]_f$ (mM)	IRN/FOA Ratio
i	7.2	0.1/1	50	60	1.21	1.74	1.0/1.4
		0.2/1			2.18	0.94	2.3/1.0
		0.1/1	65		1.05	0.51	2.1/1.0
		0.2/1			1.73	0.21	8.2/1.0
ii	6.13	0.1/1	50	10	1.23	3.7	1.0/3.0
				30	1.14	3.11	1.0/2.7
				60	2.29	2.05	1.0/1.1
iii	8.69	0.1/1	40	30	1.08	2.43	1.0/2.2
		0.2/1			1.93	1.81	1.1/1 .0
		0.1/1	45		1.15	3.61	1.0/3.1
		0.2/1			2.1	1.41	1.5/1.0
iv	4.56	0.05/1	50	30	0.56	2.03	1.0/3.6
		0.075/1			0.77	1.78	1.0/2.3
		0.1/1			1.07	1.53	1.0/1.5
		0.15/1			1.51	1.21	1.2/1.0
v	4.77	0.025/1	50	30	0.39	2.13	1.0/5.4

$[FOA]_o$: initial FOA concentration **D/L**: drug to lipid ratio **$[IRN]_f$** : final IRN concentration **$[FOA]_f$**: final FOA concentration

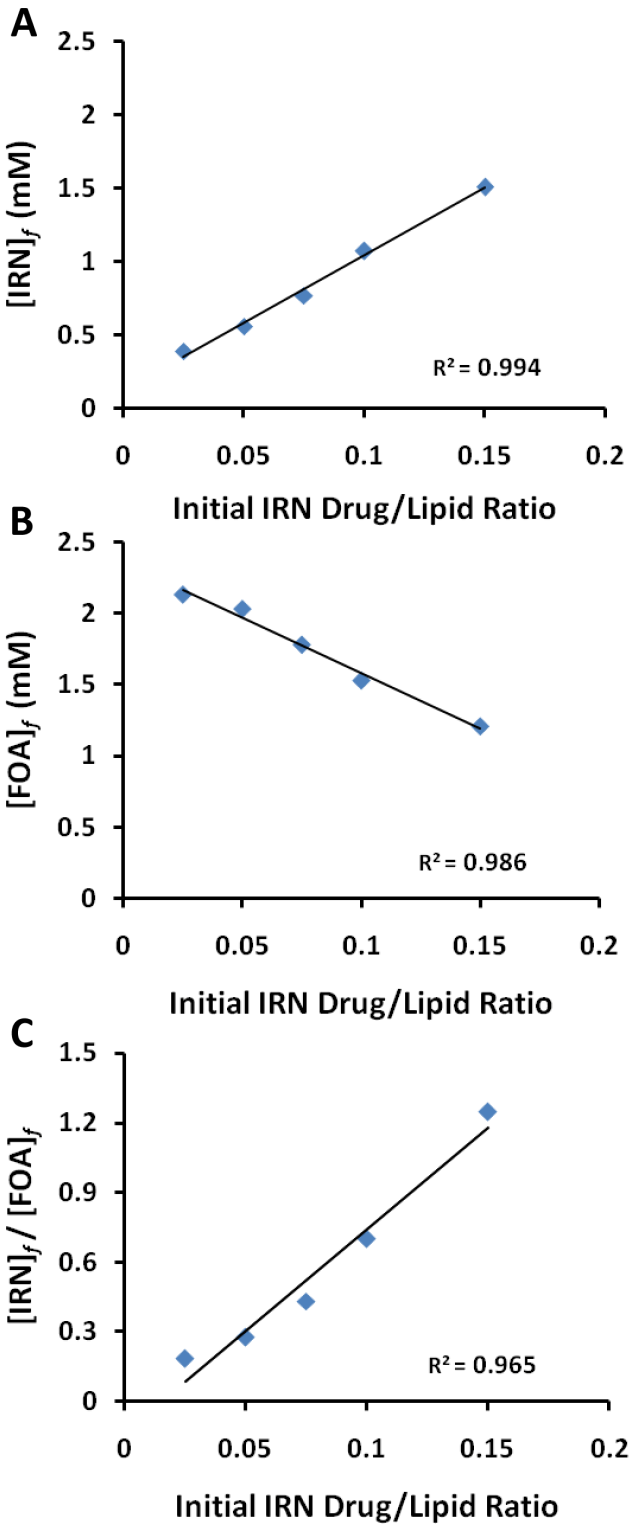

Figure 3.6 Effect of IRN drug to lipid ratio on IRN and FOA co-encapsulation at 1:5 ratio. Loading temperature was 50 °C and loading time was 30 min. **A**. Effect of initial IRN drug/lipid ratio on the final encapsulated IRN concentration ($[IRN]_f$). **B**. Effect of initial IRN drug/lipid ratio on the final encapsulated FOA concentration ($[FOA]_f$). **C**. Effect of initial IRN drug/lipid ratio on the final ratio of IRN and FOA in the liposomes ($[IRN]_f$ / $[FOA]_f$).

Table 3.3 Summary of Conditions and Outcomes to Co-encapsulate IRN+FOA into Liposomes at 1:1 Ratio

Trial	Chol (mol%)	IRN D/L Ratio	Load Temp (°C)	Load Time (min)	$[IRN]_f$ (mM)	$[FOA]_f$ (mM)	IRN/FOA Ratio
i	40	0.1/1	50	10	1.05	1.63	1.0/1.6
		0.15/1			1.43	1.29	1.1/1.0
		0.2/1			2.03	0.75	2.7/1.0
ii	30	0.125/1	50	10	0.95	0.55	1.7/1.0
				30	1.0	0.47	2.2/1.0
iii	20	0.125/1	50	10	1.14	0.67	1.7/1.0
				30	1.19	0.14	8.5/1.0
iv	10	0.125/1	50	10	1.22	1.26	1.0/1.0
				30	1.23	0.86	1.4/1.0
v*	40	0.125/1	50	10	2.4	3.26	1.0/1.4
		0.15/1			2.82	2.48	1.1/1.0
vi*	40	0.1375/1	50	10	2.8	2.87	1.0/1.0

D/L: drug to lipid ratio **$[IRN]_f$** : final IRN concentration **$[FOA]_f$**: final FOA concentration

***** The lipid concentration in these formulations are twice that of the previous formulations.

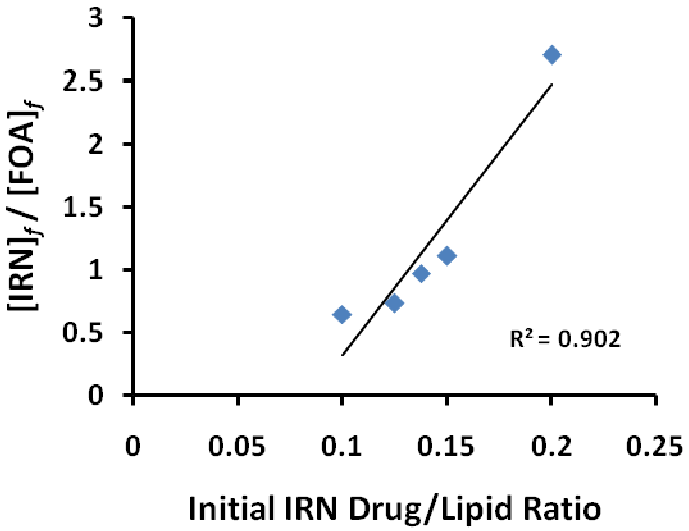

Figure 3.7 Effect of IRN drug to lipid ratio on IRN and FOA co-encapsulation at 1:1 ratio. Loading temperature was 50 °C and loading time was 10 min.

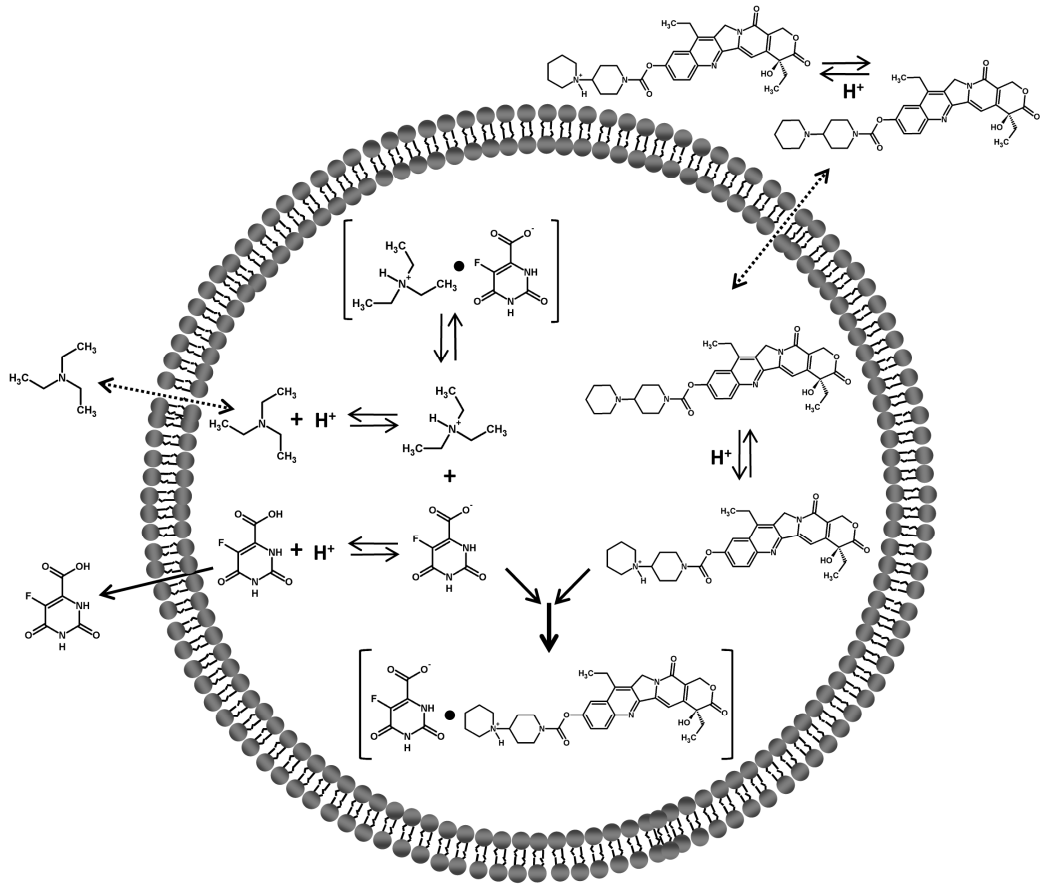

Figure 3.8 Schematic diagram of proposed mechanism of co-encapsulation of IRN + FOA in liposomes

3.4.7 Anti-tumor Effect in and Survival of C26 tumor-bearing mice treated with Liposomal IRN and FOA

We compared the therapeutic activity of this co-formulation to the single formulations and to mixtures of the single formulations in C26 tumor-bearing mice. The results of the animal study are shown in Figure 3.9, and the details of the treatment groups are summarized in Table 3.4. NTL-FOA 57.4 μmol/kg (10 mg/kg) had a superior tumor growth inhibition and significantly longer survival rate (p=0.0027 log rank test) than NTL-IRN 73.8 μmol/kg (50 mg/kg). None of the combinations were more effective than NTL-FOA. Mice treated with NTL-IRN-FOA 1:5 had an increased survival compared to mice treated with NTL-IRN + NTL-FOA 1:5 (p=0.0414, log rank test). Furthermore, mice treated with NTL-IRN + NTL-FOA 1:5 2x lived longer than mice given NTL-IRN + NTL-FOA 1:5 (p=0.0015, log rank test). The mice were treated on a 2xq7d schedule instead of a 3xq7d schedule as planned because the mice from two groups, NTL-IRN and NTL-IRN + NTL-FOA 1:5, were steadily losing weight after the second i.v. injection (Figure 3.10).

Table 3.4 Drug Content in Formulations Used in Combination Therapy Study

Formulation	**IRN (μmol/kg)**	**FOA (μmol/kg)**
NTL-FOA	-	57.4
NTL-IRN	73.8	-
NTL-IRN-FOA (1:5)	5.74	28.7
NTL-IRN + NTL-FOA (1:5)	5.74	28.7
NTL-IRN + NTL-FOA (1:5) 2x	11.5	57.4

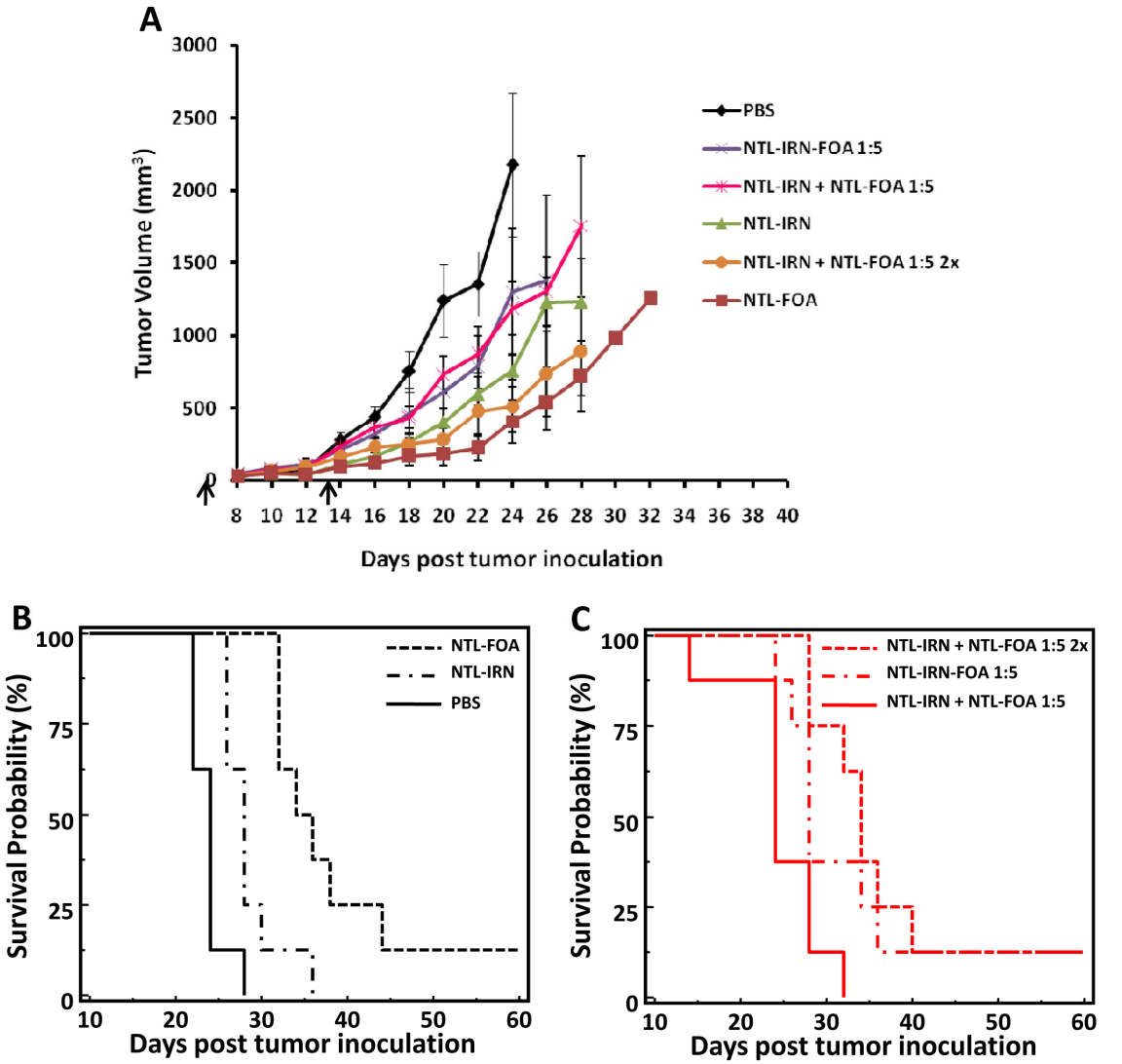

Figure 3.9 NTL-IRN-FOA combination therapy in C26 tumor-bearing mice. Balb/c mice (n=8) were treated with i.v. injections on Days 8 and 15 (as indicated by arrows). **A**. Anti-tumor activity. Error bars represent SEM. **B and C**. Survival curves. The treatment groups are PBS, NTL-FOA (57.4 µmol/kg), NTL-IRN (73.8 µmol/kg), NTL-IRN-FOA 1:5 (5.74 µmol/kg IRN; 28.7 µmol/kg FOA), NTL-IRN + NTL-FOA 1:5 (5.74 µmol/kg IRN; 28.7 µmol/kg FOA), and NTL-IRN + NTL-FOA 1:5 2x (11.5 µmol/kg IRN; 57.4 µmol/kg FOA).

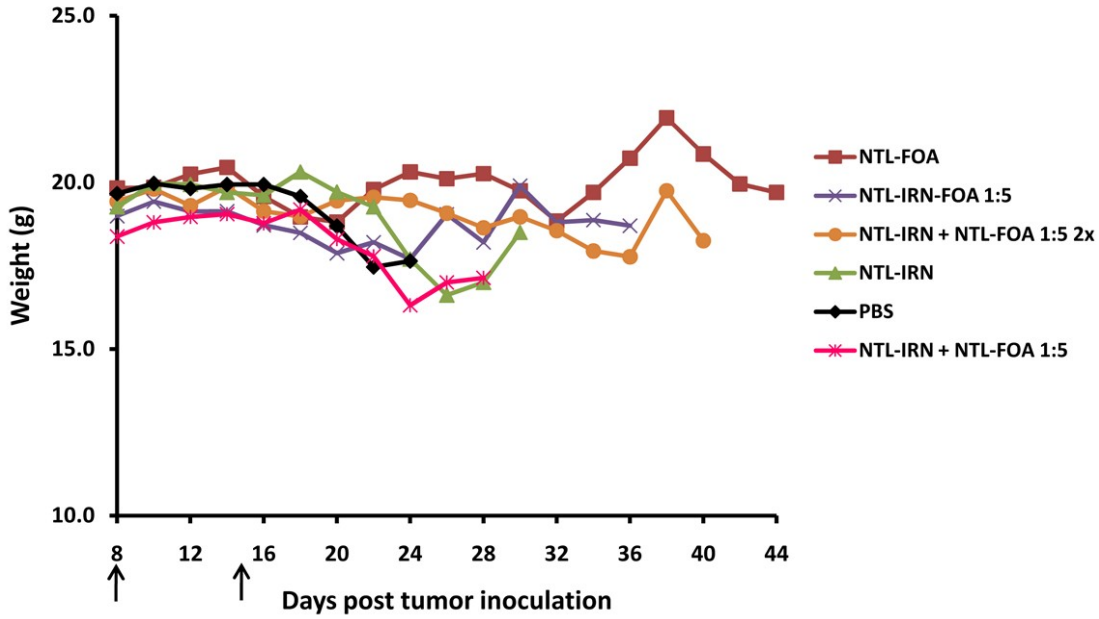

Figure 3.10 Effect of combination therapy on weight of C26 tumor-bearing mice. Arrows indicate treatment days.

3.5 Discussion

The objective of the research done in this chapter was to develop non-targeted liposome formulations of IRN, FOA, and IRN+FOA combination to investigate the hypothesis that targeted liposomes can enhance the efficacy of synergistic agents.

Initially, the combination activity of IRN+FOA was tested in C26 cells. We found that IRN + FOA at a 1:5 molar ratio was synergistic in C26 cells *in vitro* (Figure 3.1). The results from the screen show that the synergism exhibited by IRN and FOA is ratio-dependent. Therefore, it is important to control the ratios *in vivo* in order to achieve maximum therapy.

We then examined liposome formulations of IRN that we believed would be compatible for use in future drug co-encapsulation studies. Remote loading IRN in liposomes containing BTCA produced the highest encapsulation efficiency. The therapeutic efficacy of NTL-IRN was tested in a HT29 human xenograft mouse model at a similar dose and schedule previously used by Drummond and coworkers [20]. The data

in Figures 3.2 and 3.3 demonstrate that NTL-IRN was efficacious and safe at the dose and schedule administered.

To prepare NTL-FOA, we initially used a method developed by Heath and coworkers [80]; however, using this method we were only able to encapsulate 1-3 mM of FOA. We found that dissolving FOA in 7M urea, which is known to disrupt hydrogen bonding between molecules, allowed us to make a more concentrated FOA solution. As a result, we could prepare liposome that encapsulated higher concentrations (~10mM) of FOA. Being able to encapsulate suitable concentrations of a drug in liposomes is critical to deliver therapeutic doses of that drug for animal studies, especially if the drug is not very potent. With our NTL-FOA formulation, we are able to deliver a maximum of a 10 mg/kg dose to mice in a 200 uL volume.

We investigated the MTD of NTL-FOA because 1) NTL-FOA has never been tested in mice and 2) we needed to determine whether NTL-FOA could be administered safely at a schedule similar to an IRN dosing schedule. From the MTD study (Figure 3.4), we observed that Balb/c and Balb/c nu/nu mice were able to tolerate a single i.v. dose of both treatments. Both mice strains could not endure multiple i.v. doses of FOA 100 mg/kg given four days apart. The Balb/c mice also could not endure multiple i.v. doses of NTL-FOA 10 mg/kg given four days apart. However, Balb/c nu/nu mice were able to tolerate at least two i.v. doses of NTL-FOA 10 mg/kg given four days apart. Therefore, NTL-FOA would not be able to be administered on the schedule followed in the NTL-IRN therapy study in HT29 mice.

We also evaluated the MTD of the two formulations in the Balb/c mice on a 3×q7d dosing schedule (Figure 3.5). This is the schedule that Mayer and coworkers have

used to evaluate the therapeutic activity of their liposome IRN + floxuridine co-formulations [27]. The formulations were not toxic to the mice at this schedule. Since the Balb/c mice were more sensitive than Balb/c nu/nu to multiple i.v doses of either FOA or NTL-IRN, we believe that Balb/c nu/nu should also be able to tolerate a 3×q7d dosing schedule. We planned to use this schedule for future animal studies with IRN and FOA liposome formulations. It is must be noted that NTL-FOA is toxic at 10 mg/kg, which is a 10 fold less dose than free FOA. This enhanced toxicity is probably due to the longer circulation, sustained release, and enhanced accumulation of FOA to sites of toxicity due to the liposome formulation. This increased toxicity for a water soluble antimetabolite has also been observed in liposomal cytosine arabinoside formulations [93].

Lastly, we developed a liposome formulation that encapsulated both IRN and FOA. Co-encapsulating these two drugs in one liposome formulation was challenging because of the disparate physico-chemical properties of these two drugs. Weakly acidic drugs like FOA are traditionally passively loaded into liposomes; while amphipathic drugs like IRN can be actively loaded into preformed liposomes. Passive loading of drugs occurs through hydrating a lipid film with an aqueous solution of drug. This method is inefficient, and the resulting encapsulated drug concentration relies on the maximum solubility of the drug in solution [45]. It is advantageous to actively load drugs into liposomes via transmembrane gradients because high encapsulated drug concentrations and stable drug retention can be achieved. It is difficult to remote load FOA because it is deprotonated in aqueous solution; therefore, FOA cannot readily cross a lipid bilayer. On the other hand, IRN can easily partition into a bilayer under the appropriate conditions.

To co-encapsulate IRN+FOA in liposomes, we passively loaded FOA into vesicles and then remote loaded IRN (Figure 3.8). This procedure caused some FOA to leak out during IRN remote loading (Tables 3.2 and 3.3, Figures 3.6 and 3.7). Therefore, it was critical to minimize FOA leakage while maximizing IRN loading. Reducing the loading temperature, loading time and IRN drug/lipid ratio enhanced FOA retention but minimized IRN loading. However, cholesterol concentration only affected FOA retention. Generally, a high cholesterol content decreased FOA release. The IRN drug/lipid ratio had the biggest impact on FOA retention and IRN loading. Regardless, these parameters can be optimized to allow reproducible encapsulation of IRN + FOA at ratios between 1:1 to 1:5. To our knowledge, these two compounds have never been co-encapsulated in liposomes.

We investigated the combination therapy of IRN+FOA in various liposome formulations in C26 tumor-bearing mice. We found that IRN +FOA at a 1:5 molar ratio is synergistic in C26 cells *in vitro.* We were encouraged but a little surprised that IRN showed good activity since it is a prodrug that has to be activated by a carboxylesterase to the active compound SN38.

The results from the animal study (Figure 3.9) show that none of the combinations were more effective than NTL-FOA 57.4 μmol/kg (10 mg/kg). In fact, NTL-FOA was more effective than NTL-IRN even though NTL-IRN was administered at a slightly higher dose and shows good anti-tumor activity in the HT-29 model. The NTL-IRN + NTL-FOA 1:5 2x combination had similar, albeit slightly less, tumor growth inhibition as NTL-FOA. The other combinations were probably less effective because they had a lower concentration of FOA. It was difficult to draw a conclusion about the efficacy of

NTL-IRN-FOA 1:5 and NTL-IRN + NTL-FOA 1:5 combinations since we did not test single formulations of equivalent doses (i.e. NTL-FOA 28.7 μmol/kg, NTL-IRN 5.75 μmol/kg). One conclusion that can be drawn from these studies is that an *in vitro* cytotoxicity assay may not predict the outcome of an *in vivo* antitumor experiment.

The studies described in this chapter provide a robust liposome formulation of co-encapsulated IRN and FOA. The *in vivo* stability, biodistribution profile, and antitumor activity of these novel liposome formulations in the KB folate receptor over-expressing tumor mouse model are further investigated in the following chapters to allow the evaluation of the hypothesis that a targeted liposome formulation co-encapsulating a synergistic pair will provide a superior anti-tumor effect than a non-targeted liposome formulation containing the same drugs.

CHAPTER 4:
Evaluation of Folate Targeted Liposome Delivery

4.1 Abstract

The effect of folate-targeted liposomal doxorubicin (FTL-Dox) has been well characterized in folate receptor (FR) over-expressing tumors *in vitro*, particularly in KB human oral carcinoma cells. However, there are few studies evaluating the *in vivo* efficacy of FTL-Dox in KB murine xenograft models. In this study, we investigated the antitumor activity of FTL-Dox injected intravenously in mice bearing KB tumors. Folate ligands comprising of folate-polyethyleneglycol-distearoylphosphatidylethanolamine (FA-PEG-DSPE) were synthesized with different MW PEG. To design an optimum FTL-Dox formulation for therapeutic studies, we prepared several FTLs of varying ligand lengths and densities and characterized their *in vitro* targeting and *in vivo* tissue biodistribution. KB tumor-bearing mice were administered a single intravenous injection of free Dox, non-targeted PEGylated liposomal Dox (PL-Dox), or FTL-Dox at different doses. The antitumor activity and survival rate were assessed. FTLs and PLs accumulated similarly in tumor tissue, despite FTLs' faster clearance from circulation. Moreover, mice treated with FTL-Dox 20 mg/kg had a slightly greater tumor growth inhibition and almost a 50% increase in life span than mice receiving PL-Dox 20 mg/kg ($P = 0.0121$; log-rank test). We conclude from the results that folate-targeted liposomes administered systemically have the potential to enhance the delivery of anticancer drugs *in vivo*; however their removal by normal tissues that express the FR may have to be blocked if the benefits from cytotoxic drug targeting to a tumor are to be realized.

4.2 Introduction

Several strategies for tumor-specific delivery of chemotherapy are currently under evaluation because of the possibility to reduce dose limiting toxicity and bypass multi-drug resistance, both of which hamper the therapeutic efficacy of potent anticancer drugs. An often proposed target for directed cancer therapy is the folate receptor (FR). FR is a 38 kDa glycosyl-phosphatidylinositol membrane anchored glycoprotein that is over-expressed on various human cancers; however, FR is present at low levels in most normal epithelial tissues [41]. Folic acid (FA) binds to the folate receptor (FR) with high affinity (Kd = 0.1 nM) and gets internalized via receptor-mediated endocytosis [40]. Folate is an attractive ligand because of its low immunogenicity, ease of modification, and low cost [41].

Folate targeted liposomes (FTL) have successfully delivered chemotherapeutic agents as well as genes, antisense oligonucleotides, and radionuclides into FR over-expressing tumor cells [42]. FTLs encapsulating doxorubicin (FTL-Dox) have increased cellular uptake and cytotoxicity as compared to non-targeted PEGylated liposomal doxorubicin (PL-Dox) and unencapsulated doxorubicin (Dox) *in vitro* [94]. These effects result from more efficient delivery of Dox after internalization into FR over-expressing tumor cells [95].

Although FTL drugs are widely studied in KB and other FR+ cell lines *in vitro*, there are very few reports on FTL drug therapy *in vivo*, especially in solid tumor mouse models such as the KB tumor mouse model. Recently, Pan and coworkers have found that KB tumor-bearing mice treated with FTL-Dox via multiple i.p. injections had greater tumor growth inhibition ($p < 0.01$) and a 31% increase in lifespan compared to mice

treated with PL-Dox [43]. However, there are no studies to date on the *in vivo* therapeutic activity of FTL drugs after intravenous administration in KB tumor-bearing mice.

We formulated various FTLs and validated their binding and targeting to KB cells *in vitro* and *in vivo*. We utilized the best FTL formulation to investigate the therapeutic efficacy of FTL-Dox in a KB tumor mouse xenograft model after a single intravenous injection. Our findings are discussed in this chapter.

4.3 Methods

4.3.1 Materials

Folic acid, cholesterol (Chol), and fluorescein isothiocyanate (FITC) were purchased from Sigma-Aldrich (St. Louis, MO). Distearoylphosphatidylcholine (DSPC), distearoyl-phosphatidylethanolamine (DSPE) and methoxy-polyethylene glycol (MW2000)-DSPE (mPEG2000-DSPE) were purchased from Genzyme (Cambridge, MA). Amino-PEG2000-DSPE was purchased from Avanti Polar Lipids (Alabaster, AL). PEG3350-bis-amine was purchased from Shearwater Polymers (Huntsville, AL). Doxorubicin (Dox) was acquired from LGM Pharmaceuticals (Boca Raton, FL). KB cells and RPMI 1640 media were purchased from University of California, San Francisco Cell Culture Facility. Folate Free RPMI 1640 media was a product of Invitrogen (Carlsbad, CA). Folate-free chow was purchased from Harlan Teklad (Madison, WI).

4.3.2 Cell Culture

KB cells were maintained in folate-free RPMI 1640 media supplemented with 10% fetal calf serum that provides the only source of folic acid. The cells were cultured as a monolayer in 5% CO_2 at 37 °C.

4.3.3 Synthesis and Characterization of FA-PEG-DSPE Ligands

FA-PEG2000-DSPE was synthesized as described previously [96]. As shown in Scheme 4.1, FA-PEG3350-DSPE was synthesized according to a modified method from Stephenson and coworkers [97]. First DSPE was converted to N-succinyl-DSPE by succinic anhydride. Then amino-PEG3350 was conjugated to N-succinyl-DSPE through the activated ester. Finally, FA-PEG3350-DSPE was obtained by coupling FA to the terminal amino group of DSPE-PEG3350-NH_2. Detailed synthetic procedures are described below.

N-Succinyl-DSPE: To a solution of DSPE (2 g) and triethylamine (1.5 mL, 4 equiv.) in dry ethanol-free chloroform (75 mL) was added succinic anhydride (535 mg, 2 equiv.) at room temperature (r.t.) with stirring. The reaction was complete after stirring at r.t. for 24 h according to TLC analysis. The reaction mixture was diluted with 35 mL methanol and extracted with 1 M HCl (22 mL) in a separation funnel. The organic layer was dried with anhydrous sodium sulfate, filtered, concentrated, and precipitated with acetone at -20 °C. The precipitate was collected and placed under high vacuum overnight. White solid was obtained. R_f = 0.47 in chloroform-methanol-ammonium hydroxide (65:25:4 v/v). The structure of the product was confirmed with ^{1}H NMR and MALDI mass spectrometry.

DSPE-PEG3350-NH_2: To a solution of N-succinyl-DSPE (400 mg) and N-hydroxysuccinimide (65.1 mg, 1.2 equiv.) in dry chloroform (10 mL) were added dimethylaminopyridine (57.6 mg, 1 equiv.), triethylamine (263 μL), and dicyclohexylcarbodiimide (DCC) (116.8 mg, 1.2 equiv.) at r.t. under argon. After 4 h reaction in the dark at r.t., a solution of PEG3350-bis-amine (3.5 g, 2.2 equiv.) in dry

chloroform (40 mL) was added to the reaction mixture. The reaction was kept at r.t. overnight. The precipitate was filtered off and the filtrate was concentrated by rotary evaporation and purified by flash column chromatography. Elution method: solvent A: chloroform, solvent B: methanol; segment 1: 0% -10% B, 240 mL; segment 2: 10%-15% B, 360 mL; segment 3: 15%-15% B, 240 mL. R_f = 0.6 in chloroform-methanol (5:1 v/v). The structure of the product was confirmed with ^{1}H NMR and MALDI mass spectrometry.

FA-PEG3350-DSPE: To a solution of folic acid (188.5 mg) and DSPE-PEG3350-NH_2 (600 mg, 3 equiv.) in dimethyl sulfoxide (20 mL) and pyridine (2 mL) was added DCC (88 mg, 3 equiv.) at r.t. under argon in the dark. After the completion of the reaction (16 h according to TLC), the product was precipitated by diethyl ether at 4 °C. The crude product was dissolved in 2 mL dimethyl sulfoxide and 1 mL pyridine, loaded on flash column, and purified with the following solvent elution scheme. Solvent A: chloroform, solvent B: MeOH-NH_4OH 25/4; segment 1: 0%-10% B, 96 mL; segment 2: 10%-20% B, 144 mL; segment 3: 20%-20% B, 144 mL. R_f = 0.85 in chloroform-methanol-ammonium hydroxide (65:25:4 v/v). The structure of the product was confirmed with ^{1}H NMR and MALDI mass spectrometry.

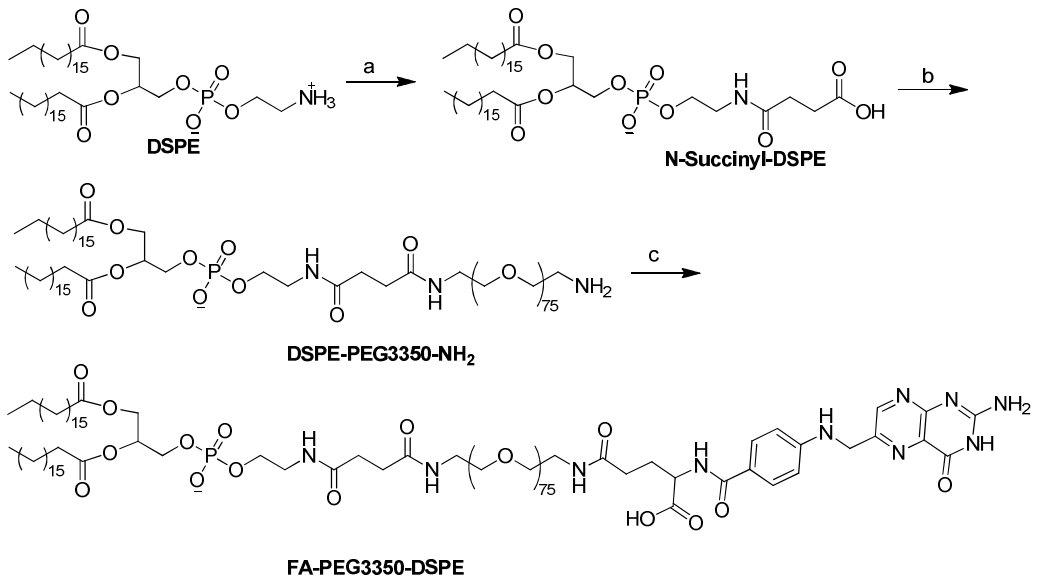

Scheme 4.1 Synthesis of FA-PEG3350-DSPE. *Reagents and conditions:* a) succinic anhydride (2 equiv.), triethylamine (4 equiv.), $CHCl_3$, r.t., 24 h; b) (i) N-hydroxylsuccinimide (1.2 equiv.), DMAP (1 equiv.), DCC (1.2 equiv.), r.t., 4 h; (ii) PEG3350-bis-amine (2.2 equiv.), $CHCl_3$, r.t., overnight; c) Folic acid (1 equiv.), DSPE-PEG3350-NH_2 (3 equiv.), DCC (3 equiv.), DMSO-Py (10/1, v/v), r.t., 16 h.

4.3.4 Synthesis of FITC-DSPE

FITC-DSPE was synthesized by the direct coupling of FITC to DSPE (Scheme 4.2). To a solution of DSPE (50 mg) in dry chloroform (5 mL) and triethylamine (37.3 μL) was added FITC (52.1 mg, 2 equiv.) in dimethyl sulfoxide. The mixture was allowed to react overnight at r.t. in the dark. The mixture was concentrated by rotary evaporation, and purified by flash column chromatography. Elution method: solvent A: chloroform, B: methanol; segment 1: 0%-20% B, 24 mL; segment 2: 20%-20% B, 48 mL; segment 3: 20%-30% B, 72 mL. Fractions of pure product were pooled, evaporated, and dried under high vacuum overnight in the dark. R_f = 0.38 in chloroform-methanol (4:1 v/v). The structure of the product was confirmed with ^{1}H NMR and MALDI mass spectrometry.

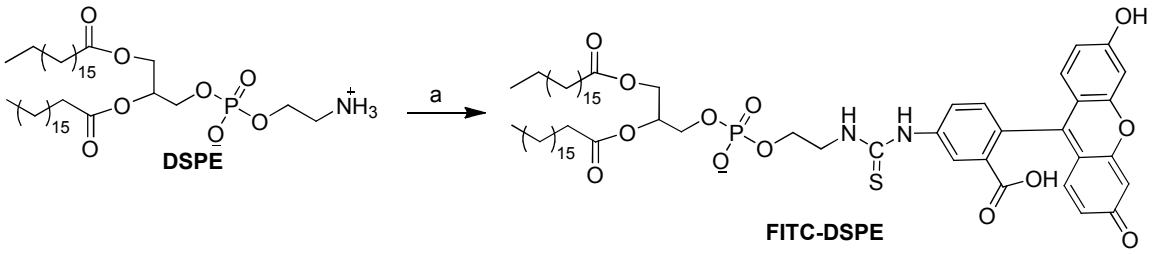

Scheme 4.2 Synthesis FITC-DSPE. *Reagents and conditions:*a) DSPE (1 equiv.), FITC (2 equiv.), triethylamine (4 equiv.), $CHCl_3$, r.t., overnight.

4.3.5 Effect of Ligand Concentration and PEG on FTL Cell Association

To investigate how ligand density effects FTL cell association, liposomes composed of DSPC/Chol (55:40) were formulated with varying mole percentages (0.01, 0.03, 0.1, 0.5 mol %) of FA-PEG2000-DSPE and 0.2 mol % FITC-DSPE. To examine the effect of PEG on FTL cell association, the following liposome formulations were prepared: *F_{2000}L(0.03)* - DSPC/Chol/FA-PEG2000-DSPE (55:40:0.03), *F_{2000}PL (0.03)* - DSPC/Chol/mPEG2000-DSPE/FA-PEG2000-DSPE (55:40:4.5:0.03), *F_{3350}L(0.03)* - DSPC/Chol/FA-PEG3350-DSPE (55:40:0.03), and *F_{3350}PL(0.03)* - DSPC/Chol/ mPEG2000-DSPE/FA-PEG3350-DSPE (55:40:4.5:0.03). These formulations were also fluorescently labeled with 0.2 mol % FITC-DSPE. All lipid mixtures (10 μmol lipid) were dissolved in chloroform and dried into a thin film by rotary evaporation then placed under high vacuum overnight. The films were subsequently hydrated with Hepes buffer (10 mM Hepes, 140 mM NaCl pH 7.4) at 60 °C and vortexed. The liposomes were then sonicated at 60 °C and extruded through 200 nm and 100 nm polycarbonate membranes (Avestin, Ottawa, CA). The liposome diameter and particle size distribution were sized by dynamic light scattering (Zetasizer 3000, Malvern Instruments, Westborough, MA). The average liposome diameter was 100-120 nm for all formulations. A schematic diagram of the FTL formulations are shown in Figure 4.1, and the liposome compositions are summarized in Table 4.1.

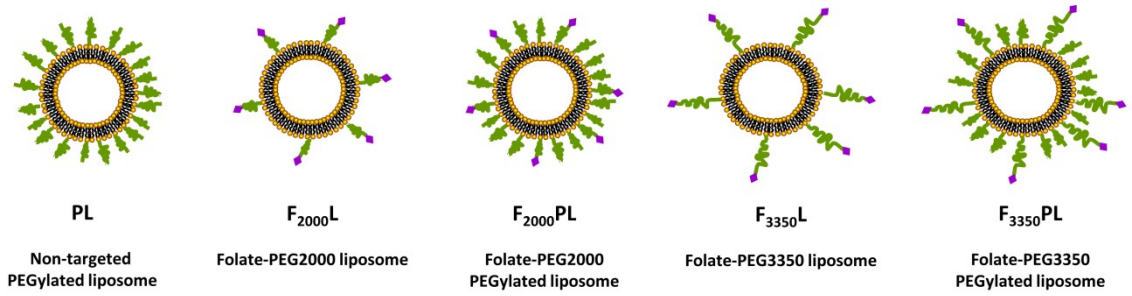

Figure 4.1 Schematic diagram of the liposome formulations.

Table 4.1 Summary of Formulations Prepared for Studies

Lipid	**Formulation**				
	PL	***F 2000 L***	***F 2000 PL***	***F 3350 L***	***F 3350 PL***
DSPC (mol %)	55	55	55	55	55
Chol (mol %)	40	40	40	40	40
mPEG2000-DSPE (mol%)	5		4.5-5	-	4.5-5
FA-PEG2000-DSPE (mol%)	-	0.01-0.5	0.03-0.3	-	-
FA-PEG3350-DSPE (mol%)	-	-	-	0.03-0.3	0.03-0.3

KB cells grown as a monolayer were washed with phosphate buffered saline ((PBS; 2.16 g/L Na_2HPO_4 $7H_20$, 0.2 g/L KH_2PO_4, 0.2 g/L KCl, 8.0 g/L NaCl) then incubated with 10 mM EDTA for 5 min at 37 °C to resuspend the cells. Then 10^6 cells were transferred to FACS tubes and centrifuged at 800 rpm for 5 min at r.t. The supernatant was aspirated and the pellets were washed with PBS. The cells were incubated with the different folate targeted liposome formulations (10 nmol lipid) in serum free folate-free RPMI 1640 medium at 37 °C for 3 hr with gentle mixing. The cells were washed twice with PBS. Then the cells were resuspended in 500 µL PBS and analyzed with a FACS Calibur flow cytometer (Becton Dickson) with a 488nm Argon laser. 10,000 events were recorded.

For some of the FTL formulations, the cell association was also measured after 24 hr incubation. KB cells were plated in 6 well plates at a density of $5x10^5$ cells per well. After 48 hr, the media was aspirated, and the cells were incubated with 1 mL of each formulation (10 nmol lipid) in serum free, Folate Free RPMI 1640 medium at 37 °C.

After 24 hr, the supernatant was aspirated, and the wells were washed with PBS. The cells (~10^6) were resuspended with 1 mL trypsin/EDTA. Then the cells were transferred to FACS tubes and centrifuged at 800 rpm for 5 min at r.t. The supernatant was aspirated, and the pellets were washed twice with PBS. Then the cells were resuspended in 500 μL PBS and analyzed by flow cytometry as stated above.

4.3.6 Animals

Balb/c nu/nu mice (8-10 weeks) were obtained from Simonsen Laboratories, Inc. (Gilroy, CA). Animal maintenance and experiments adhered to the "Principles of Laboratory Animal Care" (NIH publication #85-23, revised in 1985) under a protocol approved by the Committee on Animal Research at the University of California, San Francisco.

4.3.7 Circulation Profile and Biodistrubution of FTLs in KB Tumor-bearing Mice

Non-targeted PEGylated liposomes (PLs) were formulated as listed in Table 4.1. FTLs incorporating FA-PEG-DSPE at three different mole percentages were formulated. The liposome compositions were DSPC/Chol/mPEG2000-DSPE/FA-PEG-DSPE (55:40:5:n) where n = 0.03, 0.1, or 0.3 mol %. The lipids (10 μmol total) were dissolved in chloroform and mixed with 200 μL of 5x10^7 CPM/ml of iodo-PHB-DPPE [98]. The lipid mixtures were dried into a thin film with N_2 gas and then placed under high vacuum overnight. The films were subsequently hydrated with Hepes buffer (10 mM Hepes, 140 mM NaCl pH 7.4) at 60 °C and vortexed. The liposomes were sonicated at 60 °C and then extruded through 200 nm and 100 nm polycarbonate membranes. The liposome diameter and particle size distribution were measured by dynamic light scattering. The mean liposome diameter was 90-110 nm for all formulations.

Balb/c nu/nu mice were placed on a folate-free diet one week before tumor inoculation and were maintained on the special feed throughout the study. KB (10^6) cells suspended in 50 μL of folate-free RPMI 1640 medium without serum were inoculated subcutaneously in the right hind flank of each mouse. On Day 15 after tumor inoculation, each formulation (~1 μmol lipid in 200 μL) was injected into the tail vein of the mice (n = 3 mice/group). At 3 and 24 hrs post-injection, blood from submandibular puncture was collected. At 48 hr post-injection, the liver, spleen, tumor, muscle tissue, and blood (from cardiac puncture) were collected and weighed. The amount of radioactivity present was quantified by gamma scintillation counting (Wallac Wizard 1480 automatic gamma counter, PerkinElmer, Waltham, MA).

4.3.8 Antitumor Activity and Survival Studies

FTLs composed of DSPC/Chol/mPEG2000-DSPE/FA-PEG-DSPE (55:40:5:0.03) and NTLs were formulated as listed in Table 1. The lipid mixtures were dissolved in chloroform, dried into a thin film by rotary evaporation, and placed under high vacuum overnight. The lipid films were rehydrated with 1 mL of 250 mM ammonium sulfate at 60 °C, vortexed, and then subjected to three freeze thaw cycles. The liposomes were sonicated at 60 °C and extruded through 200 nm and 100 nm polycarbonate membranes. The formulations were added to a dialysis cassette (10, 000 MWCO) and dialyzed against 5% dextrose at 4 °C. Then Dox was remote loaded into the liposomes at a 0.1/1 drug to lipid molar ratio for 1 hr at 65 °C. To separate the liposome encapsulated Dox from unencapsulated Dox, a column packed with Dowex 50 Wx4 resin was used. The encapsulated Dox concentration was determined after dissolving a liposome sample into acidified isopropryl alcohol (90% isopropryl alcohol, 75 mM HCl) and comparing the

fluorescence (ex 490 nm, em 585 nm) to a standard curve prepared in the same solvent. The remote loading efficiency was ~90% for all formulations. The liposome diameter and particle size distribution were measured by dynamic light scattering. The mean liposome diameter was ~120 nm for all formulations.

Balb/c nu/nu mice were placed on a folate-free diet two weeks before tumor inoculation and maintained on the special feed throughout the study. KB cells (10^6), resuspended in 50 μL folate free RPMI 1640 medium without serum, were inoculated subcutaneously in the right hind flank of each mouse. On Day 8 after tumor implantation, mice were randomly distributed into treatment groups of 7-8 mice. On Day 10 after tumor implantation, the tumors were 30-60 mm^3. Each formulation (200 μL) was administered by a single tail vein injection. Tumor volume was determined by measuring the tumor in three dimensions with calipers and calculated using the formula: tumor volume = length x width x height. Mice were sacrificed due to tumor burden (volume ≥ 2000 mm^3) or decrease in body weight (> 15% loss). The percent tumor growth delay (%TGD) was calculated from the equation %TGD = (T-C)/C x 100, where T is the average time for the tumor volume of a treatment group to reach a designated volume of 500 mm^3 and C is the mean time for the control group to reach the designated volume of 500 mm^3. Mouse survival was analyzed by using MedCalc 8.2.1.0 for Windows (MedCalc Software, Mariakerke, Belgium).

4.4 Results

4.4.1 Effect of Ligand Density and PEG on Folate Targeting to KB Cells in vitro

To determine the optimum ligand concentration for folate targeting to KB cells, we evaluated the cellular association of FITC labeled FTLs with varying mole

percentages of FA-PEG2000-DSPE by flow cytometry. As depicted in Figure 4.2, FTL association with KB cells was dependent on ligand concentration. $F_{2000}L$ with 0.03 mol% of FA-PEG2000-DSPE - $F_{2000}L(0.03\%)$ - had the greatest mean fluorescence (~14 fold above blank) and the most association to KB cells compared to the other formulations ($p<0.05$). In fact, increasing the ligand density to 0.1 mol% decreased the cellular association to 11 fold above blank. In addition, $F_{2000}L(0.5\%)$ had a similar cellular association as $F_{2000}L$ (0.01%). Therefore, these results demonstrated that as little as 0.03 mol% of the ligand was optimal for binding.

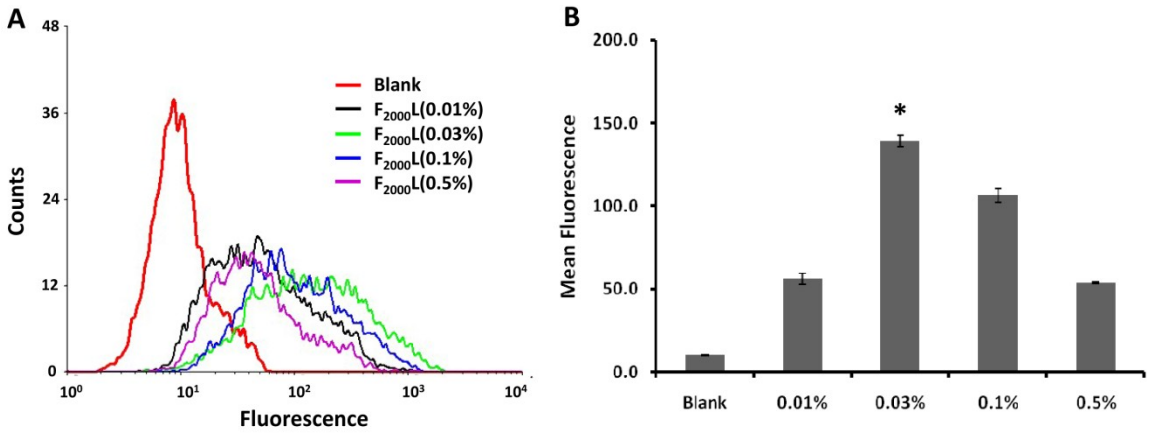

Figure 4.2 Cell association of FTLs of varying FA-PEG(2000)-DSPE mole percentages with KB cells. Cells were incubated with liposomes labeled with FITC-DSPE and containing either 0.01, 0.03, 0.1, or 0.5 mole% of Folate-PEG(2000)-DSPE for 3 hours at 37 °C and analyzed by flow cytometry. **A**. Flow cytometry spectrum. **B.** Mean fluorescence of formulations. Data shown as average ± standard deviation of at least two measurements. ***** Statistical significance ($p<0.05$) between cells treated with $F_{2000}L(0.03\ \%)$ and other $F_{2000}L$ groups as measured by Student's t-test of the geometric mean of the fluorescence.

We next examined the cell association of FTLs with and without mPEG2000-DSPE by flow cytometry. The data in Figure 4.3 (A and C) demonstrate that additional PEG significantly decreased the cellular association of FTLs. $F_{2000}PL$ had about 5 fold less association than $F_{2000}L$ ($p < 0.01$), and $F_{3350}PL$ had approximately 3 fold less cell association than $F_{3350}L$ ($p < 0.01$). The cellular association of $F_{2000}PL$ and $F_{3350}PL$ were similar. Co-incubation of $F_{2000}L$ and $F_{3350}L$ with 2mM folic acid further reduced the

cellular association, thus demonstrating the specific binding of the FTLs to the KB cells. The cellular association of PLs was similar to the cell association of FTLs + 2 mM FA (data not shown). After 24 hr incubation of cells with the formulations (Figure 4.3 B and D), the cellular association of $F_{2000}PL$ was approximately 9 fold less than $F_{2000}L$ ($p < 0.01$) whereas the cellular association of $F_{3350}PL$ was only about 2 fold less than $F_{3350}L$. Again, the KB cellular association of $F_{2000}PL$ and $F_{3350}PL$ were similar.

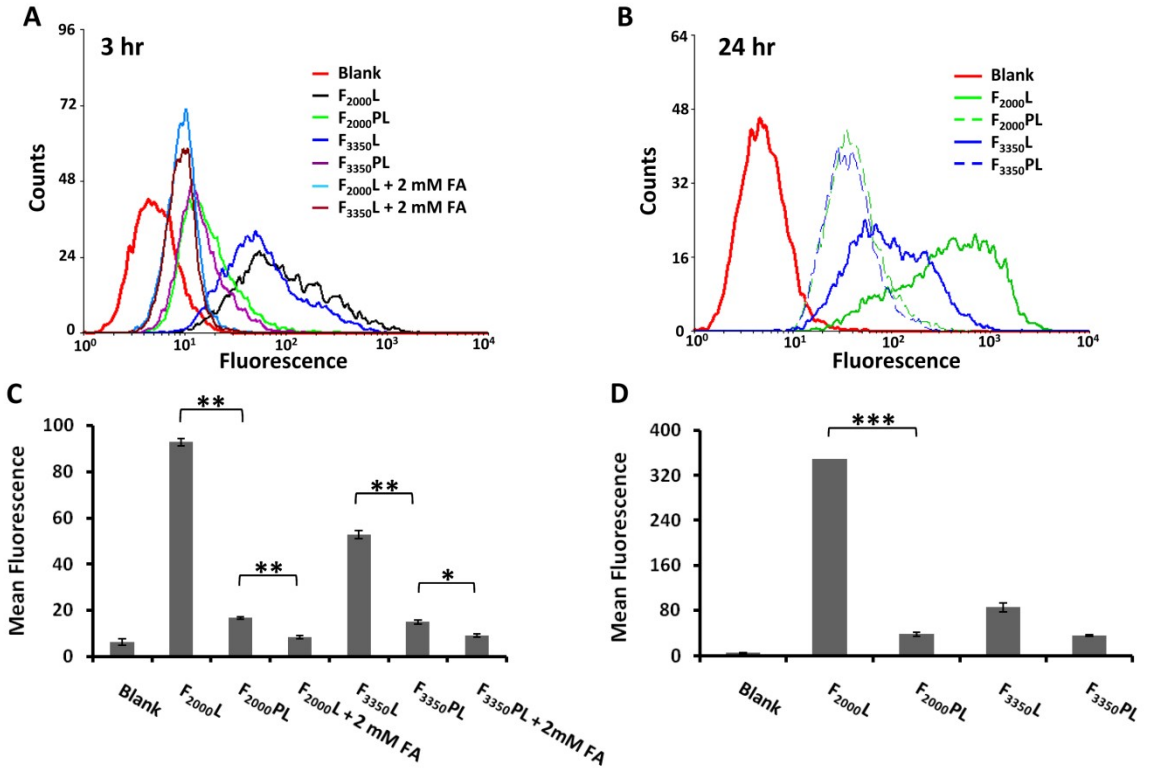

Figure 4.3 Cell association of FTLs with and without mPEG2000-DSPE. Cells were incubated with liposomes labeled with FITC-DSPE and containing 0.03 mole % of Folate-PEG(2000)-DSPE or Folate-PEG(3350)-DSPE and analyzed by flow cytometry. **A, C.** 3 hour incubation at 37 °C. **B, D.** 24 hr incubation at 37 °C. Data shown as average ± standard deviation of at least two measurements. ***** $p<0.05$, ****** $p<0.01$, *******$p<0.005$ as measured by Student's t-test of the geometric mean of the fluorescence.

4.4.2 Blood Concentration Profile and Biodistribution of FTLs

The circulation profile and biodistribution properties of the PEGylated FTL formulations with various ligand densities were studied in KB tumor mouse model. Figure 4.4 illustrates the circulation profile of the various FTL formulations. There were

more PLs present in the circulation at the measured time points compared to all the FTL formulations. There was no significant difference among the various F_{2000}PL formulations at 3, 24 or 48 hr. However, the ligand density affected the circulation properties of the various F_{3350}PL formulations. There was significantly more F_{3350}PL (0.03%) than F_{3350}PL(0.3%) in the blood at 24 hr and 48 hr ($p<0.05$). Also, there was significantly more F_{3350}PL(0.1%) than F_{3350}PL(0.3%) in the blood at 48 hr ($p<0.05$). Thus, there was a trend that FTLs with lower mol% of the targeting ligand circulated longer.

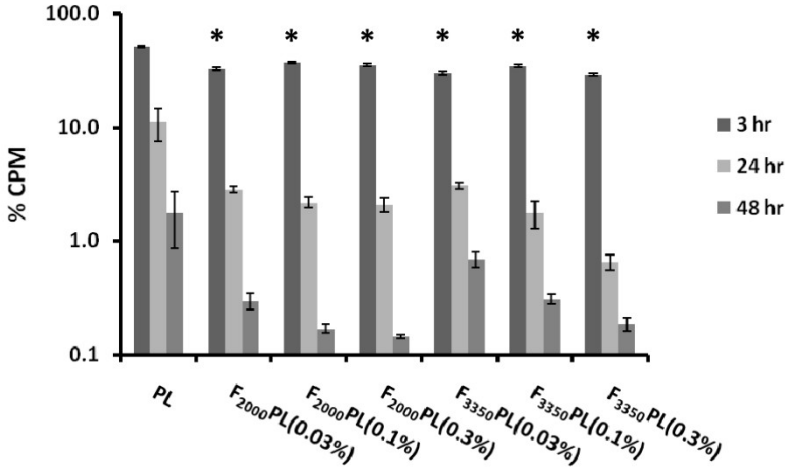

Figure 4.4 Blood circulation profile of FTLs with varying FA-PEG-DSPE mole percentages in KB tumored Balb/c nu/nu mice. Blood was collected by submandibular puncture at 3 hr and 24 hr and by heart puncture at 48 hr after i.v. injection of 1 µmol lipid/mouse (n=3 mice). The values are presented as mean ± standard deviation. *****Statistical significance between PL compared to all other formulations at 3 hr time point ($p < 0.05$) as measured by Student's t-test.

We also investigated the biodistribution of the various PEGylated FTL formulations in the blood, tumor, liver, spleen and muscle tissue 48 hr post-injection (Figure 4.5). Although there were some differences in the blood circulation profiles of the various formulations as described above, there were no significant differences in the tumor accumulation. F_{2000}PL(0.03%) had significantly more liver uptake compared to the PL ($p < 0.01$) and other FTL formulations ($p<0.05$). Furthermore, F_{3350}PL(0.03%) had

significantly more spleen uptake as compared to $F_{2000}PL$ (0.03%) ($p < 0.05$) and the other $F_{3350}PL$ formulations ($p < 0.05$). Thus, the FTLs with the lower ligand density and the longer PEG spacer had enhanced uptake by the liver and spleen. Despite the longer systemic circulation of PLs and the increased RES uptake of FTLs, all the formulations had similar levels of tumor accumulation.

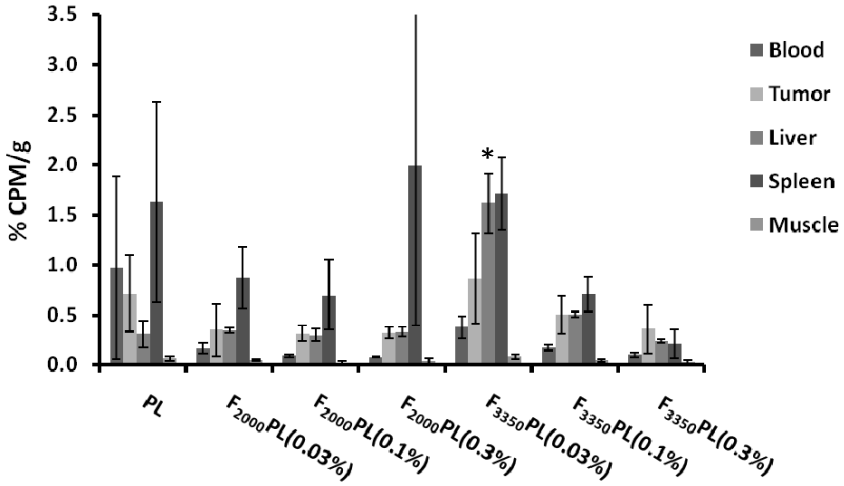

Figure 4.5 Biodistribution of radiolabeled FTLs and PLs in KB tumored Balb/c nu/nu mice sacrificed 48 hr after i.v. injection of 1 μmol lipid/mouse (n=3 mice). The values are mean ± standard deviation. *****Statistical significance between $F_{3350}PL(0.03\%)$ compared to all other formulations ($p<0.05$) as measured by Student's t-test.

4.4.3 Effect of FTL-Dox on Tumor Growth and Survival Rate

The antitumor activity of Dox encapsulated in PLs (PL-Dox) and in $F_{3350}PL(0.03$ mol%), $F_{3350}PL(0.03\%)$-Dox, after a single intravenous tail injection in KB tumor-bearing mice was evaluated. As depicted in Figure 4.6, all the liposomal formulations were more effective than PBS and Dox 10 mg/kg as expected. $F_{3350}PL(0.03\%)$-Dox 10 mg/kg and PL-Dox 10 mg/kg had similar antitumor activity and had the same TGD of 43% (Table 4.2). $F_{3350}PL(0.03\%)$-Dox 20 mg/kg had the greatest therapeutic efficacy with 86% TGD. NTL-Dox 20 mg/kg had the second best therapeutic effect with 64% TGD. However, the difference between the tumor volumes of $F_{3350}PL(0.03\%)$-Dox 20

mg/kg and PL-Dox 20 mg/kg groups were not statistically significant. Table 4.3 summarizes the statistical comparisons of the tumor growth inhibition data.

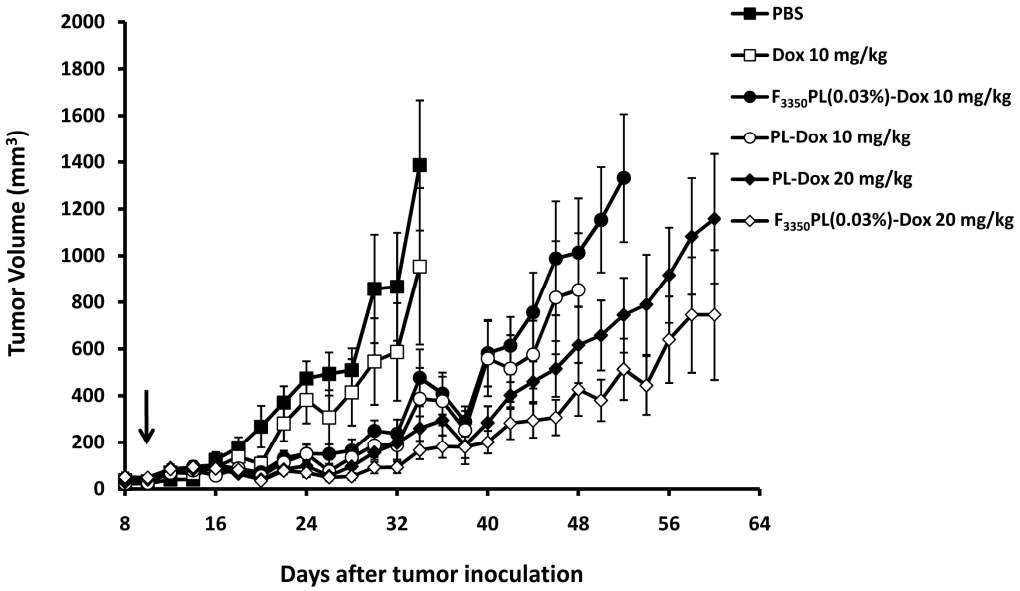

Figure 4.6 Antitumor activity of PL-Dox and F_{3350}PL(0.03%)-Dox. KB tumored Balb/c nu/nu mice (n=7 or 8) were treated with a single i.v. injection on Day 10 (as indicated by arrow). Error bars represent SEM.

Table 4.2 Quantification of Antitumor and Survival Data

Formulation	TGD (%)	MST (Days)	ILS (%)
PBS	-	47 ± 19	-
Dox 10 mg/kg	7	58 ± 21	21
PL-Dox 10 mg/kg	43	67 ± 19	42
F_{3350}PL(0.03%)-Dox 10 mg/kg	43	55 ± 7	16
PL-Dox 20 mg/kg	64	55 ± 22	16
F_{3350}PL(0.03%)-Dox 20 mg/kg	86	78 ± 12	65

TGD - tumor growth delay; MST - mean survival time; ILS - increase in life span

Table 4.3 Multiple Statistical Comparison of Average Tumor Size Data*

	PBS	Dox 10 mg/kg	PL-Dox 10 mg/kg	F_{3350}PL(0.03%)-Dox 10 mg/kg	PL-Dox 20 mg/kg	F_{3350}PL(0.03%)-Dox 20 mg/kg
PBS	-	NS	0.0108	0.016	0.0064	0.0045
Dox 10 mg/kg	NS	-	NS	NS	NS	NS
PL-Dox 10 mg/kg	0.0108	NS	-	NS	NS	NS
F_{3350}PL(0.03%)-Dox 10 mg/kg	0.016	NS	NS	-	NS	NS
PL-Dox 20 mg/kg	0.0064	NS	NS	NS	-	NS
F_{3350}PL(0.03%)-Dox 20 mg/kg	0.0045	NS	NS	NS	NS	-

* p values determined by Student's t-test. $p > 0.05$ considered not significant (NS).

The effect of the NTL-Dox and FTL-Dox formulations at the maximum tolerated dose on the survival rate of the KB tumored mice is shown in Figure 4.7. Mice treated with F_{3350}PL(0.03%)-Dox 20 mg/kg had the longest mean survival time and the highest percent increase in life span (Table 4.2). The F_{3350}PL(0.03%)-Dox 20 mg/kg group lived significantly longer than the PL-Dox 20 mg/kg group ($P = 0.0121$; log-rank test). These findings in combination with the antitumor data indicate that F_{3350}PL(0.03%)-Dox 20 mg/kg is therapeutically more effective than PL-Dox 20 mg/kg in treating KB tumors even after only a single intravenous tail vein injection. Table 4.4 summarizes the statistical comparisons of the survival data.

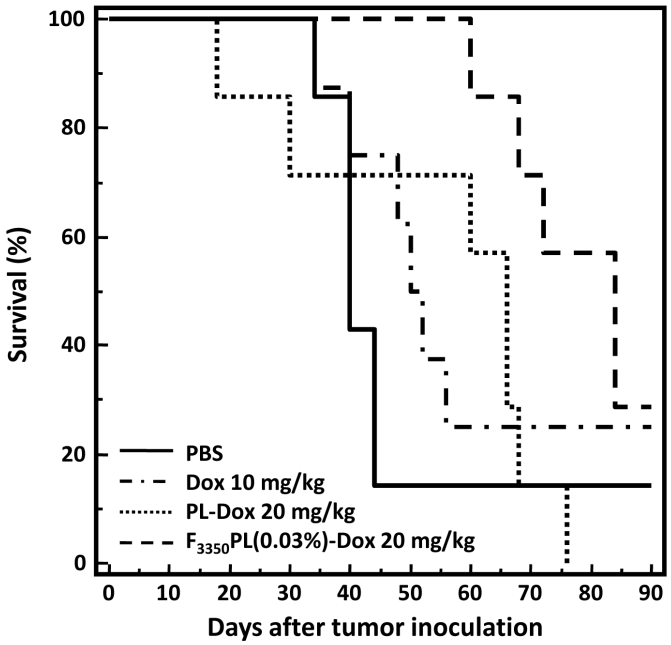

Figure 4.7 Effect of PL-Dox and F_{3350}PL(0.03%)-Dox on the survival of KB tumored Balb/c nu/nu mice. Mice (n=7 or 8) were treated with a single i.v. injection on Day 10. The F_{3350}PL(0.03%)-Dox 20 mg/kg group lived significantly longer than PL-Dox 20 mg/kg group (p = 0.0121; log-rank test).

Table 4.4 Multiple Statistical Comparison of Survival Data*

	PBS	Dox 10 mg/kg	PL-Dox 10 mg/kg	F_{3350}PL(0.03%)-Dox 10 mg/kg	PL-Dox 20 mg/kg	F_{3350}PL(0.03%)-Dox 20 mg/kg
PBS	-	NS	0.0437	NS	NS	0.049
Dox 10 mg/kg	NS	-	NS	NS	NS	NS
PL-Dox 10 mg/kg	0.0437	NS	-	NS	NS	NS
F_{3350}PL(0.03%)-Dox 10 mg/kg	NS	NS	NS	-	NS	NS
PL-Dox 20 mg/kg	NS	NS	NS	NS	-	0.0121
F_{3350}PL(0.03%)-Dox 20 mg/kg	0.049	NS	NS	NS	NS	-

* p values determined by long-rank test. p > 0.05 considered not significant (NS).

4.5 Discussion

The purpose of this study was to evaluate folate-targeted liposome drug delivery and assess whether this targeting strategy has the potential to enhance cancer therapy. We focused our efforts on the KB tumor cell line since it is a model cell line for FR targeted delivery.

We first synthesized folate lipid conjugates then prepared and characterized various FTLs formulations. We found that including only 0.03 mol% of the folate ligand in the liposome formulations resulted in the best liposome cell association to KB cells *in vitro* (Figure 4.2). This result was consistent with previous findings [99, 100]. Reddy and coworkers hypothesized that only a small density of ligands are optimal for binding because folates can bind to each other at high surface densities and inhibit binding to FRs [99]. Additionally, an optimal folate ligand density can depend on a number of factors: the accessibility of the folate moiety, PEG length, PEG-folate chemical linkage, and type of folate-lipid conjugate [99-102]. PEG is widely used in lipsome formulations because it is known to prolong the retention of the liposomes in the systemic circulation and to enhance tumor accumulation [21]. We investigated whether the presence of PEG in the liposome formulation decreases FTL cell association since there are divergent views on the influence of PEG on folate-mediated targeting [96, 103, 104]. We found that the presence of PEG in the liposome decreases FTL cell association. We also determined that PEGylated liposomes with FA attached via a PEG2000 spacer or a PEG3350 spacer had equivalent levels of binding to KB cells (Figure 4.3).

An increase in folate ligand density decreased the circulation lifetime of FTLs and increased the fraction of the dose in the spleen. In spite of this more rapid elimination of FTLs (Figures 4.4 and 4.5), the PLs and FTLs equivalently distributed to the tumor tissue. The fact that FTLs were cleared faster from blood but accumulated similarly in the tumor tissue as PLs suggests that the FTLs were targeting to KB cells *in vivo*. It is interesting that F_{3350}PL at the optimal binding density of 0.03 mol % is targeted to the liver significantly more than the other formulations yet has a comparable level of tumor

accumulation after 48 hrs. Similar findings have been previously reported [101, 105]. Putting the mice on a folate-free diet may have led to upregulation of FR in the liver, spleen, and kidney in addition to the tumor tissue [103]. This may lead to increased clearance of FTL drugs and further compromise FTL accumulation in tumor tissue.

There are few studies reporting on the antitumor efficacy of FTL therapeutics *in vivo*. Pan and coworkers have found that F_{3350}PL-Dox 5 mg/kg administered via three i.p. injections improved the survival of mice bearing murine lymphocytic L1210-JF FR+ cell ascites more than mice receiving PL-Dox 5mg/kg ($P = 0.0259$; log-rank test) [106]. KB tumor-bearing mice treated with F_{3350}PL-Dox 10 mg/kg via six i.p. injections had greater tumor growth inhibition and a slight increase in lifespan compared to mice treated with PL-Dox [43]. However, in mice bearing murine lung carcinoma M109 FR+ tumors, F_{5000}PL-Dox 8 mg/kg administered after a single intravenous injection had a lower tumor-killing effect than PL-Dox 8 mg/kg [107]. Therefore, the literature is unclear whether there is a therapeutic advantage of folate-targeted delivery.

Although KB cells have been widely utilized for investigating folate targeting to FR+ cells, there are no studies reporting on the efficacy of FTL therapeutics after intravenous administration in KB tumor-bearing mice. This motivated us to further investigate the therapeutic efficacy of FTL-Dox in a KB tumor mouse model (Figures 4.6 and 4.7). We found that KB tumor-bearing mice treated with a single i.v. injection of F_{3350}PL(0.03%)-Dox 20 mg/kg had a slightly greater tumor growth inhibition and longer life span than mice treated with PL-Dox at the same dose ($P=0.0121$; log-rank test). This result is surprising given that the FTLs were cleared faster than PLs. However, F_{3350}PL(0.03%)-Dox 10 mg/kg was slightly less effective than PL-Dox 10 mg/kg. The

enhanced therapeutic efficacy of F_{3350}PL (0.03%)-Dox compared to PL-Dox at the higher dose could be explained by saturation of RES uptake mechanisms since at the higher dose, there is an increase in the lipid concentration. Therefore, more of the FTLs are able to reach the tumor tissue.

The pharmacokinetic, biodistribution, and antitumor results imply that minimizing folate targeting to the liver and other tissues of the RES may help to improve the antitumor efficacy of FTL drugs. Gabizon and coworkers investigated the effect of co-dosing FTLs with free FA on FTL biodistribution. They determined that co-dosing with free FA significantly reduced FTL liver uptake as well as clearance from the blood, but had neglible effect on FTL accumulation in tumors [101]. They explained that free folic acid inhibits FTLs from being taken up by Kuppfer cells in the liver via receptor mediated endocytosis. However, co-dosing with free FA did not affect the tumor accumulation of FTLs because the distribution of the FTLs in tumor tissue is primarily due to passive extravasation via the enhanced permeation and retention (EPR) effect [22] rather than ligand-mediated targeting. Therefore, increasing the circulation time of FTLs might enhance tumor localization of folate-targeted liposomes. One tactic to accomplish this may be to decrease the folate ligand density below the optimal concentration so as to minimize binding to non-target, FR expressing tissues, and thus enhance the circulation time and tumor accumulation. Alternatively, masking the folate ligand with a longer PEG that can be removed from the liposome surface may enable the FTLs to avoid clearance in the liver [108]. The decreased binding avidity of the FTLs may also lead to their increased penetration into the solid tumor [38].

Overall, our studies indicate that under certain conditions folate targeting can improve delivery and efficacy of liposome drug carriers to tumors. We observed that *in vitro* optimization of folate targeting does not necessarily translate to an enhancement in *in vivo* targeting to FR+ tumors. Further modification of FTLs to reduce liver and spleen uptake may increase FTL circulation time and therefore enhance the tumor accumulation and antitumor efficacy of FTL therapeutics.

CHAPTER 5:
Therapeutic Activity of Folate Targeted Liposome Co-encapsulated Irinotecan and Fluoroorotic Acid in a KB (FR+) Tumor Model

5.1 Abstract

We propose that targeted liposomes can enhance the efficacy of synergistic anticancer drug combinations *in vivo* by facilitating the intracellular co-delivery of multiple agents at their synergistic ratio and dose. To investigate this hypothesis, we first determined in an *in vitro* cytotoxicity assay in KB folate receptor over-expressing cells that irinotecan (IRN) and fluoroorotic acid (FOA) were highly synergistic at a 1:1 molar ratio. We devised a liposome drug loading procedure that solubilized FOA in 7 M urea, then used the encapsulated FOA as the agent to remote load irinotecan into the liposome. This method achieved a synergistic ratio of 1:1 with a high concentration of the two drugs in the liposome. Encapsulation of the irinotecan with the FOA had the beneficial effect of reducing the leakage of FOA from the liposome compared to when it was encapsulated as a single agent. The reduced leakage of FOA helped to maintain the IRN/FOA ratio closer to 1:1 than when the drugs encapsulated in separate liposomes were mixed to create a 1:1 drug ratio. KB tumor-bearing Balb/c nu/nu mice were treated with the IRN at 50 mg/kg, free FOA 100mg/kg, or the single agents encapsulated in non-targeted liposomes (NTLs) or folate targeted liposomes (FTLs; IRN = 50 mg/kg, FOA = 10 mg/kg) on Days 10 and 17. The order of tumor growth suppression was NTL-IRN = FTL-IRN > IRN = FOA = FTL-FOA > NTL-FOA > PBS. Treatment with FTL-IRN, NTL-IRN, FOA, FTL-FOA resulted in similar increase in survival time. In the combination experiment, 25 mg/kg

IRN and 6.4 mg FOA were administered on Days 10, 17, and 24 in either individual NTLs /FTLs, mixtures of the two individual drugs in NTLs/FTLs at a 1:1 ratio, or in NTLs/FTLs with the two agents co-encapsulated at the 1:1 ratio. The mixture of NTL drugs provided a statistically superior increase in tumor growth delay and mean survival time compared to the free drug combination and other NTL co-formulations. The FTL co-encapsulated formulation provided a statistically superior increase in tumor growth delay and mean survival time compared to the free drug combination and other FTL co-formulations. The non-targeted mixture and folate-targeted combination were equivalent in their anti-tumor activity in the KB model. Thus, combination dosing was superior to treatment with the single agents; however, delivering the drugs in folate-targeted liposomes did not provide a therapeutic advantage over drug delivery in the non-targeted liposome in the KB tumor model.

5.2 Introduction

Drug cocktails are commonly used to treat life-threatening diseases such as cancer. The underlying principle behind this practice is that multiple drugs can act against the diverse targets implicated in disease progression. Combination chemotherapy regimens have the potential to be extremely effective without causing dose limiting toxicity if the drugs are synergistic. Drug synergism occurs when the combined effect of two or more drugs is more than additive. A rational and cost-effective way to determine what drugs will synergize is to systematically screen different drug combinations at various ratios and concentrations in cell culture. What is evident from such *in vitro* studies is that drug synergism is dependent on the ratio and dose of the combined drugs [33, 109]. Even slight alterations in drug ratios can transform a synergistic effect into an

antagonistic (less than additive) effect. As a consequence, synergistic drug combinations administered *in vivo* maintained at the synergistic ratio range identified *in vitro* may maximize therapeutic activity.

Recent reports show that synergistic drug combinations encapsulated in liposomal drug carriers have superior efficacy compared to the free synergistic drug combinations *in vivo* [27, 31, 32]. Liposomes are effective drug combination vehicles because they can control the pharmacokinetic properties of the encapsulated drugs in a manner that allows the drug combination to reach target cells at the optimal ratio and concentration [33, 34]. It seems logical that receptor-targeted liposomes can further enhance the efficacy of synergistic anticancer drug combinations *in vivo* by maintaining the optimal ratio and concentration that is delivered intracellularly to tumor cells.

To investigate this hypothesis, we used folic acid to target liposome encapsulated synergistic drug combinations to KB folate receptor (FR) over-expressing human nasopharyngeal cancer cells. Folate binds to FR with high affinity (K_d = 0.1 nM) and is internalized via receptor-mediated endocytosis [40]. FR is a 38 kDa glycosyl-phosphatidylinositol membrane anchored glycoprotein that is over-expressed on many tumor types, but is present at low levels in normal epithelial tissue. Folate-targeted liposomes (FTL) have successfully delivered diverse therapeutic agents into FR over-expressing tumor cells *in vitro* and *in vivo* [42, 43, 94, 95, 100, 105, 107]. Hence, folate-mediated targeting of liposomes is an appropriate system to investigate whether the intracellular delivery of a fixed synergistic ratio and dose will enhance the *in vivo* efficacy of synergistic anticancer drug combinations.

This chapter discusses the studies undertaken to investigate the influence of folate targeted liposome delivery on the *in vivo* efficacy for the synergistic IRN + FOA drug pair.

5.3 Methods

5.3.1 Materials

5-Fluoroorotic acid (FOA) was purchased from Research Products International (Mt. Prospect, Illinois). Irinotecan-HCl trihydrate (IRN) was purchased from Ivy Fine Chemicals (Cherry Hill, NJ). Cholesterol (Chol) and sulforhodamine B (SRB) were products of Sigma-Aldrich (St. Louis, MO). Distearoylphosphatidylcholine (DSPC) and methoxy-polyethylene glycol (MW2000)-DSPE (mPEG2000-DSPE) were purchased from Genzyme (Cambridge, MA). KB cells were purchased from the University of California, San Francisco Cell Culture Facility. Folate-free RPMI 1640 media was acquired from Invitrogen (Carlsbad, CA). Folate-free chow was a product of Harlan Teklad (Madison, WI). The folate-PEG3350-DSPE lipid was synthesized, purified and characterized by MALDI-TOF and NMR following a modified procedure of Stephenson and coworkers (see Chapter 4) [97].

5.3.2 Cell Culture

KB human nasopharyngeal cells were maintained in folate-free RPMI 1640 media supplemented with 10% fetal calf serum that provides the only source of folic acid. The cells were cultured as a monolayer in 5% CO_2 at 37 °C.

5.3.3 Cytotoxicity Assay

KB cells were seeded in 96 well plates and incubated for 24 hr at 37 °C to allow for cell attachment. IRN+FOA in a fixed ratio (10:1, 5:1, 1:1, 1:5, and 1:10) were

simultaneously added to cells at eight doses that capture the full range of cytotoxicity of the most potent drug. The cells were continuously exposed to the single drugs and pairs of drugs for 72 hr at 37 °C. Each concentration was tested in triplicate per plate. Each data set was repeated three times. Cytotoxicity was evaluated using the (SRB) assay [85]. Briefly, the cells were fixed with 50 % trichloroacetic acid and stained for 30 min with 0.4% SRB in 1% acetic acid (w/v). Then, the protein bound dye was solubilized with 10 mM unbuffered Tris base, and the absorbance of each well was measured at 564 nm.

5.3.4 Drug Interaction Analysis

Dose-effect curves consisting of eight data points were generated for each drug alone and in the combinations. The effect for each concentration was normalized to the untreated controls as a percent of cell survival and then converted to fraction of affected cells. CalcuSyn software (Biosoft, Ferguson, MO) was used to analyze the drug interaction between IRN and FOA. This program uses the median effect principle to determine the combination index (CI) that quantitatively describes the degree of synergism or antagonism of a drug interaction [1, 15]. Synergism is indicated for $CI < 1$, additivity for $CI = 1$, and antagonism for $CI > 1$.

5.3.5 Preparing Liposomal IRN

Non-targeted liposomes (NTLs) were composed of DSPC:Chol:mPEG-DSPE at a 55:40:5 molar ratio while folate targeted liposomes (FTLs) were composed of DSPC:Chol:mPEG-DSPE: FA-PEG3350-DSPE at a 55:40:5:0.03 molar ratio. This mole ratio of folate ligand provides the best binding enhancement to KB cells in vitro. Lipid mixtures were dissolved in chloroform and dried into a thin film by rotary evaporation under reduced pressure then placed under high vacuum overnight. The films were subsequently

hydrated with 300 mM butane tetracarboxylic acid (adjusted to pH 5.0 with NH_4OH) at 60 °C and vortexed to obtain a lipid concentration of 100 mM. The liposomes were then sonicated at 65 °C and extruded through 200 nm and 100 nm polycarbonate membranes (Avestin, Ottawa, CA) at 65 °C. The preparations were exchanged into 5 mM Hepes, 5% dextrose pH 6.5 by size exclusion chromatography using a Sephadex G25 column. IRN was loaded by incubating the drug with liposomes (0.2/1 drug to lipid molar ratio) at 65°C for 1 hr. The liposome preparations were exchanged into Hepes buffer (5 mM Hepes, 140 mM NaCl pH 7.4) by size exclusion chromatography using a Sephadex G25 column. To measure the encapsulated IRN concentration, an aliquot of the liposomes was mixed with 1% Triton X-100, heated to 100°C until the cloud point was reached, and cooled down to room temperature. The encapsulated IRN concentration was determined by comparing the absorbance at 370 nm to an IRN standard curve in the appropriate buffer. The liposome diameter and particle size distribution were measured by dynamic light scattering on a Zetasizer 3000 (Malvern Instruments, Westborough, MA). The average liposome diameter was ~100 nm.

5.3.6 Preparing Liposomal FOA

The same lipid mixtures were used for the FOA encapsulation and processed as described above. The films were subsequently hydrated with 500 mM FOA in 7 M urea (adjusted to pH 7 with triethylamine) at 65 °C and vortexed to obtain a lipid concentration of 50 mM. The preparations were then sonicated at 65 °C, added to a dialysis cassette (10,000 MWCO), and dialyzed against 500 ml of 5 mM Hepes, 5% dextrose pH 7.4. To assay for the encapsulated FOA, liposome samples were diluted with phosphate buffered saline (PBS; 2.16 g/L Na_2HPO_4 $7H_20$, 0.2 g/L KH_2PO_4, 0.2 g/L KCl, 8.0 g/L NaCl) and mixed with methanol:chloroform (1:1:1 v/v/v), vortexed, and centrifuged at 1000 rpm for 10

min. Then the upper phase was mixed with 1M HCl. The encapsulated FOA concentration was determined by comparing the absorbance at 284 nm to a standard curve prepared with a solution from a blank extraction. The liposome diameter and particle size distribution were measured by dynamic light scattering. The average liposome diameter was ~120 nm.

5.3.7 Liposome Coencapsulation of IRN and FOA

The same lipid mixtures were processed to the thin film stage as described above. The lipid films were subsequently hydrated with 500 mM FOA in 7 M urea (adjusted to pH 7 with triethylamine) at 65 °C and vortexed to obtain a lipid concentration of 50 mM. The preparations were subsequently sonicated at 65 °C, added to dialysis cassettes (10,000 MWCO), and dialyzed against 500 ml of 5 mM Hepes, 5% dextrose pH 6.5. IRN was loaded by incubating the drug with liposomes (0.1375/1 drug to lipid molar ratio) at 50°C for 10 min to achieve a 1:1 encapsulated molar ratio of IRN + FOA. The liposome preparations were exchanged into Hepes buffer (5 mM Hepes, 140 mM NaCl pH 7.4) by size exclusion chromatography using a Sephadex G25 column. To assay the drug content of the liposomes, an aliquot was mixed with 1% Triton X-100, heated to 100°C until the cloud point was reached and then cooled to room temperature. The encapsulated IRN concentration was determined by comparing the absorbance at 370 nm to a standard curve. A second liposome aliquot was diluted with PBS and mixed with methanol:chloroform (1:1:1 v/v/v), vortexed, and centrifuged at 1000 rpm for 10 min. Then the upper phase was mixed with 1M HCl. The encapsulated FOA concentration was determined by 1) calculating the absorbance due to FOA in the coformulation at 284 nm according to the equation $(A284)_{FOA} = (A284)_{FOA+IRN} - R(A284)_{IRN}$ where R = [IRN

Dilution Factor / FOA Dilution Factor] and 2) comparing $(A284)_{FOA}$ to a standard curve. The liposome diameter and particle size distribution were measured by dynamic light scattering. The average liposome diameter was ~120 nm.

5.3.8 Drug Release Studies

Liposome formulations were incubated in 33% fetal bovine serum at 37 °C. At selected time-points, samples (in triplicate) were exchanged into 5 mM Hepes, 140 mM NaCl pH 7.4 by size exclusion chromatography using a Sepharose 4B-CL column. Drug concentrations were determined as described above.

5.3.9 Animals

Balb/c nu/nu mice (8-10 weeks) were obtained from Simonsen Laboratories, Inc. (Gilroy, CA). Animal maintenance and experiments adhered to the NIH principles of laboratory animal care under a protocol approved by the Committee on Animal Research at the University of California, San Francisco.

5.3.10 Liposomal IRN and FOA Individual and Combination Therapy in KB Model

Balb/c nu/nu mice were put on a folate-free diet two weeks before tumor inoculation and maintained on the special feed until Day 30 of the study. KB cells (10^6) suspended in 50 μL folate free RPMI 1640 medium without serum were inoculated subcutaneously in the right hind flank of each Balb/c nu/nu mouse. On Day 10 after tumor implantation, mice were randomly distributed into treatment groups (n = 8 - 10). Each formulation (~200 μL) was administered by tail vein injection on Days 10 and 17 for individual therapy studies and on Days 10, 17 and 24 for combination therapy studies. Tumor volume was determined by measuring the tumor in three dimensions with calipers and calculated using the formula: tumor volume = length x width x height. The tumor

growth delay (TGD) was calculated from the equation TGD = (T-C)/C x 100, where T is the mean time for the tumor volume of a treatment group to reach a designated volume of 500 mm^3 and C is the mean time of the control group to reach the designated volume of 500 mm^3. Mice were sacrificed due to tumor burden (volume $\geq$ 2000 mm^3) or decrease in body weight (> 20% loss). Mouse survival was analyzed by using MedCalc 8.2.1.0 for Windows (MedCalc Software, Mariakerke, Belgium).

5.4 Results

5.4.1 Combination Activity of IRN and FOA in KB Cells

After screening an array of two drug pairs in KB cells (see Chapter 2), we determined that the combination of irinotecan (IRN) and fluoroorotic acid (FOA) was the most synergistic. FOA also has the advantage in that it is a liposome dependent drug, that is the activity of liposome encapsulated FOA increases compared to the free compound when it trafficks into the endosome in the liposome [80, 87]. We evaluated the combination activity of five molar ratios of IRN and FOA using the median effect method. Figure 5.1A shows the results of the screen for different doses of IRN and FOA at fixed molar ratios added simultaneously and continuously exposed to KB cells for 72 hrs. Figure 5.1B shows the combination index (CI) values at the concentrations causing 50%, 75%, and 90% tumor growth inhibition (E50, EC75 and EC90 that correspond to f_a = 0.5, 0.75 and 0.9 respectively). The CI values varied as a function of drug ratio and dose. For all the ratios tested, antagonism (CI > 1) was observed at the low fractions affected (low concentrations). However, the 1:10 molar ratio also showed antagonism at the higher fractions affected. Synergism (CI < 0.9) occurred for the 10:1, 5:1, 1:1, and 1:5 molar ratios, particularly at the high drug concentrations (high fractions affected). In a

chemotherapy situation, one is striving to reach a high fraction of cells affected; thus, we consider synergy estimations using f_a values greater than 0.5 to be more predictive for drug pairs that are good candidates for a tumor treatment. Based on this criterion, the 5:1 and 1:1 molar ratios were the most synergistic (CI <0.5 at ED90 and higher).

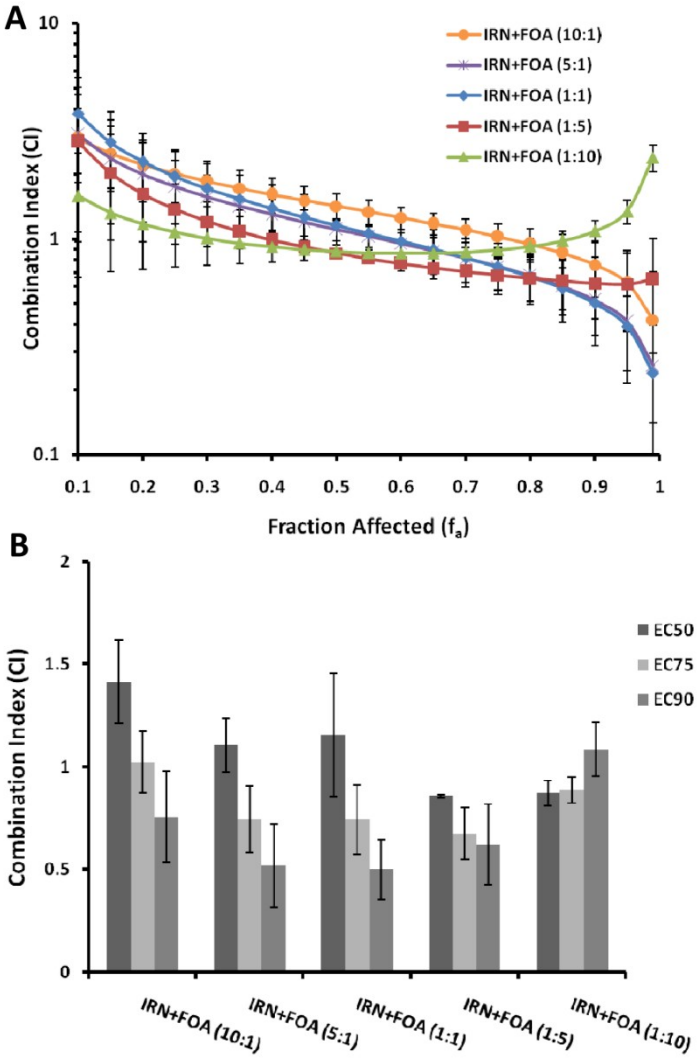

Figure 5.1 *In vitro* combination activity of IRN and FOA at fixed dose ratios in KB cells. Data shown here include additional replicates not performed for data in Chapter 2. **A**. Combination index (CI) plot for various ratios of IRN + FOA. CI < 0.9 indicates synergy, 0.9 < CI < 1.1 indicates additivity, and CI > 1.1 indicates antagonism. The points displayed are CI values ± standard deviation at various f_a simulated by CalcuSyn software based upon the data from the cytotoxicity experiment. **B**. Combination index values for the various ratios at the EC50, EC75, and EC90. Error bars represent standard deviation.

5.4.2 Encapsulation and Release Profile of IRN and FOA from Liposomes

To attain a high co-encapsulation level of the two compounds in the same liposome we had to devise a new procedure for loading the IRN into the liposome. The procedure (Figure 5.2) used the carboxylate of FOA to provide the ion pair partner for the protonated amine on irinotecan. We investigated a number of different loading conditions in order to attain 1:1 loading (see Chapter 3). We found that including 1,2,3,4-butanetetracarboxylic acid (BTCA) in the loading mixture decreased the retention of FOA in the liposomes. Loading the IRN for an extended period or at high temperatures also compromised FOA retention in liposomes. The final co-encapsulation procedure that was adopted loaded the IRN for 10 min at 50°C into the FOA liposome and permitted the co-encapsulation of a 1:1 ratio of IRN: FOA at a sufficiently high amount so that chemotherapy experiments were readily accomplished.

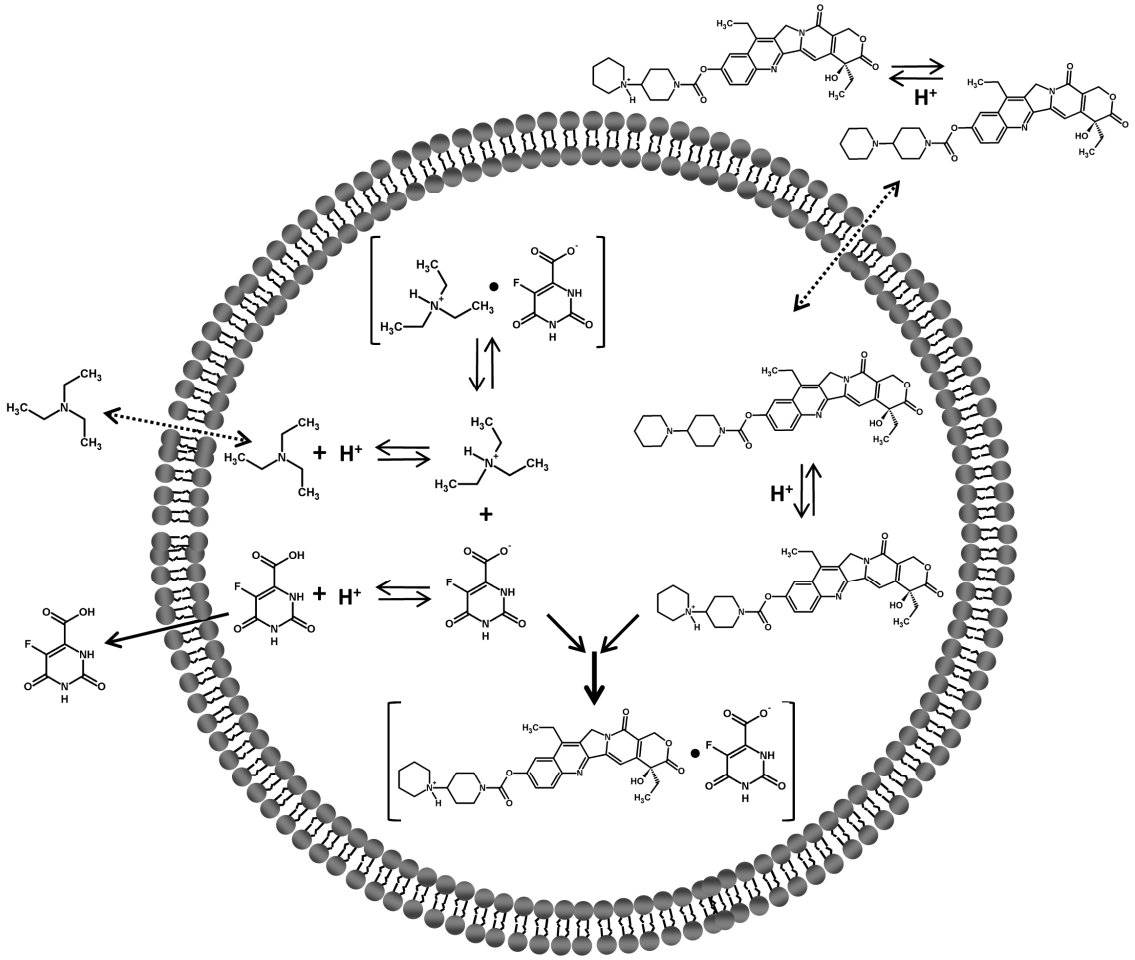

Figure 5.2 Schematic diagram of proposed mechanism of co-encapsulation of IRN +FOA in liposomes.

We compared the drug release of the co-encapsulated, non-targeted liposome formulation (NTL-IRN-FOA) to the drug release of each individually encapsulated preparation (NTL-IRN and NTL-FOA). Figure 5.3 shows the release profile of IRN and FOA from the formulations after incubation in 33% serum at 37 °C. IRN was maintained in both the NTL-IRN and NTL-IRN-FOA formulations over the 96 hr period. However, FOA was released less from the NTL-IRN-FOA formulation than from the NTL-FOA preparation. In the FOA liposome, approximately 60% of FOA remained in NTL-FOA after 24 hrs and 40% remained after 96 hrs; whereas in NTL-IRN-FOA liposome, about 90% FOA remained after 24 hr and 70% remained after 96 hrs. The IRN/FOA molar ratio changed from 1:1 to 1.4:1 over the 96 hr period. Therefore, NTL-IRN-FOA formulation was able to maintain the IRN/FOA ratio near 1:1 for an extended period of time.

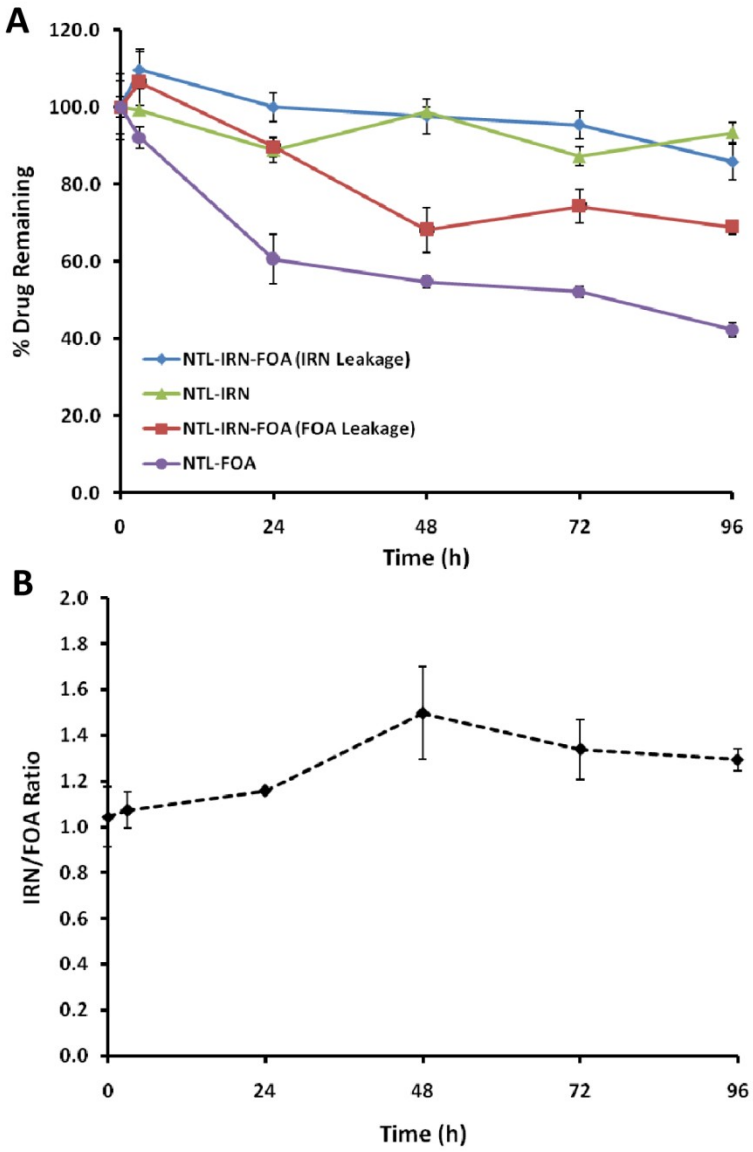

Figure 5.3 IRN and FOA release profile from NTL formulations. **A**. *In vitro* leakage from NTLs after 96 hr incubation in 33% serum at 37°C. **B**. Ratio of IRN and FOA released from the co-encapsulated NTL formulation (NTL-IRN-FOA).

5.4.3 Therapeutic Activity of Individual Liposomal Agents in the KB Tumor Model

The anti-tumor activity of NTL and FTL individually encapsulated formulations of IRN and FOA were assessed in KB tumor-bearing mice. Both NTL and FTL formulations of IRN and FOA have activity in KB tumors (Figure 5.4). FTL-FOA 10 mg/kg had better tumor growth inhibition and a significant increase in survival rate ($p = 0.002$; log-rank test) compared to NTL-FOA 10 mg/kg. FOA 100 mg/kg also had better

tumor growth inhibition and a significant increase in survival rate ($p = 0.0486$; log-rank test) compared to NTL-FOA 10 mg/kg. Interestingly, FOA 100 mg/kg and FTL-FOA 10 mg/kg had similar antitumor activity although the dose of free FOA was 10 fold more than that of FTL-FOA. The IRN formulations were more effective than the FOA formulations. NTL-IRN 50 mg/kg and FTL-IRN 50 mg/kg were more effective than free IRN 50 mg/kg in tumor growth inhibition ($p < 0.05$). The mice treated with FTL-IRN had a significant increase in survival ($p = 0.0064$; log-rank test) than mice administered IRN. There was no statistical difference between NTL-IRN and FTL-IRN in tumor growth inhibition or mouse survival rate.

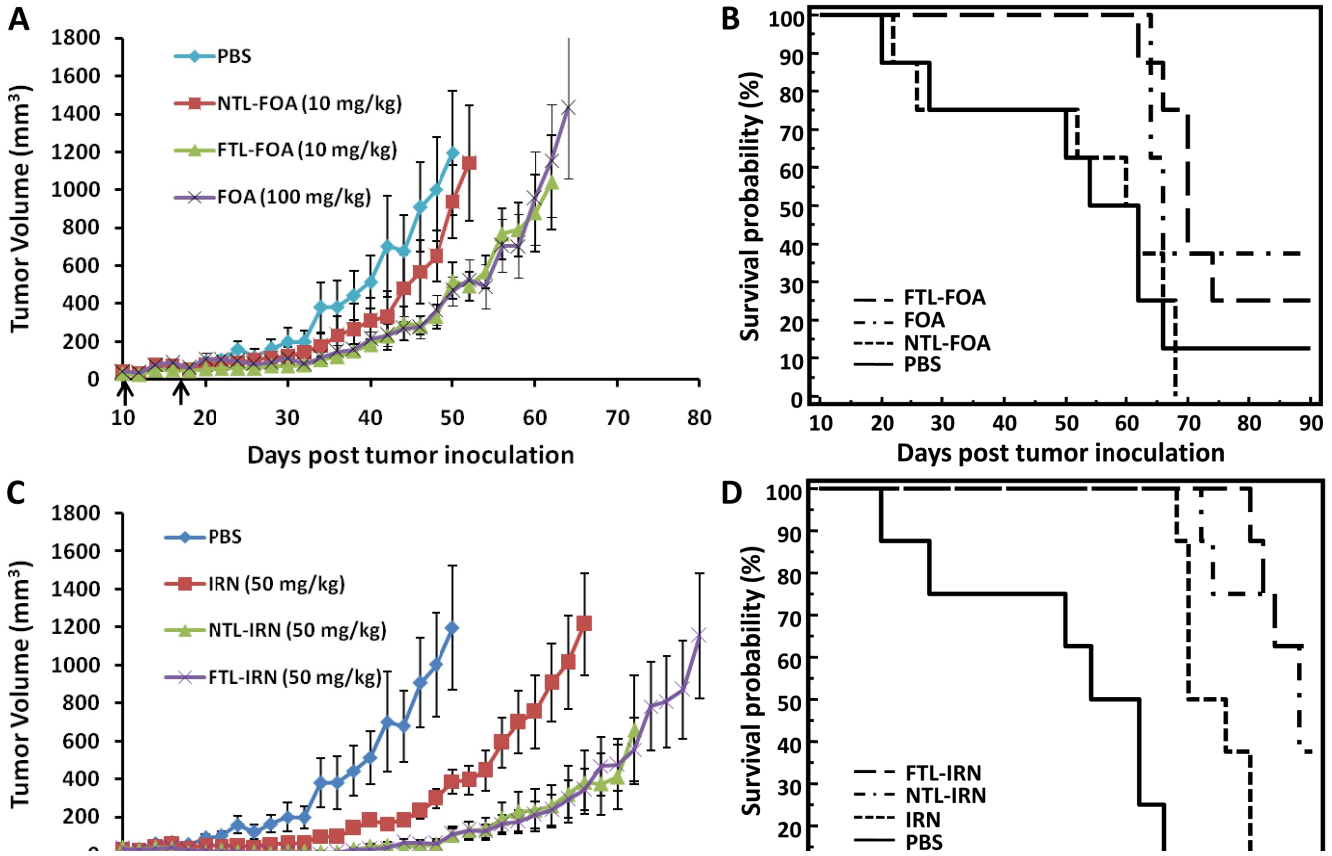

Figure 5.4 Efficacy of NTL and FTL formulations of IRN or FOA alone in KB tumor-bearing mice. KB tumored athymic nu/nu mice (n=8) were administered i.v. injections on Days 10 and 17 (as indicated by arrows). **A and C.** Tumor growth inhibition. Error bars represent SEM. NTL-IRN and FTL-IRN groups had significantly smaller tumors than IRN group ($p < 0.05$ Student's t-test). **B and D.** Survival curves. FTL-IRN group lived significantly longer than IRN ($p=0.0064$ log rank test). FTL-FOA group lived significantly longer than NTL-FOA group ($p = 0.002$; log-rank test).

5.4.4 Therapeutic Activity of the Liposomal Combinations in KB Tumor-bearing Mice

We investigated the therapeutic activity of NTL and FTL formulations of the IRN+FOA 1:1 combination in the KB tumor model to determine whether folate-targeted delivery could improve the *in vivo* effectiveness of this combination. To compare the impact of delivering the combinations in one liposome carrier versus a mixture of separate liposome carriers, we also examined the efficacy of a 1:1 mixture of the drugs encapsulated in separate NTL or FTL formulations. In combination dose studies, the doses of the individual agents in the combination treatment are often reduced to avoid potential toxic outcomes. Therefore, we reduced the dose of the two agents in the combination study by about one half and added a third dose on Day 24 so that the total dose was about 0.75 of the maximum dose studied in the individual dosing study. The dose administered for each agent was 37μmol/kg, which is equivalent to 25 mg/kg for IRN and 6.4 mg/kg for FOA. The effect of these formulations on KB tumor growth inhibition is shown in Figure 5.5 and summarized in Table 5.1.

Free IRN+FOA had a significant but modest effect on KB tumor growth inhibition ($p < 0.05$) as compared to PBS. The FOA liposome formulation, NTL-FOA, had negligible tumor growth inhibition. Although the single liposome agent, NTL-IRN, was significantly more effective than free IRN+FOA (TGD of 93.3% versus 26.7%), the NTL formulations of IRN + FOA performed better. The liposome mixture, NTL-IRN +NTL-FOA, and the liposome co-encapsulated combination, NTL-IRN-FOA, had 140.0% TGD and 173.3% TGD, respectively.

The tumor growth inhibition of NTL-IRN-FOA was significantly better compared to the free IRN+FOA combination and NTL-IRN ($p < 0.05$). However, the tumor-killing

activity of the liposome mixture, NTL-IRN + NTL-FOA, was only statistically different from free IRN+FOA ($p < 0.05$). The NTL co-encapsulated combination also had a slightly larger effect on tumor growth inhibition than the NTL drug mixture.

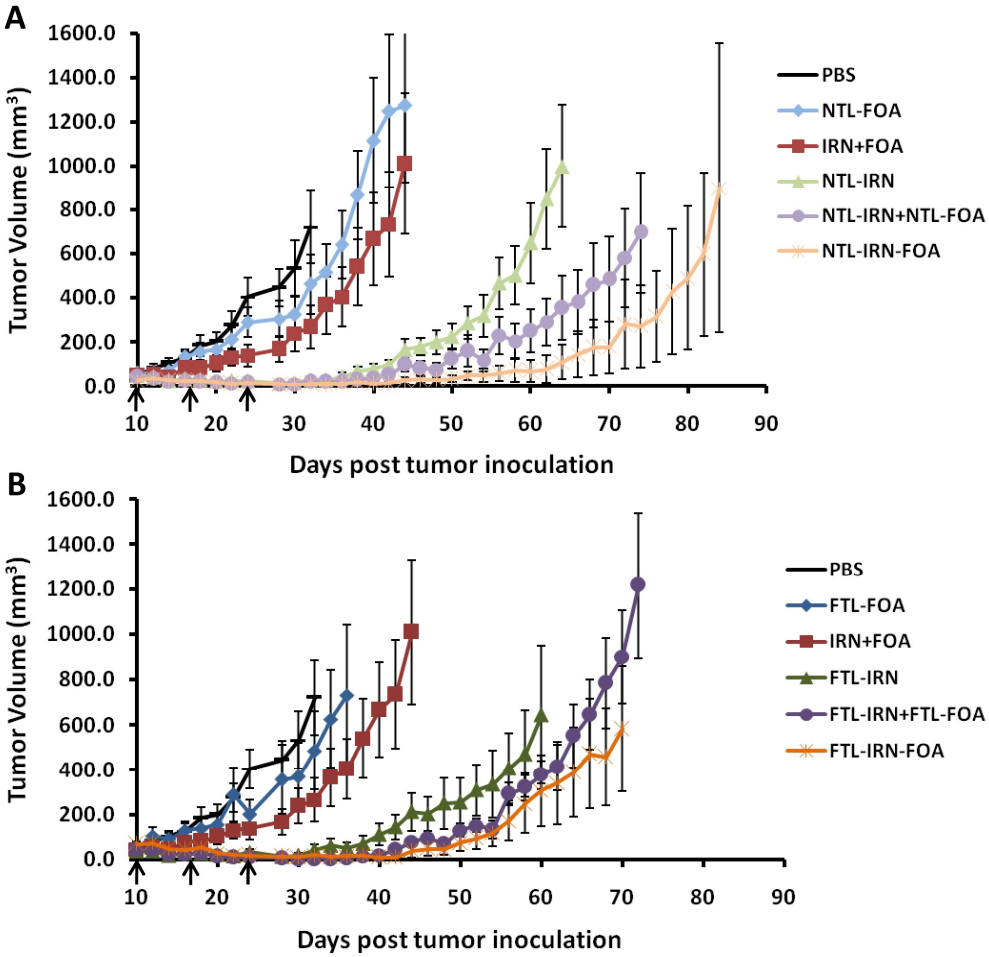

Figure 5.5 Tumor growth inhibition of NTL and FTL combination therapy in KB tumor-bearing mice. Balb/c nu/nu mice (n=8) were treated with i.v. injections on Days 10, 17, and 24 (as indicated by arrows). **A**. NTL Formulations. **B**. FTL formulations. Error bars represent SEM. The dose of each drug is 37 µmol/kg, and the molar ratio is 1:1.

The FTL co-encapsulated combination and FTL drug mixture were also more effective than free IRN+FOA ($p<0.05$). FTL-IRN-FOA had TGD of 133.3% while FTL-IRN + FTL-FOA had TGD of 113.3%. FTL-IRN-FOA and FTL-IRN+FTL-FOA were more superior to FTL-FOA (13.3%TGD) and slightly more effective than FTL-IRN

(100%TGD). Furthermore, FTL-IRN-FOA had slightly better tumor growth inhibition than the FTL drug mixture.

Comparing panels A and B in Figure 5.5, it is evident that the targeted and non-targeted formulations had similar anti-tumor properties. For instance, the NTL-IRN-FOA formulation was slightly more effective than the FTL-IRN-FOA formulation. Table 5.2 summarizes the multiple comparison statistics of the tumor growth inhibition data.

Table 5.1 Quantification of Antitumor and Survival Data

Formulation	TGD (%)	MST (Days)	ILS (%)
PBS	-	58 ± 18	-
IRN+FOA	26.7	60 ± 15	3.5
NTL-FOA	13.3	47 ± 15	-19.5
NTL-IRN	93.3	78 ± 10	34.6
NTL-IRN + NTL-FOA	140.0	87 ± 6	50.2
NTL-IRN-FOA	173.3	67 ± 31	15.6
NTL-IRN-FOA*	173.3	89 ± 3	53.8
FTL-FOA	13.3	56 ± 20	-3.0
FTL-IRN	100.0	83 ± 10	44.2
FTL-IRN + FTL-FOA	113.3	79 ± 13	37.2
FTL-IRN-FOA	133.3	86 ± 8	48.9

TGD-tumor growth delay; MST-mean survival time; ILS-increase in life span
* Data if mice that died due to toxicity were removed from study

Table 5.2 Multiple Statistical Comparison of Average Tumor Size Data*

	PBS	IRN+FOA	NTL-FOA	NTL-IRN	NTL-IRN +NTL-FOA	NTL-IRN-FOA	FTL-FOA	FTL-IRN	FTL-IRN +FTL-FOA	FTL-IRN-FOA
PBS	-	NS	NS	0.0053	0.0051	0.0048	NS	0.0062	0.0047	0.0049
IRN+FOA	NS	-	NS	ND	0.024	0.0175	NS	NS	0.0222	0.0185
NTL-FOA	NS	NS	-	ND	0.0191	0.016	NS	ND	ND	ND
NTL-IRN	0.0053	ND	ND	-	NS	0.015	ND	NS	ND	ND
NTL-IRN +NTL-FOA	0.0051	0.024	0.0191	NS	-	NS	ND	ND	NS	ND
NTL-IRN-FOA	0.0048	0.0175	0.016	0.015	NS	-	ND	ND	ND	NS
FTL-FOA	NS	NS	NS	ND	ND	ND	-	ND	NS	NS
FTL-IRN	0.0062	ND	ND	NS	ND	ND	ND	-	NS	NS
FTL-IRN +FTL-FOA	0.0047	0.0222	ND	ND	ND	ND	NS	NS	-	NS
FTL-IRN-FOA	0.0049	0.0185	ND	ND	ND	NS	NS	NS	NS	-

* p-values were determined by Student's t-test. $p > 0.05$ considered not significant (NS).
ND-not determined.

The effect of the different treatment groups on the survival rate is shown in Figure 5.6. Of the NTL formulations, the 1:1 mixture produced the longest mean survival time (87 days) and increase in life span (50.2%). Mice treated with this formulation had a significantly longer life span than mice treated with free IRN+FOA ($p = 0.0037$; log rank test). Furthermore, mice with NTL-IRN + NTL-FOA lived an average of 9 days longer than mice treated with NTL-IRN and 20 days longer than mice treated with NTL-IRN-FOA. NTL-IRN-FOA had only a minor improvement on the MST compared to IRN+FOA (67 versus 60 days) despite the superior tumor growth delay induced by this formulation.

Of the FTL preparations, FTL-IRN-FOA produced the longest mean survival time (86 days) and increase in life span (48.9%). Mice administered this treatment had a significantly longer survival time than mice treated with IRN+FOA ($p=0.0025$; log rank test). Also, mice treated with the liposome mixture FTL-IRN+FTL-FOA had longer survival time than mice treated with IRN+FOA ($p = 0.0285$; log rank test). Treatment

with FTL-IRN-FOA resulted in an average of 7 day longer survival than mice treated with FTL-IRN + FTL-FOA and 3 days longer than mice treated with FTL-IRN. There was not a significant difference in the survival rates between NTL and FTL formulations of the combinations. NTL-IRN-FOA had the least effect on the survival rate compared to the other liposome combinations even though it produced the greatest effect on tumor progression. If this combination were not very toxic, it could have had the longest survival rate (ILS of 53.8%).

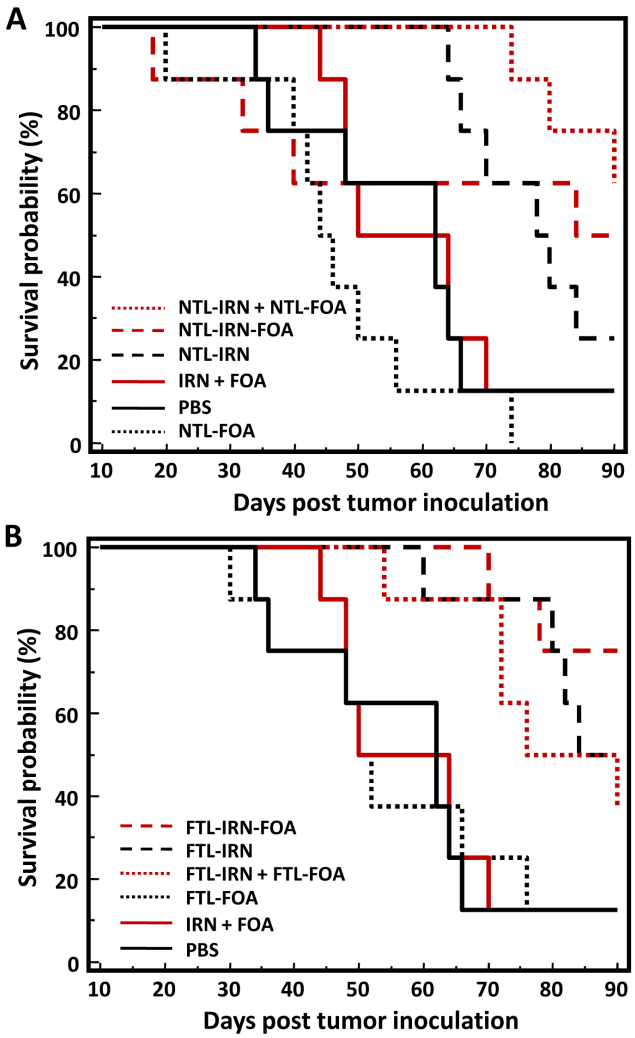

Figure 5.6 Effect of NTL and FTL combination therapy on survival rate in KB tumor-bearing mice. Balb/c nu/nu mice (n=8) were treated with i.v. injections on Days 10, 17, and 24. **A**. NTL Formulations. **B**. FTL formulations. The dose of each drug is 37μmol/kg, and the molar ratio is 1:1

Table 5.3 Multiple Statistical Comparison of Survival Data*

	PBS	IRN+FOA	NTL-FOA	NTL-IRN	NTL-IRN +NTL-FOA	NTL-IRN-FOA	FTL-FOA	FTL-IRN	FTL-IRN +FTL-FOA	FTL-IRN-FOA
PBS	-	NS	NS	0.0485	0.0035	NS	NS	0.0201	0.0319	0.0018
IRN+FOA	NS	-	ND	ND	0.0037	NS	NS		0.0285	0.0025
NTL-FOA	NS	NS	-	ND	0.0001	NS	NS	ND	ND	ND
NTL-IRN	0.0485	ND	ND	-	NS	NS	ND	NS	ND	ND
NTL-IRN + NTL-FOA	0.0035	0.0037	0.0001	NS	-	NS	ND	ND	NS	ND
NTL-IRN-FOA	NS	NS	NS	NS	NS	-	ND	ND	ND	NS
FTL-FOA	NS	NS	NS	ND	ND	ND	-	ND	0.0461	0.0027
FTL-IRN	0.0201	ND	ND	NS	ND	ND	ND	-	NS	NS
FTL-IRN + FTL-FOA	0.0319	0.0285	ND	ND	ND	ND	0.0461	NS	-	NS
FTL-IRN-FOA	0.0018	0.0025	ND	ND	ND	NS	0.0027	NS	NS	-

* p-values were determined by lo-rank test. $p > 0.05$ is considered not significant (NS).
ND-not determined.

Treatment with NTL-IRN-FOA and FTL-IRN-FOA significantly affected the weight of the mice after the third i.v. injection (Figure 5.7). This suggests that there was some drug toxicity to the mice due to the liposome co-encapsulated drugs at the dose level that was used.

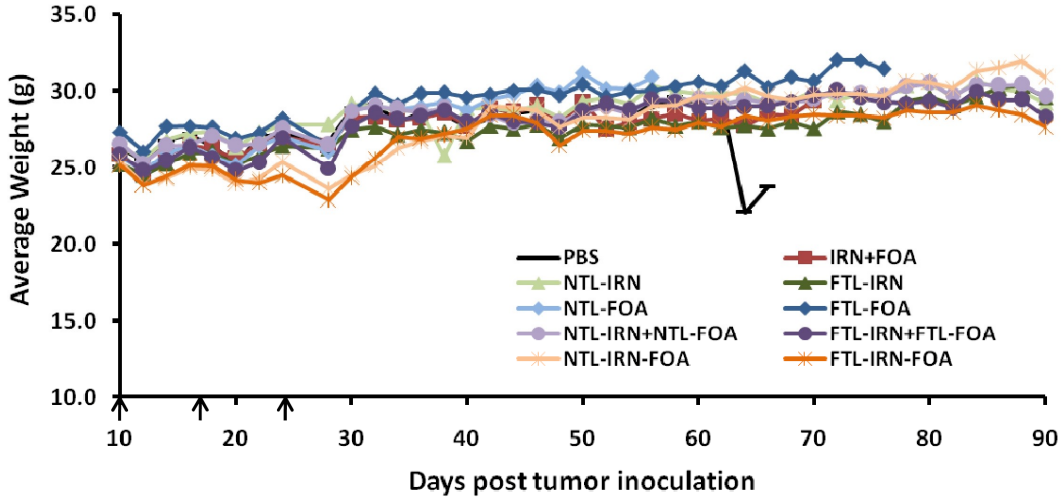

Figure 5.7 Effect of treatments on weight of KB tumor-bearing mice. Arrows indicate treatment days.

5.5 Discussion

The goal of this study was to evaluate the hypothesis that folate-targeted liposome would provide a superior delivery vehicle for synergistic combinations of anti-cancer drugs.

After screening several drug pairs in KB FR+ human nasopharyngeal cancer cells, we determined that the combination of IRN and FOA was synergistic. This drug pair was included in the screen because of a number of reports that IRN and fluoropyrimidines such as 5-fluorouracil (5-FU) are synergistic [50, 57, 62, 86]. 5-FU is an antimetabolite that inhibits RNA synthesis and also DNA synthesis via the enzyme thymidylate synthase. FOA is a prodrug of 5-FU that is able to be encapsulated into liposomes and is more effective in the liposome encapsulated form than as the free drug in cytotoxicity studies in vitro [79, 80, 87]. IRN is a camptothecin prodrug that exerts its cytotoxicity by inhibiting the enzyme topoisomerase I, a process which prevents the religation of DNA after replication and causes single strand breaks. The combination of IRN and 5-FU is very effective and is widely used for treatment of colorectal cancer. Although the exact mechanism of synergism is not clearly understood, it is believed that IRN recruits cells in S phase which allows increased fluoropyrimidine incorporation into DNA and induces apoptosis [27, 57, 86].IRN + FOA exhibited ratio dependent synergism in the KB cells (Figure 5.1). This combination was very synergistic at the 1:1 and 5:1 molar ratios, particularly at the high fractions cell kill. The mechanism of IRN+FOA synergism is probably similar to that of IRN and other fluoropyrimidines.

Since we observed synergy in the KB cells with IRN, we assumed that release of IRN from the liposome in the tumor environment would result in a local conversion of

IRN into SN38. IRN is enzymatically converted by liver and tumor carboxylesterases in to its active metabolite SN-38 [110]. However, we chose not to incorporate SN38 into the liposomes because SN38 is not retained in liposomes *in vivo* due to the high lipophilicity of this drug whereas IRN can be stably incorporated into liposomes [26-28]. Furthermore, combinations of SN-38 and FOA were mostly antagonistic, especially at 5:1, 1:1 and 1:10 molar ratios, in KB cells (see Chapter 2). It may be that the synergism observed between FOA and IRN is not due to the classic topoisomerase activity of the active compound SN38 but rather IRN itself may be altering gene expression in the KB cells that makes them more susceptible to killing by FOA.

IRN and FOA were co-encapsulated in liposomes at 1:1 molar ratio by passively loading FOA into the liposomes then remote loading IRN. The proposed mechanism of coencapsulation is shown in Figure 5.2. We believe that during the remote loading process, triethylamine present in the liposome internal buffer transfers out of the liposome interior. This causes a transmembrane pH gradient across the liposome bilayer (high [H+] in the interior, low [H+] in the exterior). IRN in the external buffer is then able to cross the liposome bilayer and become protonated. Thus, IRN is positively charged (pKa = 8.1) within the liposomes and interacts with FOA, which is negatively charged (pKa = 2.4), forming a complex [23, 88, 92]. The release profiles of IRN from the NTL-IRN and NTL-IRN-FOA formulations were similar (Figure 5.3). However, the leakage of FOA from NTL-IRN-FOA was slower than from NTL-FOA. This observation supports the idea that IRN and FOA form a complex within liposomes.

The therapeutic efficacy of IRN and FOA had not previously been tested in the KB model. Liposomal FOA formulations were dosed at MTD of 10 mg/kg, while the

liposomal IRN preparations were administered at 50 mg/kg. The liposomal IRN formulations had superior therapeutic activity compared to the liposomal FOA formulations (Figure 5.4). The first experiment was designed to treat mice on a 3xq7d schedule; however, all the treated mice were losing weight after the first two i.v. injections (data not shown) so the third dose was not administered. We concluded that it was necessary to dose the liposome combinations at lower doses in order to compare all the treatment groups and to manage the toxicity.

NTL and FTL combinations were significantly more effective than the free IRN + FOA combination (Figures 5.5 and 5.6). This result indicates that liposome delivery enhances the efficacy of synergistic drug pairs *in vivo*. The NTL combinations had a modestly greater antitumor activity than the FTL combinations. Therefore folate-targeted liposome delivery to KB cells did not improve the efficacy of the IRN + FOA combination. It is possible that the hypothesized increase in antitumor activity of the FTL combinations due to targeting is reduced because of the faster elimination of FTLs from the systemic circulation compared to NTLs [11, 32] (see Chapter 4). It is also possible that FTLs traffic into cells differently than the NTL and this interferes with the IRN + FOA synergistic effect.

The IRN and fluoropyrmidine combination is known to be very toxic [57]. We observed that the NTL-IRN-FOA combination was more toxic to the mice than were the other formulations. Three mice out of eight in this group died or were sacrificed early in the study due to significant loss in body weight. It is interesting, however, that neither the FTL-IRN-FOA combination nor the liposome mixtures caused a similar level of toxicity. The mice in these groups were sacrificed only due to tumor burden. It is plausible that

FTL-IRN-FOA had lesser toxicity because FTL formulations are eliminated faster (see Chapter 4).

As predicted, the co-encapsulated combinations showed a trend towards having superior antitumor activity compared to the liposome mixtures. This is probably because the co-encapsulated liposome drug formulations had matched released rates of IRN and FOA compared to the combined drugs in separate carriers (Figure 5.3).

This is the first report that investigates if targeted liposome delivery affects the synergism of anticancer drug combinations *in vivo*. Our studies support the concept that delivery of synergistic combinations in liposomes can enhance the antitumor activity of synergistic combinations. However, we found that folate-targeting of the liposome drug combinations did not provide an increase in activity compared to the non-targeted liposomes formulations. Whether this is specific to the folate receptor or is a general phenomenon will require additional studies with other ligand receptor pairs.

CHAPTER 6:
Conclusions

6.1 Summary of Findings

The goal of this dissertation project was to investigate the hypothesis that targeted liposomes can enhance the efficacy of synergistic drug combinations by controlling the ratio that gets delivered to tumor cells. The motivation behind this study was to exemplify an improved way to translate *in vitro* synergy results to an *in vivo* setting as well as to provide an effective approach for delivering drug combinations to treat cancer.

We tested this hypothesis by first investigating the combination activity of several combinations of free anticancer drugs in KB human oral cancer cells that over-express the folate receptor (FR+). This cell line was selected because of the strong literature evidence supporting that the KB tumor model can be successfully targeted by folate linked liposomes. In Chapter 2, we identified that irinotecan (IRN) + fluoroorotic acid (FOA) was the most synergistic drug pair in KB cells because of its synergism at a wide range of concentrations at particular molar ratios. Furthermore, the synergism of this drug combination was ratio and dose dependent. This synergistic drug pair gave us a means to investigate the concept that liposome delivery can enhance the *in vivo* efficacy of this combination.

The next aim of the study was to develop liposomal formulations that effectively encapsulate IRN and FOA alone and together as well as to design folate-targeted liposomes that can successfully target to KB (FR+) tumors. Therefore in Chapter 3, we developed new, non-targeted liposome (NTL) formulations for IRN alone, FOA alone, and their combination. We found that IRN can be efficiently remote loaded into pre-

formed liposomes by using BTCA. The efficacy and safety of this NTL-IRN formulation was validated in a HT29 human colorectal xenograft tumor model. We found that dissolving FOA in 7M urea allowed us to make a 10 fold more concentrated FOA solution. As a result, we could prepare liposomes that encapsulated a 10 fold higher concentration of FOA. With the NTL-FOA formulation, we are able to deliver a maximum of a 10 mg/kg dose to mice in a 200 μL volume. From safety studies conducted in normal mice, we determined that NTL-FOA was well tolerated at the 10 mg/kg dose given in a 3×q7d dosing schedule, which was the schedule we planned to use for combination therapy studies. We established a method to incorporate IRN and FOA within the same liposome by first passively loading FOA then remote loading IRN. By optimizing the loading temperature and time as well as the initial IRN drug to lipid ratio, we were able to reproducibly co-encapsulate IRN+FOA at 1:1-1:5 molar ratios. In a preliminary combination therapy study, we compared the anti-tumor activity of the NTL single and dual loaded agents in a C26 murine colorectal cancer model. The most potent formulation was NTL-FOA. Single doses of the combinations exhibited a modest tumor suppressive effect. Two doses of the NTL-IRN + NTL-FOA 1:5 combination, which had the same total amount of FOA as the NTL-FOA and $1/7^{th}$ of the dose of the NTL-IRN, provide a slightly lower tumor suppressive effect. Thus, liposomes prepared at a drug ratio that was synergistic in cell culture on the C26 colon carcinoma did not display synergism in the C26 tumor model. These studies point out the challenges to design synergistic treatment protocols based upon results from *in vitro* cytotoxicity studies.

In Chapter 4, we describe the synthesis of folate-PEG-lipid conjugates (FA-PEG-DSPE) with different MW of PEG and their use in targeted liposome formulations.

Various folate targeted liposome (FTL) formulations were prepared and characterized for targeting to KB tumor cells *in vitro* and *in vivo*. Including only 0.03 mol% of FA-PEG-DSPE in the liposome formulation resulted in optimal *in vitro* and *in vivo* targeting. Although FTLs were cleared faster than NTLs from the systemic circulation; both formulations had similar levels of accumulation in tumor tissue. This indicated that the folate-targeted liposomes may be targeted to the tumor tissue. The therapeutic activity of NTL- and FTL-doxorubicin was also examined in KB tumor-bearing mice. The FTL-doxorubicin had slightly better tumor growth inhibition and resulted in a significant increase in survival rate compared to NTL-doxorubicin; however, the enhancement in therapy was only observed for the higher drug dose administered. We propose that the enhanced efficacy at the higher dose could be due to saturation of RES uptake mechanisms since at the higher dose there is an increase in the lipid concentration. As a result of the reduced uptake by RES tissue, more of the FTLs are able to reach the tumor tissue. Further alterations of FTLs to reduce liver and spleen uptake may increase FTL circulation time and improve FTL drug delivery. However, these studies raise a cautionary note for multivalent targeting to solid tumors with low MW ligands attached to drug carriers. What limits uptake for a high-affinity ligand is accessibility to the receptor and not usually the affinity. Putting multiple ligands onto a liposome may modestly increase the affinity of the liposome to the target receptor that is over expressed on tumor cells; however, the multiple ligands will also cause an increase in affinity to sparsely expressed receptors on normal cells as well as non-specific binding sites in the body. Since there are usually many more non-specific sites or sites with low receptor densities, the result of using multiple low MW ligands to target a carrier may cause the

carrier to be more rapidly eliminated from circulation. The net result could be to decrease drug availability to the target tumor and increase drug delivery to normal cells.

The last aim of this thesis was to evaluate the biodistribution and antitumor activity of synergistic drug combinations encapsulated within targeted and non-targeted liposomes. Thus in Chapter 5, we prepared NTL and FTL formulation of IRN, FOA and the IRN + FOA combination in 1:1 molar synergistic ratio. Results from an *in vitro* drug release assay revealed that the co-encapsulated formulation (NTL-IRN-FOA) was able to control the release of the two drugs at the 1:1 ratio. Therapy studies in KB tumor-bearing mice demonstrated that the NTL and FTL combinations were more effective than free IRN + FOA. This adds support to the concept that liposomes can enhance the *in vivo* efficacy of synergistic drug combinations. We observed that co-delivery of the drugs in one liposome showed a trend towards being more effective than co-delivery of drugs via a mixture of two liposomes for both NTL and FTL formulations. Furthermore, the non-targeted liposome formulations of the combinations had slightly greater antitumor efficacy than the folate targeted liposome formulations of the combinations. We believe that the lack of enhanced efficacy of the FTL treatments is due to FTLs increased systemic clearance. Biodistribution studies conducted with the NTL and FTL combinations in the KB model will confirm this assumption.

6.2 Future Directions

We focused the studies in this thesis on the KB tumor cell line (Chapter 2, 4, and 5) because it is widely used as a model for folate receptor targeting. However, the folate receptor is over-expressed on many tumor types, particularly ovarian cancers, and there are several other folate receptor cell lines. These cell lines are not as well studied as the

KB cell line. Anti-cancer drug combinations could be screened in these cells lines for synergism. One could compare folate-targeted liposome of synergistic agents to non-targeted liposome formulations in the multiple FR+ cell lines. Then, one would be able to assess whether folate-targeted liposomes are generally less effective than non-targeted liposomes at delivering synergistic agents or if the therapeutic advantage of folate-targeting is tumor dependent.

It is probable that other ligands that target receptors that are ubiquitously expressed-especially in eliminating organs-may suffer the same fate as folic acid. Therefore, ligands that are uniquely expressed in target tissues are probably the best to employ for targeted delivery. However, such ligands are rare. Therefore, one strategy is to mask the ligand until it reaches the target tissue. Another approach is to include a minimal concentration of the ligand on the surface of the nanocarrier such that only the tissues that over-express the target receptor will bind strongly to the drug delivery vehicle. In Chapter 4, we proposed that FTL delivery may be enhanced by decreasing the folate ligand density below the optimal concentration so as to minimize binding to non-target, FR expressing tissues. This approach could enhance the circulation time and hence tumor accumulation. The decreased binding avidity of the less dense FTLs may also enhance the penetration of FTLs into the solid tumor. Finally, masking the folate ligand with a longer PEG that can be removed from the liposome surface may enable the FTLs to avoid clearance in the liver. This is the first report that investigates if targeted liposome delivery affects the synergism of anticancer drug combinations *in vivo.* Further investigations with different targeting strategies are warranted to determine if targeting can enhance combination drug delivery.

REFERENCES

1. Chou, T.C., *Theoretical basis, experimental design, and computerized simulation of synergism and antagonism in drug combination studies.* Pharmacol Rev, 2006. **58**(3): p. 621-81.
2. Chou, T.C., *The median-effect principle and the combination index for quantitation of synergism and antagonism*. Synergy and antagonism in chemotherapy, ed. T.C. Chou, Rideout, D.C. 1991, San Diego (California): Academic Press.
3. Zimmermann, G.R., J. Lehar, and C.T. Keith, *Multi-target therapeutics: when the whole is greater than the sum of the parts.* Drug Discov Today, 2007. **12**(1-2): p. 34-42.
4. Jia, J., et al., *Mechanisms of drug combinations: interaction and network perspectives.* Nat Rev Drug Discov, 2009. **8**(2): p. 111-28.
5. Loewe, S., *Antagonisms and antagonists.* Pharmacol Rev, 1957. **9**(2): p. 237-42.
6. Berenbaum, M.C., *The expected effect of a combination of agents: the general solution.* J Theor Biol, 1985. **114**(3): p. 413-31.
7. Berenbaum, M.C., *What is synergy?* Pharmacol Rev, 1989. **41**(2): p. 93-141.
8. Bliss, C.I., *The toxicity of poisons applied jointly.* The Annals of Applied Biology, 1939. **26**: p. 585-615.
9. Webb, J.L., *Effect of more than one inhibitor*. Enzymes and Metabolic Inhibitors. Vol. 1. 1963, New York: Academic Press.
10. Greco, W.R., H.S. Park, and Y.M. Rustum, *Application of a new approach for the quantitation of drug synergism to the combination of cis-diamminedichloroplatinum and 1-beta-D-arabinofuranosylcytosine.* Cancer Res, 1990. **50**(17): p. 5318-27.
11. Greco, W.R., G. Bravo, and J.C. Parsons, *The search for synergy: a critical review from a response surface perspective.* Pharmacol Rev, 1995. **47**(2): p. 331-85.
12. Lee, J.J., et al., *Interaction index and different methods for determining drug interaction in combination therapy.* J Biopharm Stat, 2007. **17**(3): p. 461-80.
13. Chou, T.C. and P. Talaly, *A simple generalized equation for the analysis of multiple inhibitions of Michaelis-Menten kinetic systems.* J Biol Chem, 1977. **252**(18): p. 6438-42.
14. Chou, T.C. and P. Talalay, *Generalized equations for the analysis of inhibitions of Michaelis-Menten and higher-order kinetic systems with two or more mutually exclusive and nonexclusive inhibitors.* Eur J Biochem, 1981. **115**(1): p. 207-16.
15. Chou, T.C. and P. Talalay, *Quantitative analysis of dose-effect relationships: the combined effects of multiple drugs or enzyme inhibitors.* Adv Enzyme Regul, 1984. **22**: p. 27-55.
16. Chou, T.C., *Preclinical versus clinical drug combination studies.* Leuk Lymphoma, 2008. **49**(11): p. 2059-80.
17. Chou, T.C.a.T., P., *Analysis of combined drug effects: a new look at a very old problem.* Trends in Pharmacological Sciences, 1983. **4**: p. 450-454.
18. Tallarida, R.J., *Drug synergism: its detection and applications.* J Pharmacol Exp Ther, 2001. **298**(3): p. 865-72.
19. Gabizon, A., H. Shmeeda, and Y. Barenholz, *Pharmacokinetics of pegylated liposomal Doxorubicin: review of animal and human studies.* Clin Pharmacokinet, 2003. **42**(5): p. 419-36.

20. Drummond, D.C., et al., *Development of a highly active nanoliposomal irinotecan using a novel intraliposomal stabilization strategy.* Cancer Res, 2006. **66**(6): p. 3271-7.
21. Allen, T.M. and P.R. Cullis, *Drug delivery systems: entering the mainstream.* Science, 2004. **303**(5665): p. 1818-22.
22. Maeda, H., *The enhanced permeability and retention (EPR) effect in tumor vasculature: the key role of tumor-selective macromolecular drug targeting.* Adv Enzyme Regul, 2001. **41**: p. 189-207.
23. Drummond, D.C., et al., *Pharmacokinetics and in vivo drug release rates in liposomal nanocarrier development.* J Pharm Sci, 2008. **97**(11): p. 4696-740.
24. Vaage, J., et al., *Therapy of mouse mammary carcinomas with vincristine and doxorubicin encapsulated in sterically stabilized liposomes.* Int J Cancer, 1993. **54**(6): p. 959-64.
25. Abraham, S.A., et al., *In vitro and in vivo characterization of doxorubicin and vincristine coencapsulated within liposomes through use of transition metal ion complexation and pH gradient loading.* Clin Cancer Res, 2004. **10**(2): p. 728-38.
26. Wang, J., et al., *In vitro cytotoxicity of Stealth liposomes co-encapsulating doxorubicin and verapamil on doxorubicin-resistant tumor cells.* Biol Pharm Bull, 2005. **28**(5): p. 822-8.
27. Mayer, L.D., et al., *Ratiometric dosing of anticancer drug combinations: controlling drug ratios after systemic administration regulates therapeutic activity in tumor-bearing mice.* Mol Cancer Ther, 2006. **5**(7): p. 1854-63.
28. Yamashita, Y., et al., *Convection-enhanced delivery of a topoisomerase I inhibitor (nanoliposomal topotecan) and a topoisomerase II inhibitor (pegylated liposomal doxorubicin) in intracranial brain tumor xenografts.* Neuro Oncol, 2007. **9**(1): p. 20-8.
29. Krauze, M.T., et al., *Convection-enhanced delivery of nanoliposomal CPT-11 (irinotecan) and PEGylated liposomal doxorubicin (Doxil) in rodent intracranial brain tumor xenografts.* Neuro Oncol, 2007. **9**(4): p. 393-403.
30. Wu, J., et al., *Reversal of multidrug resistance by transferrin-conjugated liposomes co-encapsulating doxorubicin and verapamil.* J Pharm Pharm Sci, 2007. **10**(3): p. 350-7.
31. Tardi, P., et al., *In vivo maintenance of synergistic cytarabine:daunorubicin ratios greatly enhances therapeutic efficacy.* Leuk Res, 2009. **33**(1): p. 129-39.
32. Tardi, P.G., et al., *Drug ratio-dependent antitumor activity of irinotecan and cisplatin combinations in vitro and in vivo.* Mol Cancer Ther, 2009. **8**(8): p. 2266-75.
33. Ramsay, E.C., et al., *The formulation of lipid-based nanotechnologies for the delivery of fixed dose anticancer drug combinations.* Curr Drug Deliv, 2005. **2**(4): p. 341-51.
34. Mayer, L.D. and A.S. Janoff, *Optimizing combination chemotherapy by controlling drug ratios.* Mol Interv, 2007. **7**(4): p. 216-23.
35. Harasym, T.O., et al., *Increased preclinical efficacy of irinotecan and floxuridine coencapsulated inside liposomes is associated with tumor delivery of synergistic drug ratios.* Oncol Res, 2007. **16**(8): p. 361-74.
36. Bayne, W.F., L.D. Mayer, and C.E. Swenson, *Pharmacokinetics of CPX-351 (cytarabine/daunorubicin HCl) liposome injection in the mouse.* J Pharm Sci, 2009. **98**(7): p. 2540-8.

37. Batist, G., et al., *Safety, pharmacokinetics, and efficacy of CPX-1 liposome injection in patients with advanced solid tumors.* Clin Cancer Res, 2009. **15**(2): p. 692-700.
38. Allen, T.M., *Ligand-targeted therapeutics in anticancer therapy.* Nat Rev Cancer, 2002. **2**(10): p. 750-63.
39. Sapra, P. and T.M. Allen, *Ligand-targeted liposomal anticancer drugs.* Prog Lipid Res, 2003. **42**(5): p. 439-62.
40. Antony, A.C., *The biological chemistry of folate receptors.* Blood, 1992. **79**(11): p. 2807-20.
41. Lu, Y. and P.S. Low, *Folate-mediated delivery of macromolecular anticancer therapeutic agents.* Adv Drug Deliv Rev, 2002. **54**(5): p. 675-93.
42. Hilgenbrink, A.R. and P.S. Low, *Folate receptor-mediated drug targeting: from therapeutics to diagnostics.* J Pharm Sci, 2005. **94**(10): p. 2135-46.
43. Pan, X.Q., H. Wang, and R.J. Lee, *Antitumor activity of folate receptor-targeted liposomal doxorubicin in a KB oral carcinoma murine xenograft model.* Pharm Res, 2003. **20**(3): p. 417-22.
44. Eder, J.P., et al., *Sequence effect of irinotecan (CPT-11) and topoisomerase II inhibitors in vivo.* Cancer Chemother Pharmacol, 1998. **42**(4): p. 327-35.
45. Abraham, S.A., et al., *The liposomal formulation of doxorubicin.* Methods Enzymol, 2005. **391**: p. 71-97.
46. Bonavida, B., et al., *Synergy is documented in vitro with low-dose recombinant tumor necrosis factor, cisplatin, and doxorubicin in ovarian cancer cells.* Gynecol Oncol, 1990. **38**(3): p. 333-9.
47. Rezk, Y.A., et al., *Use of resveratrol to improve the effectiveness of cisplatin and doxorubicin: study in human gynecologic cancer cell lines and in rodent heart.* Am J Obstet Gynecol, 2006. **194**(5): p. e23-6.
48. Schabel, F.M., Jr., et al., *cis-Dichlorodiammineplatinum(II): combination chemotherapy and cross-resistance studies with tumors of mice.* Cancer Treat Rep, 1979. **63**(9-10): p. 1459-73.
49. Peleg-Shulman, T., et al., *Characterization of sterically stabilized cisplatin liposomes by nuclear magnetic resonance.* Biochim Biophys Acta, 2001. **1510**(1-2): p. 278-91.
50. Fischel, J.L., et al., *Ternary combination of irinotecan, fluorouracil-folinic acid and oxaliplatin: results on human colon cancer cell lines.* Br J Cancer, 2001. **84**(4): p. 579-85.
51. Kanzawa, F., et al., *In vitro synergistic interactions between the cisplatin analogue nedaplatin and the DNA topoisomerase I inhibitor irinotecan and the mechanism of this interaction.* Clin Cancer Res, 2001. **7**(1): p. 202-9.
52. Kogure, T., et al., *The efficacy of the combination therapy of 5-fluorouracil, cisplatin and leucovorin for hepatocellular carcinoma and its predictable factors.* Cancer Chemother Pharmacol, 2004. **53**(4): p. 296-304.
53. Tanaka, R., et al., *Synergistic interaction between oxaliplatin and SN-38 in human gastric cancer cell lines in vitro.* Oncol Rep, 2005. **14**(3): p. 683-8.
54. Boulikas, T., *Clinical overview on Lipoplatin: a successful liposomal formulation of cisplatin.* Expert Opin Investig Drugs, 2009. **18**(8): p. 1197-218.
55. Schroeder, A., et al., *Ultrasound triggered release of cisplatin from liposomes in murine tumors.* J Control Release, 2009. **137**(1): p. 63-8.

56. Woo, J., et al., *Use of a passive equilibration methodology to encapsulate cisplatin into preformed thermosensitive liposomes.* Int J Pharm, 2008. **349**(1-2): p. 38-46.
57. Azrak, R.G., et al., *Therapeutic synergy between irinotecan and 5-fluorouracil against human tumor xenografts.* Clin Cancer Res, 2004. **10**(3): p. 1121-9.
58. Cao, S., F.A. Durrani, and Y.M. Rustum, *Selective modulation of the therapeutic efficacy of anticancer drugs by selenium containing compounds against human tumor xenografts.* Clin Cancer Res, 2004. **10**(7): p. 2561-9.
59. Fakih, M., et al., *Selenium protects against toxicity induced by anticancer drugs and augments antitumor activity: a highly selective, new, and novel approach for the treatment of solid tumors.* Clin Colorectal Cancer, 2005. **5**(2): p. 132-5.
60. Fakih, M.G., et al., *A Phase I and pharmacokinetic study of selenomethionine in combination with a fixed dose of irinotecan in solid tumors.* Cancer Chemother Pharmacol, 2008. **62**(3): p. 499-508.
61. Fakih, M.G., et al., *A phase I and pharmacokinetic study of fixed-dose selenomethionine and irinotecan in solid tumors.* Clin Cancer Res, 2006. **12**(4): p. 1237-44.
62. Grivicich, I., et al., *The irinotecan/5-fluorouracil combination induces apoptosis and enhances manganese superoxide dismutase activity in HT-29 human colon carcinoma cells.* Chemotherapy, 2005. **51**(2-3): p. 93-102.
63. Janss, A.J., et al., *Synergistic cytotoxicity of topoisomerase I inhibitors with alkylating agents and etoposide in human brain tumor cell lines.* Anticancer Drugs, 1998. **9**(7): p. 641-52.
64. Jonsson, E., et al., *Synergistic interactions of combinations of topotecan with standard drugs in primary cultures of human tumor cells from patients.* Eur J Clin Pharmacol, 1998. **54**(7): p. 509-14.
65. Messerer, C.L., et al., *Liposomal irinotecan: formulation development and therapeutic assessment in murine xenograft models of colorectal cancer.* Clin Cancer Res, 2004. **10**(19): p. 6638-49.
66. Ramsay, E., et al., *Transition metal-mediated liposomal encapsulation of irinotecan (CPT-11) stabilizes the drug in the therapeutically active lactone conformation.* Pharm Res, 2006. **23**(12): p. 2799-808.
67. Ramsay, E., et al., *A novel liposomal irinotecan formulation with significant anti-tumour activity: use of the divalent cation ionophore A23187 and copper-containing liposomes to improve drug retention.* Eur J Pharm Biopharm, 2008. **68**(3): p. 607-17.
68. Zeghari-Squalli, N., et al., *Cellular pharmacology of the combination of the DNA topoisomerase I inhibitor SN-38 and the diaminocyclohexane platinum derivative oxaliplatin.* Clin Cancer Res, 1999. **5**(5): p. 1189-96.
69. Lei, S., et al., *Enhanced therapeutic efficacy of a novel liposome-based formulation of SN-38 against human tumor models in SCID mice.* Anticancer Drugs, 2004. **15**(8): p. 773-8.
70. Pal, A., et al., *Preclinical safety, pharmacokinetics and antitumor efficacy profile of liposome-entrapped SN-38 formulation.* Anticancer Res, 2005. **25**(1A): p. 331-41.
71. Zhang, J.A., et al., *Development and characterization of a novel liposome-based formulation of SN-38.* Int J Pharm, 2004. **270**(1-2): p. 93-107.

72. Barret, J.M., C. Etievant, and B.T. Hill, *In vitro synergistic effects of vinflunine, a novel fluorinated vinca alkaloid, in combination with other anticancer drugs.* Cancer Chemother Pharmacol, 2000. **45**(6): p. 471-6.
73. Drummond, D.C., et al., *Improved pharmacokinetics and efficacy of a highly stable nanoliposomal vinorelbine.* J Pharmacol Exp Ther, 2009. **328**(1): p. 321-30.
74. Semple, S.C., et al., *Optimization and characterization of a sphingomyelin/cholesterol liposome formulation of vinorelbine with promising antitumor activity.* J Pharm Sci, 2005. **94**(5): p. 1024-38.
75. Webb, M.S., et al., *In vitro and in vivo characterization of a combination chemotherapy formulation consisting of vinorelbine and phosphatidylserine.* Eur J Pharm Biopharm, 2007. **65**(3): p. 289-99.
76. Zhigaltsev, I.V., et al., *Liposome-encapsulated vincristine, vinblastine and vinorelbine: a comparative study of drug loading and retention.* J Control Release, 2005. **104**(1): p. 103-11.
77. Goa, K.L. and D. Faulds, *Vinorelbine. A review of its pharmacological properties and clinical use in cancer chemotherapy.* Drugs Aging, 1994. **5**(3): p. 200-34.
78. Bono, V.H., Jr., et al., *Mehtyl-5-Fluoroorotate: Synthesis and Comparison with 5-Fluoroorotic Acid with Respect to Biological Activity and Cell Entry.* Cancer Res, 1964. **24**: p. 513-7.
79. Heath, T.D., et al., *Antiproliferative and anticontractile effects of liposome encapsulated fluoroorotate.* Invest Ophthalmol Vis Sci, 1987. **28**(8): p. 1365-72.
80. Heath, T.D., et al., *5-Fluoroorotate: a new liposome-dependent cytotoxic agent.* FEBS Lett, 1985. **187**(1): p. 73-5.
81. Straubinger, R.M., et al., *Liposome-based therapy of human ovarian cancer: parameters determining potency of negatively charged and antibody-targeted liposomes.* Cancer Res, 1988. **48**(18): p. 5237-45.
82. Caddeo, C., et al., *Effect of resveratrol incorporated in liposomes on proliferation and UV-B protection of cells.* Int J Pharm, 2008. **363**(1-2): p. 183-91.
83. Hung, C.F., et al., *Development and evaluation of emulsion-liposome blends for resveratrol delivery.* J Nanosci Nanotechnol, 2006. **6**(9-10): p. 2950-8.
84. Narayanan, N.K., et al., *Liposome encapsulation of curcumin and resveratrol in combination reduces prostate cancer incidence in PTEN knockout mice.* Int J Cancer, 2009. **125**(1): p. 1-8.
85. Skehan, P., et al., *New colorimetric cytotoxicity assay for anticancer-drug screening.* J Natl Cancer Inst, 1990. **82**(13): p. 1107-12.
86. Peters, G.J., et al., *Basis for effective combination cancer chemotherapy with antimetabolites.* Pharmacol Ther, 2000. **87**(2-3): p. 227-53.
87. Heath, T.D., *Methodology and experimental design for the study of liposome-dependent drugs.* Methods Enzymol, 2005. **391**: p. 186-99.
88. Dicko, A., et al., *Role of copper gluconate/triethanolamine in irinotecan encapsulation inside the liposomes.* Int J Pharm, 2007. **337**(1-2): p. 219-28.
89. Tardi, P.G., et al., *Coencapsulation of irinotecan and floxuridine into low cholesterol-containing liposomes that coordinate drug release in vivo.* Biochim Biophys Acta, 2007. **1768**(3): p. 678-87.

90. Clerc, S. and Y. Barenholz, *Loading of amphipathic weak acids into liposomes in response to transmembrane calcium acetate gradients.* Biochim Biophys Acta, 1995. **1240**(2): p. 257-65.
91. Heidelberger, C., et al., *Studies on fluorinated pyrimidines. II. Effects on transplanted tumors.* Cancer Res, 1958. **18**(3): p. 305-17.
92. Dicko, A., et al., *Intra and inter-molecular interactions dictate the aggregation state of irinotecan co-encapsulated with floxuridine inside liposomes.* Pharm Res, 2008. **25**(7): p. 1702-13.
93. Mayhew, E., et al., *Role of cholesterol in enhancing the antitumor activity of cytosine arabinoside entrapped in liposomes.* Cancer Treat Rep, 1979. **63**(11-12): p. 1923-8.
94. Lee, R.J. and P.S. Low, *Folate-mediated tumor cell targeting of liposome-entrapped doxorubicin in vitro.* Biochim Biophys Acta, 1995. **1233**(2): p. 134-44.
95. Goren, D., et al., *Nuclear delivery of doxorubicin via folate-targeted liposomes with bypass of multidrug-resistance efflux pump.* Clin Cancer Res, 2000. **6**(5): p. 1949-57.
96. Gabizon, A., et al., *Targeting folate receptor with folate linked to extremities of poly(ethylene glycol)-grafted liposomes: in vitro studies.* Bioconjug Chem, 1999. **10**(2): p. 289-98.
97. Stephenson, S.M., P.S. Low, and R.J. Lee, *Folate receptor-mediated targeting of liposomal drugs to cancer cells.* Methods Enzymol, 2004. **387**: p. 33-50.
98. Abra, R.M., H. Schreier, and F.C. Szoka, *The use of a new radioactive-iodine labeled lipid marker to follow in vivo disposition of liposomes: comparison with an encapsulated aqueous space marker.* Res Commun Chem Pathol Pharmacol, 1982. **37**(2): p. 199-213.
99. Reddy, J.A., et al., *Folate-targeted, cationic liposome-mediated gene transfer into disseminated peritoneal tumors.* Gene Ther, 2002. **9**(22): p. 1542-50.
100. Shmeeda, H., et al., *Intracellular uptake and intracavitary targeting of folate-conjugated liposomes in a mouse lymphoma model with up-regulated folate receptors.* Mol Cancer Ther, 2006. **5**(4): p. 818-24.
101. Gabizon, A., et al., *In vivo fate of folate-targeted polyethylene-glycol liposomes in tumor-bearing mice.* Clin Cancer Res, 2003. **9**(17): p. 6551-9.
102. Zhao, X.B., et al., *Cholesterol as a bilayer anchor for PEGylation and targeting ligand in folate-receptor-targeted liposomes.* J Pharm Sci, 2007. **96**(9): p. 2424-35.
103. Gabizon, A., et al., *Tumor cell targeting of liposome-entrapped drugs with phospholipid-anchored folic acid-PEG conjugates.* Adv Drug Deliv Rev, 2004. **56**(8): p. 1177-92.
104. Lee, R.J. and P.S. Low, *Delivery of liposomes into cultured KB cells via folate receptor-mediated endocytosis.* J Biol Chem, 1994. **269**(5): p. 3198-204.
105. Lu, Y., et al., *Role of formulation composition in folate receptor-targeted liposomal doxorubicin delivery to acute myelogenous leukemia cells.* Mol Pharm, 2007. **4**(5): p. 707-12.
106. Pan, X.Q., et al., *Strategy for the treatment of acute myelogenous leukemia based on folate receptor beta-targeted liposomal doxorubicin combined with receptor induction using all-trans retinoic acid.* Blood, 2002. **100**(2): p. 594-602.
107. Yamada, A., et al., *Design of folate-linked liposomal doxorubicin to its antitumor effect in mice.* Clin Cancer Res, 2008. **14**(24): p. 8161-8.

108.Kale, A.A. and V.P. Torchilin, *Enhanced transfection of tumor cells in vivo using "Smart" pH-sensitive TAT-modified pegylated liposomes.* J Drug Target, 2007. **15**(7-8): p. 538-45.
109.Hu, Y., et al., *Synergistic cytotoxicity of pyrazoloacridine with doxorubicin, etoposide, and topotecan in drug-resistant tumor cells.* Clin Cancer Res, 2004. **10**(3): p. 1160-9.
110.Senter, P.D., et al., *Identification and activities of human carboxylesterases for the activation of CPT-11, a clinically approved anticancer drug.* Bioconjug Chem, 2001. **12**(6): p. 1074-80.

APPENDIX A:
Hyaluronan-Lipid Conjugates for Targeted Liposomal Delivery

This chapter contains reprinted material from the technical report "Efficient synthesis of an aldehyde functionalized hyaluronic acid and its application in the preparation of hyaluronan-lipid conjugates" by Dipali Ruhela,, Kareen Riviere, and Francis C. Szoka Jr. in Bioconjugate Chemistry 2006;17:1360-1363. Kareen conducted the enzymatic digestion, purification, and MALDI-TOF characterization of the HA oligosaccharides; assisted with the synthesis and purification of the HA-lipid conjugates; and characterized the lipoligosaccharides via MALDI-TOF mass spectrometry.

A.1 Abstract

An efficient method to synthesize hyaluronan oligosaccharide lipid conjugates is described. This strategy is based on the introduction of a double bond in the glucuronic acid of the hyaluronic acid (HA), by the biodegradation of HA with hyaluronate lyase, followed by the generation of a free aldehyde group at the non-reducing end of hyaluronic acid via ozonolysis and the subsequent reduction of the generated ozonide. The resulting aldehyde functionalized HA is then coupled to dipalmitoyl phosphatidylethanolamine (DPPE) using reductive amination chemistry. This methodology can be extended to link molecules such as biotin, polymers, or proteins to HA for numerous applications in drug delivery and in the creation of biocompatible materials for tissue repair and engineering.

A.2 Introduction

Hyaluronic acid (HA) is a high molecular weight linear polysaccharide which is composed of a simple repeating disaccharide unit of D-glucuronic acid (GlcA) and N-acetyl-D-glucosamine (GlcNAc) linked through a β 1-3 glycosidic bond (Figure A.1). The disaccharides are in turn linked to each other through a β 1-4 glycosidic bond. HA is

found in the extracellular matrix and is the main ligand for CD44, a type 1 transmembrane glycoprotein that is over-expressed in many cancers.

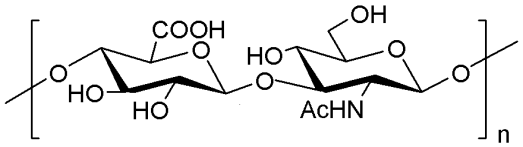

Figure A.1 Disaccharide repeat unit of HA

HA has numerous applications in tissue repair and engineering and in gene and drug delivery. Cross-linked HA has been used as a biomaterial for cartilage repair (*1*). For gene delivery applications, HA-DNA microspheres and a DNA-HA matrix have been used for the controlled release of DNA and are adaptable for site specific targeting (*2, 3*). Various HA conjugates have been tested for targeting drugs to CD44. HA-Taxol and HA-HPMA-Doxorubicin, both synthesized from high molecular weight HA, have been shown to have an increased uptake by tumor cells and therefore have a potential to target drugs selectively to tumors (*4, 5*). Both high molecular (*6, 7*) and low molecular (*8*) weight HA-lipid conjugates have been shown to successfully target liposomes to CD44 expressing cancers and to increase cell killing both *in vitro* and *in vivo*. However, certain liver receptors specifically recognize high molecular weight HA and rapidly clear it from the systemic circulation (*9*). In addition, high molecular weight HA may not be ideal since the frequency of attachment between HA and the conjugated drug is often unknown. Therefore, HA conjugates having small, defined oligosaccharides may avoid clearance by the liver while still preferentially target CD44 over-expressing tumor cells. Understanding the significance of oligomer length for receptor binding is important for furthering drug targeting studies using HA.

Several HA oligosaccharides, having different lengths and modified sequences, have been synthesized over the past decade (*10*) but there are no published studies of well defined lipooligosaccharides. Reductive amination chemistry has been used to conjugate HA with lipids (*11, 12*), polymers (*13*) and a fluorescent tag (*14*). In our ongoing efforts to synthesize lipooligosaccharides, we have designed a more efficient strategy for the synthesis of HA-lipid conjugates of defined length. In this paper, we summarize the results of a methodology, which is based on the generation of a free aldehyde group at the non-reducing end of hyaluronic acid (HA) via enzymatic digestion of high molecular weight HA using hyaluronate lyase, ozonolysis and the subsequent reduction of the generated ozonide. The aldehyde is much more reactive than the hemiacetal so the resulting functionalized hyaluronic acid is easily coupled to DPPE through the aldehyde rather than via the reducing end using an equimolar concentration of the lipid.

A.3 Materials and Methods

A.3.1 Enzymatic Digestion of HA

Sodium hyaluronate (Genzyme Biosurgery) was dissolved in digest buffer (200 mM NaCl and 50 mM sodium acetate, adjusted to pH 6.0) at a concentration of 200 mg/40 mL and stirred at room temperature for 1 day. To 40 mL of dissolved HA, 4000 U of hyaluronate lyase (*Streptomyces hyalurolyticus*, Sigma, St. Louis, MO) was added and allowed to incubate for 4 h at 37 °C. The enzyme was inactivated by immersing the flask in boiling water for 10 min, and the contents were lyophilized.

A.3.2 Size Exclusion Chromatography

The resulting white powder was dissolved in 1 mL of 0.05 M NH_4HCO_3 buffer, filtered through a 0.45 μm filter and loaded via a sample injector onto a 50 mm x 100 cm

Bio-Gel Column (Biorad P-30, medium grade, 300 g). The column was equilibrated in 0.05 M NH_4HCO_3. The first 450 mL of eluate was not collected. Thereafter, fractions of 8 mL each were collected, and their absorbances were read at 232 nm. Fractions containing HA-oligomers were pooled as individual length oligomers, lyophilized, redissolved in H_2O, and lyophilized again to remove residual ammonium bicarbonate salt. The masses of the oligomers were confirmed by MALDI-TOF.

A.3.3 Ozonolysis/Reduction of the HA Oligomers

The HA oligomer (**1**) was dissolved in a mixture of $(CH_3)_2SO$, H_2O and CH_3OH. The solution was cooled to -78 °C and ozone was bubbled into the solution via a sintered glass pipette until a pale blue color persisted. This treatment yielded ozonide (**2**) and ozonide (**3**). Oxygen was then bubbled through the solution to remove the excess ozone until the solution became colorless. After the addition of dimethyl sulfide, the solution was allowed to stir at room temperature for 2 h to reduce the ozonides to yield products **4** and **5**. This mixture was thoroughly dried and used immediately for coupling.

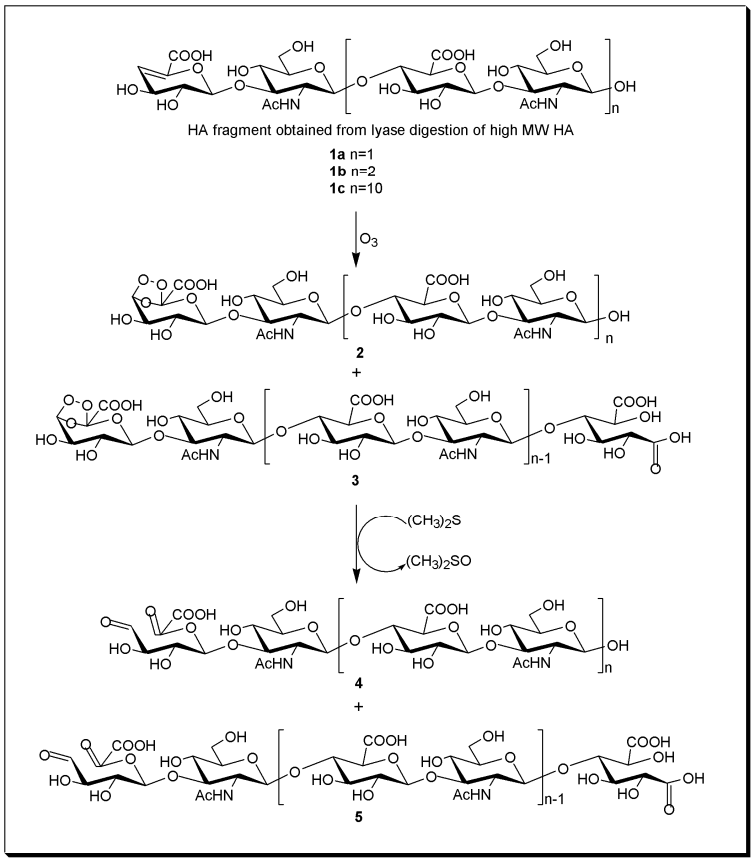

Scheme A.1 Ozonolysis/reduction of the HA oligomers

A.3.4 Synthesis of the Lipooligosaccharide

The crude mixture of **4** and **5** was resuspended in a suitable combination of $(CH_3)_2SO$ and CH_3OH. To this, 1.05 eq of DPPE (Avanti Polar Lipids, Alabaster, AL) in CH_3OH-$CHCl_3$ was added, and the mixture was stirred at 60 °C for 2 h. Thereafter, a 50-fold molar excess of freshly prepared reducing agent solution (1% w/v of $NaCNBH_3$ (Aldrich, St. Louis, MO) in $CHCl_3/CH_3OH$ (1:1 by volume) containing 0.1% CH_3COOH) was added in five portions in 1 h increments. The resulting yellow solution was then allowed to stir at 60 °C for 2 days to yield the HA_n-DPPE conjugate (**6**), which contains DPPE at the non-reducing end, and the HA_{n-1}-DPPE conjugate (**7**), which bears DPPE on the non-reducing residue and contains a lactone at the other end. The solvent was evaporated under vacuum. The residue was resuspended in a modest amount of water and

repeatedly precipitated (three times) in acetone to remove excess $NaCNBH_3$. The resultant pellet was then resuspended in minimal $CHCl_3/CH_3OH/H_2O$ (65:25:4 by volume) and loaded onto a prepacked Biotage silica column. The column was first washed with $CHCl_3$, and then a gradient program of $CHCl_3/CH_3OH/H_2O$ was run to elute out the two products separately. The purified conjugates were characterized by MALDI-TOF.

The HA_4-DPPE conjugate was fully characterized by NMR using pyridine $D_5/DCl/CD_3OD/CDCl_3$ in a volume ratio of 1:1:2:10 (*16*). ^{1}H-NMR (400 MHz) with characteristic peaks: δ 5.2 (1H, H-1α), 4.39 (d, 2H, H-1'β, H-1''), 4.36 (d, 2H, H-1'''β, H-1'α), 4.32 – 4.11 (20H, sugar ring protons), 3.81 – 3.29 (12H, sugar ring protons), 2.25 – 1.29 (56H, methylene protons of DPPE), 2.01 (6H, NHCOCH_3), 1.56 (4H, NH-CH_2-CH_2), 0.87 (6H, terminal CH_3 of DPPE).

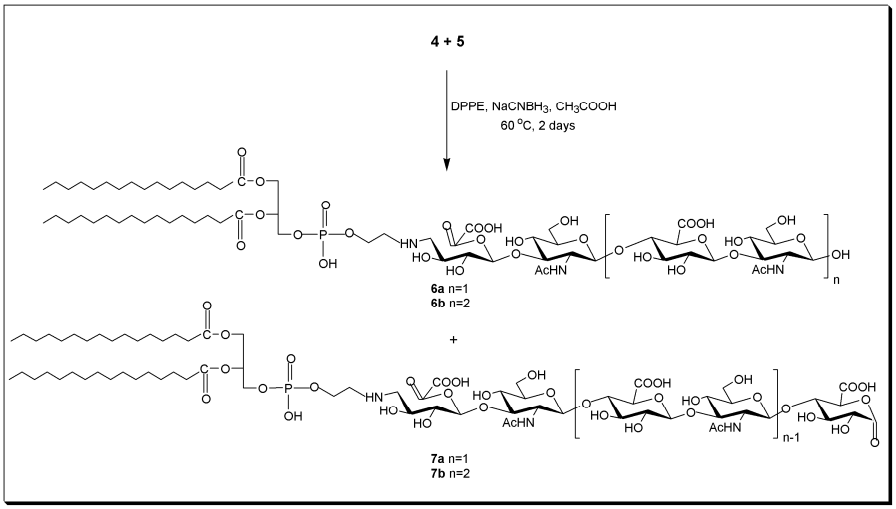

Scheme A.2 Synthesis of the lipooligosaccharide

A.4 Results and Discussion

Conventionally, HA derivatives are directly prepared from oligomers obtained by enzymatic digestion of high molecular weight HA with hyaluronidase. Alternatively, high molecular weight HA can be digested with hyaluronate lyase, an endo-hexosaminidase

whose catalytic activity introduces an α, β unsaturated carboxylic acid moiety at the non-reducing end of the oligomers. We decided to exploit this unique double bond on HA for the synthesis of small, well defined HA-lipid conjugates. The double bond can efficiently be cleaved and converted to an aldehyde functionality via ozonolysis and subsequent reductive workup. Previously, Weingarten and Thiem (*17*) have synthesized aldehyde functionalized carbohydrate derivatives by first introducing a functionality, containing a double bond, on the sugar which was then efficiently converted to a free aldehyde via ozonolyis. Coupling of amino acids with this aldehyde functionalized carbohydrate by reductive amination led to novel carbohydrate-amino acid conjugates. However, in our case, we can generate a double bond within the HA oligomer directly by digestion with hyaluronate lyase. Ozone-assisted cleavage of this double bond can then generate a free aldehyde functionality which can be easily coupled to proteins and phospholipid amino groups by reductive amination. To test our hypothesis, we carried out this sequence of reactions on small HA oligomers and characterized the products formed.

In order to obtain well defined, small HA oligomers, ranging from 4-12 sugar residues containing a double bond at the non-reducing end (having the structure β-D-4en-thrHexA-(1→3)-[β-D-GlcNAc-(1→4)-β-D-GlcA]$_n$-(1→3)-D-GlcNAc), we followed a published procedure by Price et al (*15*). High molecular weight HA was digested with hyaluronate lyase to yield hyaluronan fragments ranging from 4 to 12 saccharides in length. The oligomers were separated on a size exclusion column and analyzed for their absorbance at 232 nm. The separation profile and MALDI-TOF results are shown in Figure A.2 and Table A.1, respectively.

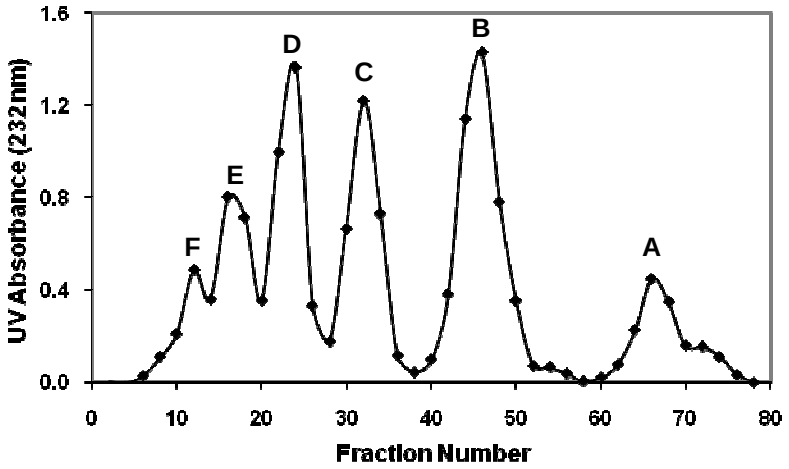

Figure A.2 Size exclusion profile of HA oligomer. Fraction volume = 8 mL.

Table A.1 MALDI-TOF MS (negative mode) Results for HA Oligosaccharides.

Peak	Oligomer	Expected MW	Observed MW
A	3-mer	554.1	- [a]
	4-mer	757.2	756.0
B	5-mer	933.2	933.9
	6-mer	1136.3	1138.1
C	7-mer	1312.3	1314.1
	8-mer	1515.4	1517.7
D	9-mer	1691.4	1691.4
	10-mer	1894.5	1894.5
E	11-mer	2070.6	-
	12-mer	2273.6	2273.6
F	13-mer	2449.7	2451.9
	14-mer	2652.9	2656.0

[a] '-' Indicates mass not observed.

The tetrasaccharide and hexasaccharide thus obtained were subjected to ozonolysis/ reduction with $(CH3)_2S$. This treatment cleanly cleaved the terminal double bond and generated a free aldehyde functionality at the non reducing end of the oligomer. Ozonolysis of the oligomers (Scheme **1**) yielded the corresponding ozonide (**2**) and ozonide (**3**) which resulted from the electrophilic attack of ozone on HA to liberate the anomeric carbon of the second sugar residue from the reducing end of the oligomer, via ozone catalyzed hydrolysis of the β 1, 3 glycosidic bond. It has been previously reported

that ozone can preferentially oxidize β-D-glycosidic linkages in unprotected carbohydrates and generate fragments of various repeat lengths (*18, 19*). As illustrated in Scheme **1**, controlled exposure of the carbohydrate to ozone yielded a mixture of even (compound **4**) and odd (compound **5**) numbered HA fragments, containing a free aldehyde functionality, from the same oligomer.

The resulting aldehyde functionalized HA oligomers were coupled to DPPE using reductive amination chemistry (Scheme **2**) in a mixture of aprotic solvents ($CHCl_3$ and CH_3OH). The reaction with the HA_4 oligomer yielded the products **6a** and **7a**, and similarly the products **6b** and **7b** were obtained from HA_6. One step purification of **6** and **7** by silica column chromatography afforded pure HA_n-DPPE and HA_{n-1}-DPPE conjugates. The products were analyzed by MALDI, and the correct masses for the even (**6a** and **6b**) and odd (**7a** and **7b**) lipooligosaccharides were obtained, as shown in Table A.2.

Table A.2 MALDI-TOF MS (positive mode) Results for HA_n-DPPE Conjugates

Starting Compound	Product	Expected MW	Observed MW
1a	6a	1464.3	1487.5 ($M + Na^+$)
	7a	1259.1	1260.3 ($M + H^+$)
1b	6b	1843.3	1866.3 ($M + Na^+$)
	7b	1638.1	1639.2 ($M + H^+$)

HA_4-DPPE and HA_6-DPPE were also characterized by ^1H NMR (Figure A.3). The NMR spectra showed characteristics peaks for both oligosaccharides and DPPE in the correct ratio. Furthermore, we observed the H-1α proton at δ 5.2 for HA_4-DPPE, which indicates that the anomeric proton at the reducing end of the tetrasaccharide is still intact. This confirms that DPPE is linked to HA via the non-reducing end. Due to line broadening and low resolution, we could not observe the peak for the anomeric proton in

HA_6-DPPE. This line broadening is commonly encountered in the analysis of glycolipids, which have a tendency to self-associate in solution.

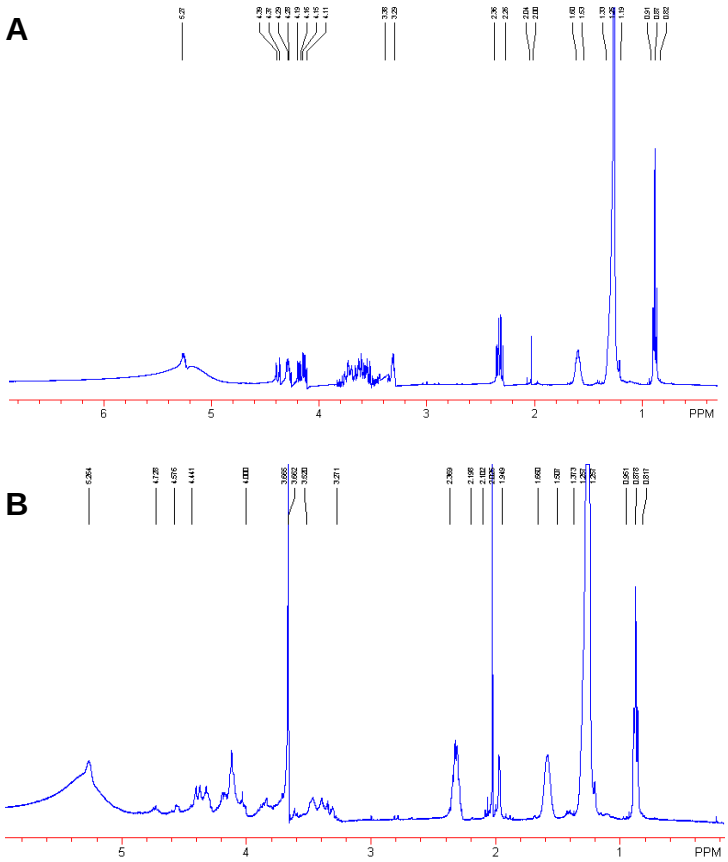

Figure A.3 ^{1}H NMR spectrum of A) HA_4-DPPE and B) HA_6-DPPE

We have demonstrated a facile synthetic approach for preparing HA derivatives. This approach generates a free aldehyde on HA that can readily react with equimolar amounts of lipids containing an amino functionality. This route is more efficient in comparison to the conjugation at the reducing end of the sugar. In addition, we can synthesize a series of conjugates containing even and odd number sugar residues, which can have potential significance in certain applications where oligomer length is critical. Although this approach is quite efficient, it seems to be more suited for small length oligomers because of the difficulty in controlling the side reaction (the fragmentation of the larger oligosaccharides) that is caused by ozone assisted hydrolysis of the glycoside

bonds. The HA lipid conjugates thus generated are currently being evaluated for their properties as targeting ligands and also as potential candidates to mask the surface of the liposomes and microspheres from nonspecific interactions with biological proteins and cells.

A.5 References

(1) Nettles, D. L., Vail, T. P., Morgan, M. T., Grinstaff, M. W., and Setton, L. A. (2004) Photocrosslinkable hyaluronan as a scaffold for articular cartilage repair. *Ann. Biomed. Eng. 32*, 391-397.
(2) Yun, Y. H., Goetz, D. J., Yellen, P., and Chen, W. (2004) Hyaluronan microspheres for sustained gene delivery and site-specific targeting. *Biomaterials 25*, 147-157.
(3) Kim, A., Checkla, D. M., Dehazya, P., and Chen, W. (2003) Characterization of DNA-hyaluronan matrix for sustained gene transfer. *J. Control. Release 90*, 81-95.
(4) Luo, Y., Ziebell, M. R., and Prestwich, G. D. (2000) A hyaluronic acid-taxol antitumor bioconjugate targeted to cancer cells. *Biomacromolecules 1*, 208-218.
(5) Luo, Y., Bernshaw, N. J., Lu, Z. R., Kopecek, J., and Prestwich, G. D. (2002) Targeted delivery of doxorubicin by HPMA copolymer-hyaluronan bioconjugates. *Pharm. Res. 19*, 396-402.
(6) Peer, D., and Margalit, R. (2004) Loading mitomycin C inside long circulating hyaluronan targeted nano-liposomes increases its antitumor activity in three mice tumor models. *Int. J. Cancer 108*, 780-789.
(7) Peer, D., and Margalit, R. (2004) Tumor-targeted hyaluronan nanoliposomes increase the antitumor activity of liposomal doxorubicin in syngeneic and human xenograft mouse tumor models. *Neoplasia 6*, 343-353.
(8) Eliaz, R. E., and Szoka, F. C. (2001) Liposome-encapsulated doxorubicin targeted to CD44: a strategy to kill CD44-overexpressing tumor cells. *Cancer Res. 61*, 2592-2601.
(9) Harris, E. N., Weigel, J. A., and Weigel, P. H. (2004) Endocytic function, glycosaminoglycan specificity, and antibody sensitivity of the recombinant human 190-kDa hyaluronan receptor for endocytosis. *J. Biol. Chem. 279*, 36201-36209.
(10) Karst, N. A., and Linhardt, R. J. (2003) Recent chemical and enzymatic approaches to the synthesis of glycosaminoglycan oligosaccharides. *Curr. Med. Chem. 10*, 1993-2031.
(11) Oohira, A., Kushima, Y., Tokita, Y., Sugiura, N., Sakurai, K., Suzuki, S., and Kimata, K. (2000) Effects of lipid-derivatized glycosaminoglycans (GAGs), a novel probe for functional analyses of GAGs, on cell-to-substratum adhesion and neurite elongation in primary cultures of fetal rat hippocampal neurons. *Arch. Biochem. Biophys. 378*, 78-83.
(12) Sugiura, N., Sakurai, K., Hori, Y., Karasawa, K., Suzuki, S., and Kimata, K. (1993) Preparation of lipid-derivatized glycosaminoglycans to probe a regulatory function of the carbohydrate moieties of proteoglycans in cell-matrix interaction. *J. Biol. Chem. 268*, 15779-15787.
(13) Asayama, S., Nogawa, M., Takei, Y., Akaike, T., and Maruyama, A. (1998) Synthesis of novel polyampholyte comb-type copolymers consisting of a poly (L-lysine)

backbone and hyaluronic acid side chains for a DNA carrier. *Bioconjugate Chem. 9*, 476-481.
(14) Calabro, A., Benavides, M., Tammi, M., Hascall, V. C., and Midura, R. J. (2000) Microanalysis of enzyme digests of hyaluronan and chondroitin/dermatan sulfate by fluorophore-assisted carbohydrate electrophoresis (FACE). *Glycobiology 10*, 273-281.
(15) Price, K. N., Tuinman, A., Baker, D. C., Chisena, C., and Cysyk, R. L. (1997) Isolation and characterization by electrospray-ionization mass spectrometry and high-performance anion-exchange chromatography of oligosaccharides derived from hyaluronic acid by hyaluronate lyase digestion: observation of some heretofore unobserved oligosaccharides that contain an odd number of units. *Carbohydr. Res. 303*, 303-311.
(16) Wang, Y., and Hollingsworth, R. I. (1995) A solvent system for the high-resolution proton nuclear magnetic resonance spectroscopy of membrane lipids. *Anal. Biochem. 225*, 242-251.
(17) Weingarten, S., and Thiem, J. (2003) Facile formation of novel carbohydrate-amino acid conjugates by reductive amination. *Synlett*. *7*, 1052-1054.
(18) Wang, Y., Hollingsworth, R. I., and Kasper, D. L. (1998) Ozonolysis for selectively depolymerizing polysaccharides containing β-D-aldosidic linkages. *Proc. Natl. Acad. Sci. 95*, 6584-6589.
(19)Wang,Y.,Hollingsworth,R. I., and Kasper, D. L. (1999) Ozonolytic depolymerization of polysaccharides in aqueous solution. *Carbohydr. Res. 319*, 141-14.

Publishing Agreement

It is the policy of the University to encourage the distribution of all theses, dissertations, and manuscripts. Copies of all UCSF theses, dissertations, and manuscripts will be routed to the library via the Graduate Division. The library will make all theses, dissertations, and manuscripts accessible to the public and will preserve these to the best of their abilities, in perpetuity.

Please sign the following statement:

I hereby grant permission to the Graduate Division of the University of California, San Francisco to release copies of my thesis, dissertation, or manuscript to the Campus Library to provide access and preservation, in whole or in part, in perpetuity.

Author

Oct. 2, 2009
Signature Date